HYDROGEOLOGY OF ROUND VALLEY, WASATCH COUNTY, UTAH

by Paul Inkenbrandt

REPORT OF INVESTIGATION 279
UTAH GEOLOGICAL SURVEY
a division of
UTAH DEPARTMENT OF NATURAL RESOURCES
2019

Blank pages are intentional for printing purposes

HYDROGEOLOGY OF ROUND VALLEY, WASATCH COUNTY, UTAH

by Paul Inkenbrandt

Cover photo: The headwaters of Little Hobble Creek, looking south towards Rattlesnake Mountain and Bald Knoll.

REPORT OF INVESTIGATION 279
UTAH GEOLOGICAL SURVEY
a division of
UTAH DEPARTMENT OF NATURAL RESOURCES
2019

STATE OF UTAH
Gary R. Herbert, Governor

DEPARTMENT OF NATURAL RESOURCES
Brian C. Steed, Executive Director

UTAH GEOLOGICAL SURVEY
R. William Keach II, Director

PUBLICATIONS
contact
Natural Resources Map & Bookstore
1594 W. North Temple
Salt Lake City, UT 84116
telephone: 801-537-3320
toll-free: 1-888-UTAH MAP
website: utahmapstore.com
email: geostore@utah.gov

UTAH GEOLOGICAL SURVEY
contact
1594 W. North Temple, Suite 3110
Salt Lake City, UT 84116
telephone: 801-537-3300
website: https://geology.utah.gov

CONTENTS

FIGURES

TABLES

PLATE

HYDROGEOLOGY OF ROUND VALLEY, WASATCH COUNTY, UTAH

by Paul Inkenbrandt

ABSTRACT

The Utah Geological Survey (UGS), in cooperation with Wasatch County, conducted a hydrologic study of the Round Valley drainage basin in Wasatch County, Utah. The primary goals of the study were to (1) characterize the hydrogeology in the area, (2) measure the flow of creeks and springs in the Round Valley watershed, and (3) compare the water chemistry of surface water to groundwater, as well as bedrock groundwater to unconsolidated valley fill (sand and gravel) groundwater.

Groundwater maps and records provide an important baseline of groundwater conditions for an area and allow hydrologists to infer groundwater flow conditions. I examined groundwater levels in Round Valley and the surrounding region by measuring depth to water in 70 wells throughout the valley, compiling Utah Division of Water Rights and U.S. Geological Survey groundwater data, and statistically analyzing the data, using analyses that included geostatistical interpolations and time-series analyses.

The first complete potentiometric surface map of Round Valley was constructed, and long-term groundwater-level trends for the region were examined. Groundwater in Round Valley generally flows from east to west at an average gradient of 3% toward Deer Creek Reservoir. The regional potentiometric surface mimics topography, indicating limited potential for flow between valleys. Examination of groundwater-level time series shows groundwater is highest in June and lowest in December but can vary locally. Long-term hydrographs indicate no significant upward or downward trend in groundwater levels in the Provo River watershed over the past six decades.

The first basin depth map of the area was also created. Deposits of unconsolidated sand, gravel, clay, and boulders vary in thickness in Round Valley. Some sediments are more than 500 feet (152 m) thick near the northeast basin-bounding fault. The maximum thickness of alluvium in the center part of the valley is generally 100 to 200 feet (30.5–61 m), thinning with distance from the stream channels.

Based on forward analytic element modeling, an average of 0.01 feet (1 mm) of groundwater-level decline is expected in wells per gallon per minute pumping increase, having up to 10 feet (3 m) of average aquifer drawdown over the area of the unconsolidated sediment at a combined steady-state pumping rate of 1000 gallons per minute (63 L/s). Drawdown near a hypothetical pumping well would be much higher than the average drawdown. Drought conditions would significantly increase the amount of observed drawdown from pumping.

Mass loading calculations indicate that adding 500 septic systems may increase the average background groundwater concentration of nitrate as nitrogen by 0.5 mg/L, where the greatest observed increases would be in areas of highest septic system density. This estimate is very sensitive to the assumed groundwater flow and the total area used in the calculation.

Water chemistry shows that groundwater in Round Valley is pristine, having total-dissolved-solid concentrations of less than 1000 mg/L and no exceedances of any inorganic drinking water standards. Surface water has a history of relatively high nutrient (phosphorous and nitrate) loads, but the loading appears to have decreased in recent years due to mitigation

efforts and/or decreased discharge. The flow of Main Creek at its mouth has likely decreased since the 1940s, when comparable precipitation produced higher discharges than those measured in 2013–2017.

Water chemistry, modeling, and the potentiometric surface indicate that the bedrock and valley-fill aquifers are connected and should be considered an inhomogeneous aquifer system. Water chemistry and discharge measurements indicate that surface water and groundwater in Round Valley are also closely connected. Reducing the potentiometric surface will impact surface water and spring flows; specifically, the flows of Main Creek and Little Hobble Creek in the alluvial fill material of Round Valley will be reduced by increased pumping.

INTRODUCTION

Purpose

Round Valley (also known as Wallsburg Valley) is a small valley in the eastern Wasatch Range in north-central Utah, south of Heber City and east of Deer Creek Reservoir in Wasatch County (figure 1). This hydrogeologic study of Round Valley by the Utah Geological Survey (UGS) was initiated by Wasatch County, spurred by potential residential development in the area (Berg Engineering, 2015). The goal of the study was to develop a water budget and hydrogeologic framework for Round Valley, which will provide water managers with tools to understand how population growth could impact water supplies in the valley.

Setting

Round Valley is in the Middle Rocky Mountains physiographic province (Roark and others, 1991) and has land elevations ranging from about 5400 feet (1646 m) at Deer Creek Reservoir to 8400 feet (2560 m) at the mountain ridges bounding the watershed. The valley margins are at an elevation of about 6200 feet (1890 m) (Roark and others, 1991). The only town in Round Valley is Wallsburg. In 2010, Round Valley had a population of 745 people, 245 of whom lived within Wallsburg city limits, and the others dispersed throughout the valley (U.S. Census Bureau, 2016). The area receives 15 to 20 inches (38–51 cm) of precipitation per year, mostly in the form of snow during the winter months (Baker and Peterson, 1970). Primary land use is irrigated agriculture (Roark and others, 1991) and some residential use concentrated near Wallsburg.

Geology

Round Valley is a fault-bounded alluvial valley underlain by upper Paleozoic rocks. Most of the geology of Round Valley consists of the Pennsylvanian-Permian Oquirrh Formation and Quaternary alluvium and alluvial-fan deposits (figures 2 and 3). Of the members of the Oquirrh Formation (figure 2), the Granger Mountain Member is more prevalent in the southern part of the valley, whereas the Wallsburg Ridge Member is more prevalent in the northern part of the valley (figure 3). Outcrops of the Wallsburg Ridge and Granger Mountain Members within Round Valley are highly fractured sandstone (Biek and Lowe, 2009). The sandstone of the Wallsburg Ridge Member is generally yellow-brown orthoquartzite interbedded with silty limestone (Baker, 1976; Biek and Lowe, 2009). The Granger Mountain Member is more calcareous, has siltier interbeds, and has fossiliferous limestone at its base. The Oquirrh Formation primarily yields water to wells and springs from fractures and solution openings. Transmissivity of the Oquirrh Formation is about 270 feet squared per day (ft^2/day [25 m^2/day]) (Baker and Peterson, 1970).

Round Valley is bounded on the northeast and southwest by the East and West Round Valley faults, respectively. Based on the cross section of Biek and Lowe (2009), the East and West Round Valley faults have approximately 1000 feet (305 m) and 1800 feet (550 m) of normal slip, respectively (figure 4). The East Round Valley fault juxtaposes the Oquirrh Formation against Quaternary fan alluvium. The West Round Valley fault vertically offsets the Oquirrh Formation (figure 4). Unnamed intra-basin normal faults cross the interior of the valley (figure 3). Well-defined triangular facets and linear scarps suggest the valley-bounding faults have been active as recently as the late Quaternary (Sullivan and others, 1988). Sullivan and others (1988) observed that the absence of mid-Tertiary deposits in the valley suggests that the faults initiated movement in the late Cenozoic.

Round Valley's alluvial fans make up a large component of the valley fill. Sediment clasts in the fans are primarily composed of weathered sandstone boulders from the Oquirrh Formation. The fans transition into late Quaternary alluvium deposited and reworked by Main Creek and its tributaries near the center of the valley. The lower parts of the alluvial fans are generally younger than the middle and upper parts of the fans near the margins of the valley.

Hydrology

Round Valley's surface water is drained by one trunk stream, Main Creek. Tributaries to Main Creek include Little Hobble Creek, Spring Creek, and Upper Main Creek (figure 1). Main Creek contributes to Deer Creek Reservoir which started filling in 1941 and has a capacity of 152,000 acre-feet (ac-ft) (0.187 km^3) (Provo River Water Users Association, 2016). The U.S. Geological Survey (USGS) operated a surface gage station (gage ID 0158500) on Main Creek from October 1, 1938, to September 30, 1950 (U.S. Geological Survey, 2019). Much of Main Creek and its tributaries are diverted for irrigation (Roark and others, 1991). According to Roark and others (1991), the U.S. Bureau of Reclamation operated the USGS station as U.S. Bureau of Reclamation (BOR) station 1013 from 1985 to 1987, but records requests to the BOR indicate that these data were lost.

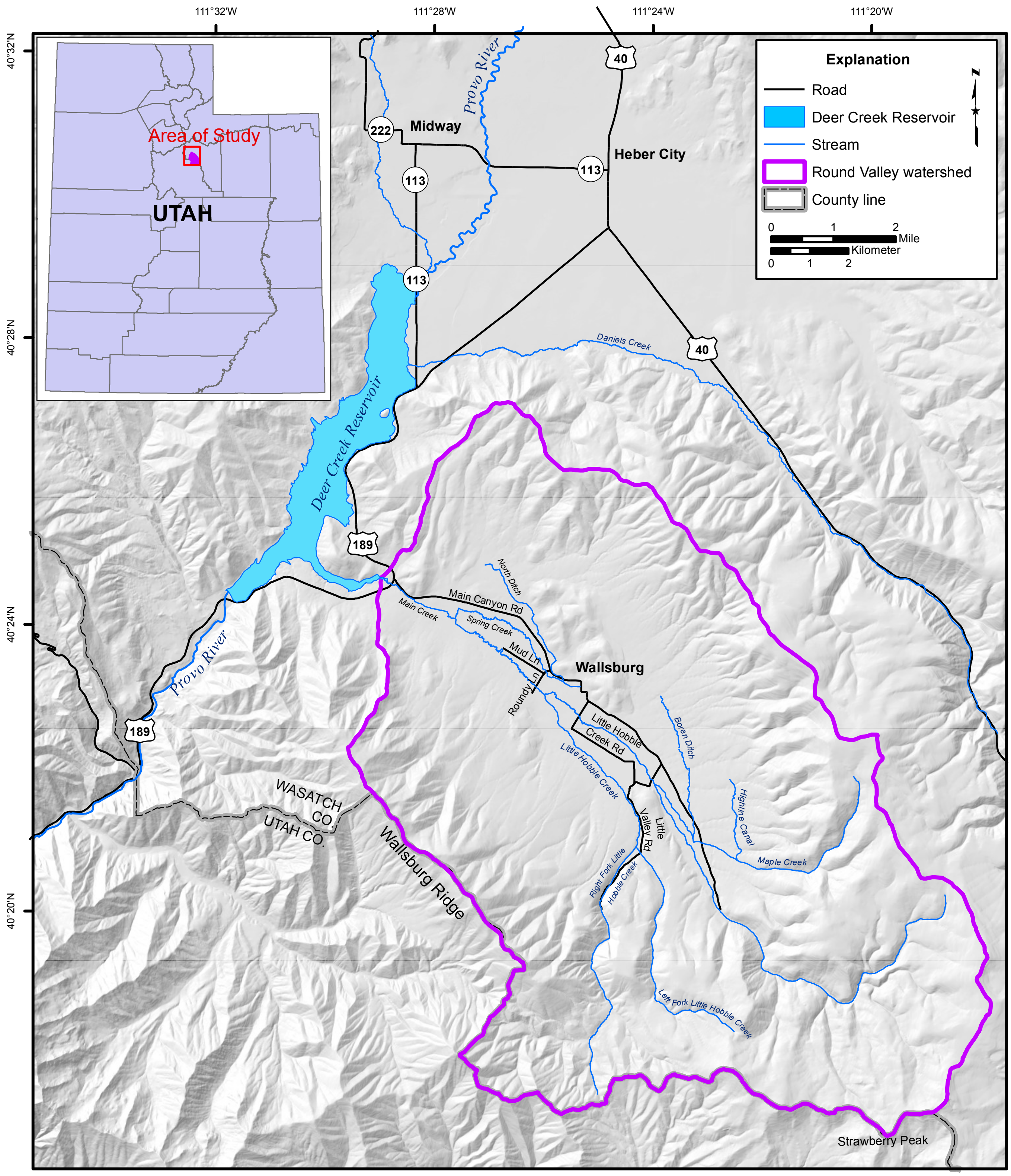

Figure 1. The study area is in north-central Utah, south of Heber, Wasatch County, Utah. Hillshade base map from the Utah Automated Geographic Reference Center (2019).

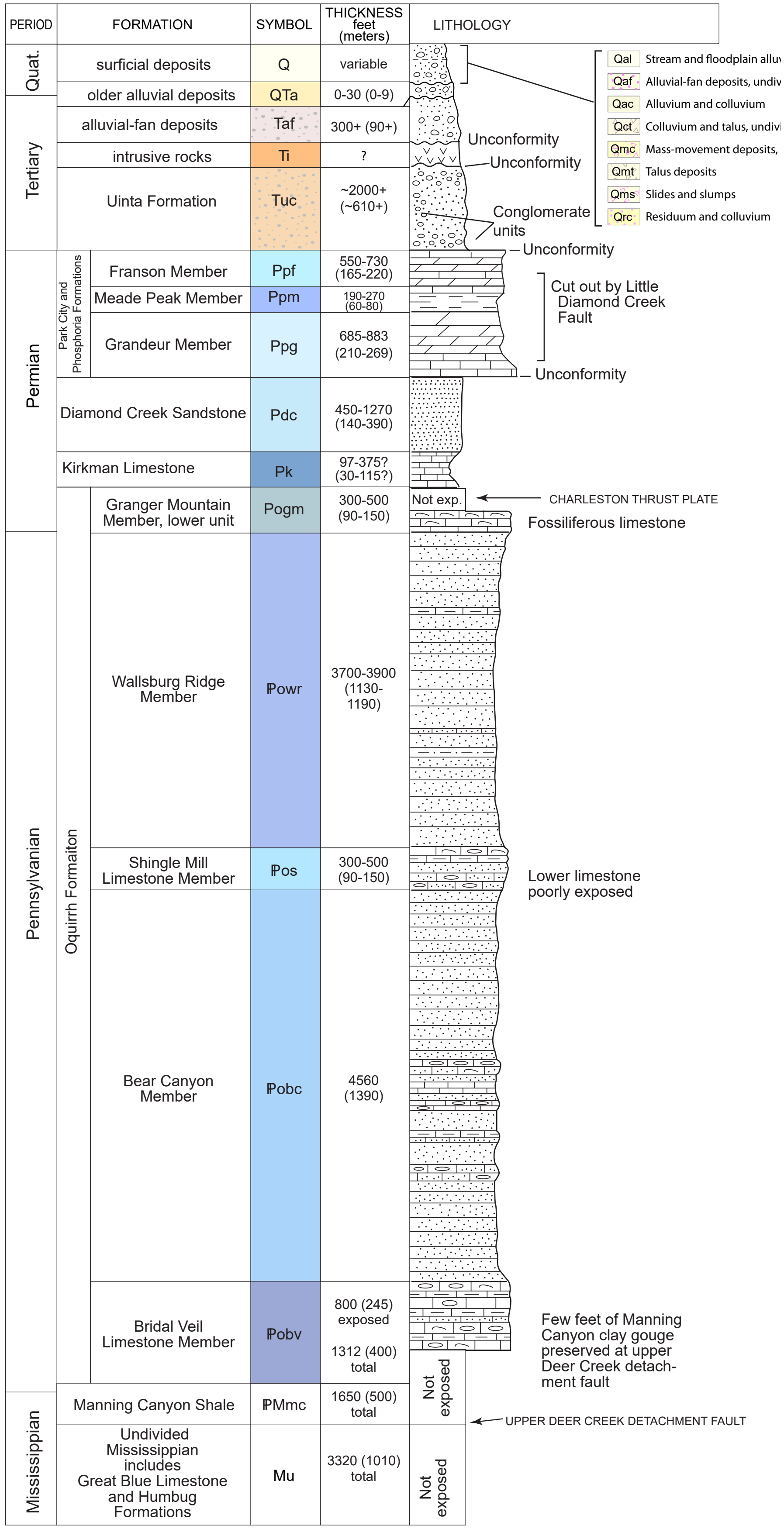

***Figure 2**. Stratigraphic column of geologic units in the region adapted from Biek and Lowe (2009) and Constenius and others (2011).*

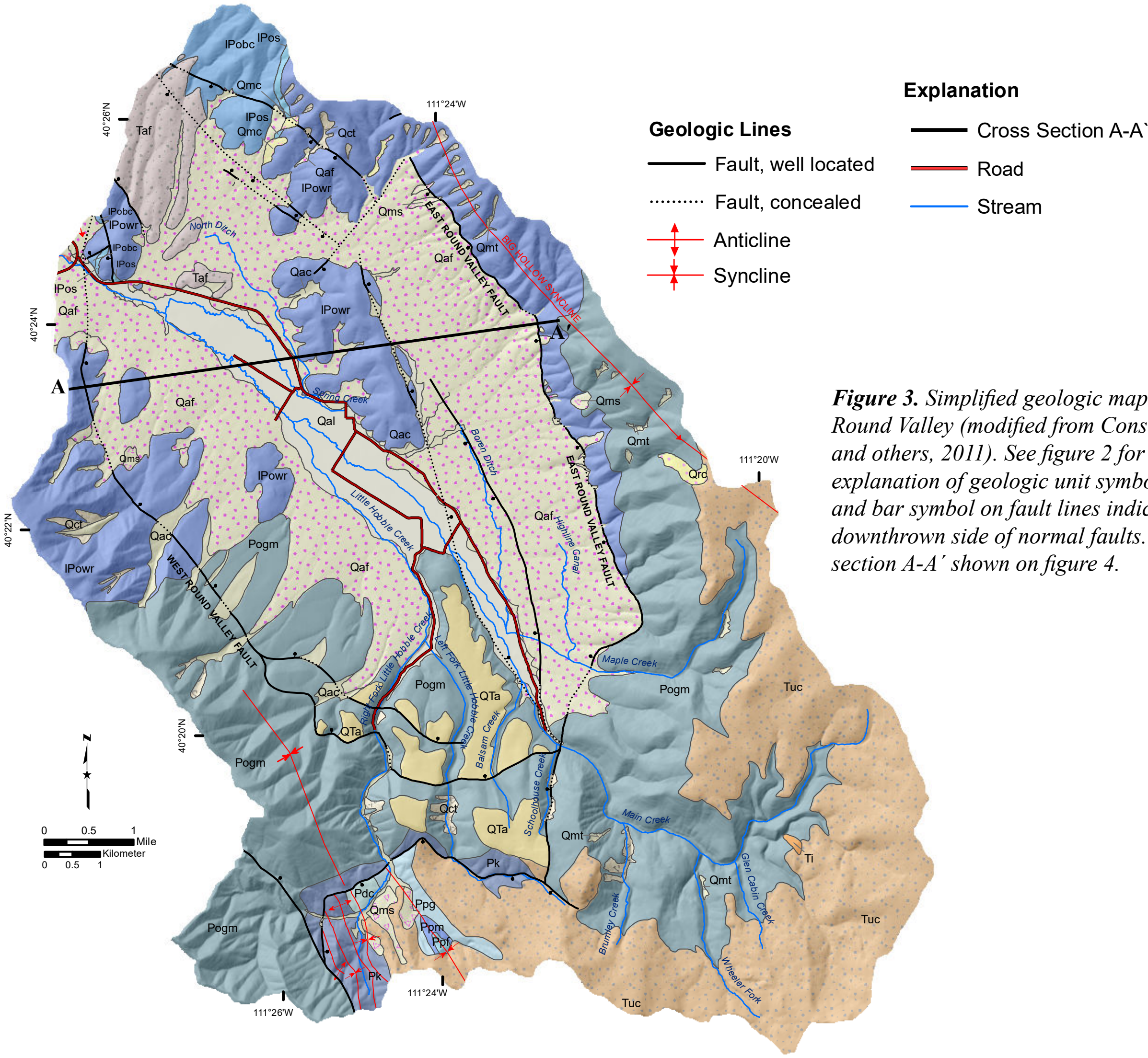

Figure 3. Simplified geologic map of Round Valley (modified from Constenius and others, 2011). See figure 2 for explanation of geologic unit symbols. Ball and bar symbol on fault lines indicates downthrown side of normal faults. Cross section A-A′ shown on figure 4.

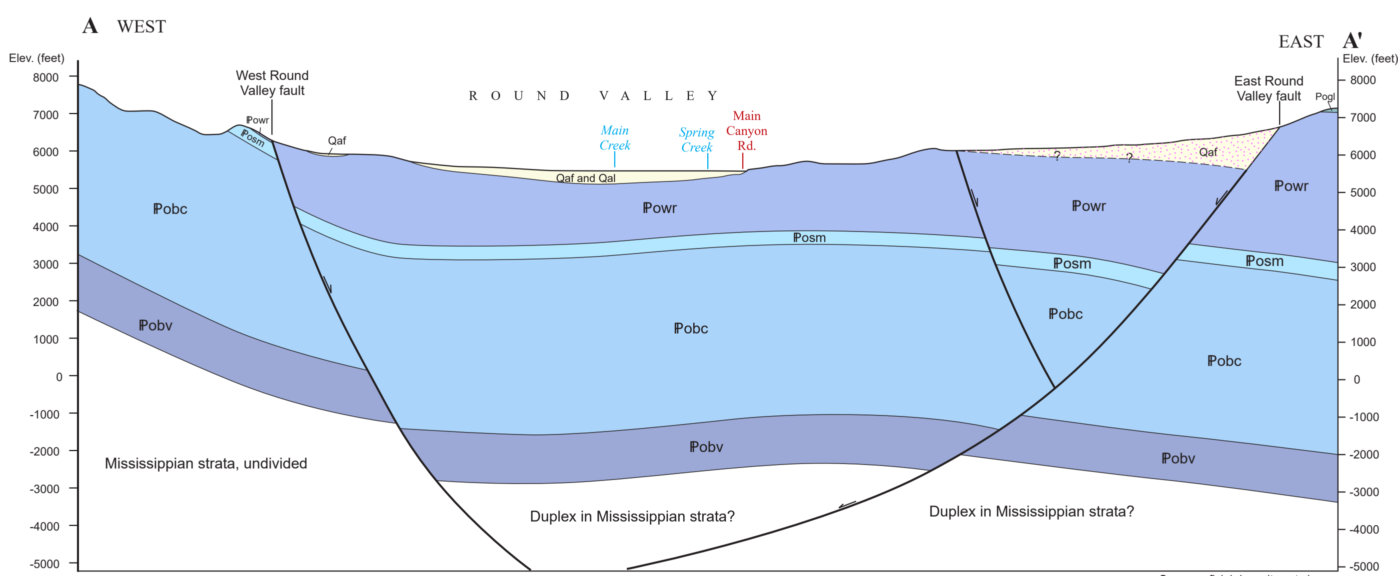

Figure 4. Geologic cross section of Round Valley, modified from Biek and Lowe (2009). This cross section is a truncated version of the original. Location of cross section shown on figure 3.

Roark and others (1991) investigated the hydrogeology of Heber and Round Valleys and initial estimated groundwater budget components for Round Valley. They estimated that the unconsolidated deposits receive 3 cubic feet per second (cfs) (85 L/s) of water from infiltrating precipitation and 5 cfs (142 L/s) of recharge from stream loss. They estimated that 115 wells were pumping approximately 0.2 cfs (6 L/s) of water from the aquifer in 1989.

In 2002, the Utah Department of Environmental Quality (UDEQ) released a Total Maximum Daily Load (TMDL) study for the Deer Creek Reservoir drainage, which includes Main Creek. UDEQ showed that although Main Creek makes up only 8% of the flow to Deer Creek Reservoir, it contributes 17% of the phosphorous load and 22% of the suspended sediment load to the reservoir (Psomas, 2002).

In 2007, the Provo River Watershed Council published the Wallsburg Coordinated Resource Management Plan (Wasatch Conservation District, 2012) due, in part, to the interest generated from the TMDL study. The plan ranked water conservation and water quality as the primary concerns for the watershed. Because of the plan, the Wasatch Conservation District initiated stream restoration on Main Creek in 2012. This restoration is ongoing and involves stabilizing the stream banks and creating meanders in the stream.

Many small-scale hydrologic studies have been conducted since the TMDL study and the management plan. In 2013, a rigorous stream geometry and flow measurement study was conducted, which continuously measured different segments of Main Creek (Allred Restoration and Bio-West, 2013). The study showed relatively high flows were from the forested area of the watershed and decreased rapidly downstream through the valley. Scientists at Brigham Young University (Johns and others, 2015; Pearce, 2017) examined spatial variation of phosphorous loading along the reaches of Main and Little Hobble Creeks, and concluded that much of the phosphorous concentration exists in the streams prior to intersecting agricultural lands, indicating a significant natural (possibly geologic) source of phosphorous.

Based on continuous gauging data from USGS station 0158500 recorded from October 1, 1938, to September 30, 1950, the average discharge of Main Creek was 13 cfs (368 L/s), ranging from close to zero to 152 cfs (4304 L/s) (U.S. Geological Survey, 2019). Discharge was highest from mid-April to mid-May, and lowest from August to October (figure 5).

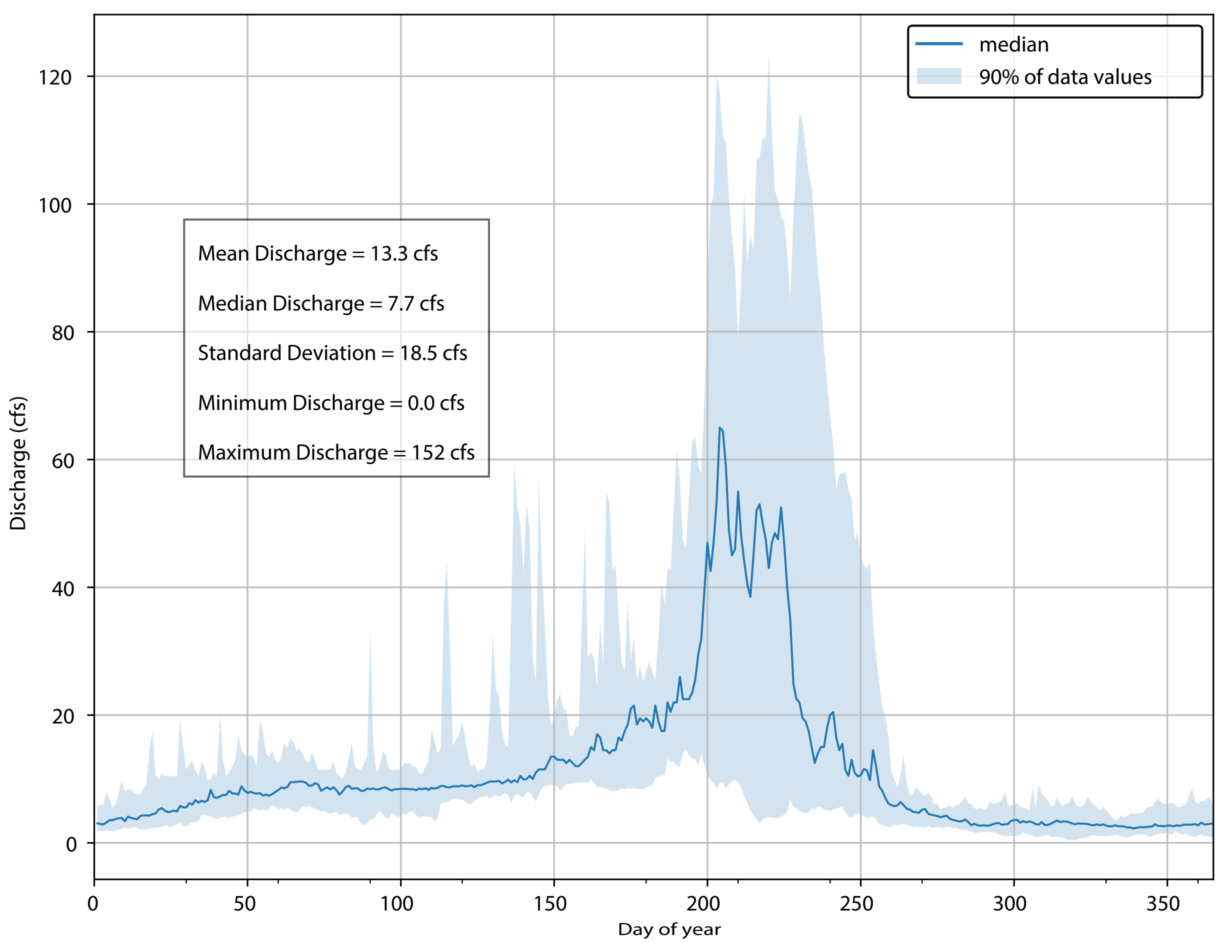

***Figure 5.** Daily median discharge data at USGS station 10158500 on Main Creek near U.S. Highway 189 from 10/1/1938 to 9/30/1950 (U.S. Geological Survey, 2019). The 90th percentile area (blue) covers 90 percent of all measured discharge values.*

METHODS

Water Chemistry

Water chemistry data were collected and compiled to characterize the water quality and type of groundwater in Round Valley. Chemistry data were used to compare surface water to groundwater, as well as bedrock groundwater to unconsolidated valley fill groundwater.

UGS Data

Water samples were collected for general water chemistry from five wells, one spring, and one stream in Round Valley (figure 6). General chemistry includes magnesium, calcium, sodium, chloride, potassium, bicarbonate, carbonate, and sulfate. The Utah Department of Health Laboratory analyzed all general chemistry samples. I measured field parameters using a handheld multiparameter probe and collected 44 stable isotope samples for 31 stream, 6 well, and 5 spring sites in the valley (figure 6; table 1). The University of Utah SIRFER laboratory conducted all the stable isotope analyses. Field parameters included specific conductance, temperature, and pH. For groundwater samples, oxidation-reduction potential (ORP) was measured. For each of the stream sites and the springs, discharge was measured along with the field parameters.

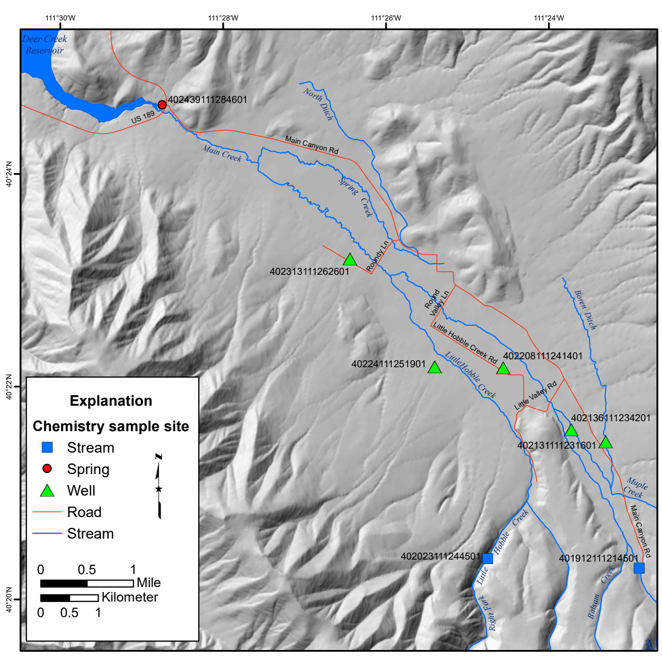

Figure 6. *Location of water samples taken for general chemistry analysis. Station identification number shown next to symbol. Hillshade base map and street data from the Utah Automated Geographic Reference Center (2019). See table 1 for field chemistry parameters of each site.*

Historical Data

I compared the results of the water chemistry analyses to compiled data from the Water Quality Portal (National Water Quality Monitoring Council, 2018), Utah Ambient Water Quality Monitoring System (AWQMS), Utah Safe Drinking Water Information System (SDWIS), and previous studies to compare to the analyses of the chemistry data. The Water Quality Portal (National Water Quality Monitoring Council, 2018) combines all data collected and recorded by the U.S. Geological Survey National Water Information System (U.S. Geological Survey, 2019) and the U.S. Environmental Protection Agency Water Quality Exchange, the primary clearinghouses for all federal water data. Utah AWQMS contains data collected by Utah regulatory agencies, including the Utah Division of Water Quality. Utah SDWIS contains water quality data of public water supplies not included in the Utah AWQMS database and not available from the Water Quality Portal. Data from previous studies includes water chemistry samples collected by Loughlin Water Associates for two studies in Round Valley, as well as data collected by the UGS for the National Groundwater Monitoring Network. The compiled data also included water chemistry analyses from the canyon to the south (South Fork), to compare Round Valley's groundwater chemistry to that of an adjacent drainage. Table 2 summarizes the compiled water chemistry samples and stations.

Data compilation took considerable effort, due to differences in how data were stored and collected. All data were processed using Python (vanRossum, 2014) and are available in detail online (Inkenbrandt, 2018). All fields (columns) in the different datasets were renamed for consistency and all concentration units were converted to milligrams per liter. For nutrient samples, all reported nitrate concentrations were converted to milligrams per liter as nitrogen and all phosphate concentrations were converted to phosphorus. For each sample containing all the major cations (sodium, calcium, magnesium, potassium) and anions (bicarbonate, carbonate, chloride, sulfate), I conducted a charge balance, which is a measure of how well the charges and concentrations of the ions balance. For samples without reported bicarbonate values but with carbonate alkalinity, I determined the relationship between alkalinity and bicarbonate for samples with measurements of both parameters and used it to estimate bicarbonate.

Septic Tank Density

The UGS has used septic-tank density analysis to help rural communities in Utah with land-use planning decisions (Lowe and Wallace, 1999; Wallace and Lowe, 1999; Lowe and others, 2000; Lowe and others, 2007). Septic-tank density analysis uses the mass-balance approach to estimate potential water-quality degradation as a function of the areal distribution of septic-tank systems. The mass-balance analysis uses nitrate, which is a conservative tracer commonly produced from septic system leachate as a contaminant. This mass-balance analysis can be applied as a first-pass planning tool

Table 1. *Water sample location and field chemistry parameters for each site. See figure 6 for sample locations.*

Station ID	Station Name	Type	Lat	Long	Site Visit Date & Time	Isotope Sample	General Chem Sample	Cont. Flow Gage	Specific Cond. (µS/cm)	Temp. (°C)	ORP (mV)[1]	pH	Q (cfs)[2]
402037111243401	Upper Rain Gage	Precip	40.3436	-111.4094	10/5/2016 12:00	1	0	0	<500				
402436111284101	Lower Rain Gage	Precip	40.4099	-111.4781	10/5/2016 13:00	1	0	0	<500				
402311111251601	Spring Creek	Spring	40.3864	-111.4213	8/15/2016 11:54	1	0	0	429	11.1	308	7.21	
402439111284601	State Park Spring	Spring	40.4109	-111.4793	8/23/2016 9:30	1	1	0	615	16	177	7.44	
402311111251601	Spring Creek	Spring	40.3864	-111.4213	9/19/2016 12:50	1	0	0	488	12.3		7.7	1.81
401747111250201	Upper Hobble seep	Spring	40.2964	-111.4174	9/21/2016 13:00	1	0	0	463	13.5	125	8.22	0.0001
402311111251601	Spring Creek	Spring	40.3864	-111.4213	10/5/2016 12:30	1	0	1	558	11.4		7.45	1.81
402310111260501	Main Creek @ Roundy Ln	Stream	40.3862	-111.4348	8/18/2016 11:30	1	0	0	370	16.3	195	8.17	0.01
402023111244501	Little Hobble FS	Stream	40.3401	-111.4123	8/18/2016 17:00	1	1	0	308	11.7	153	8.55	0.47
402051111241101	Left Fork Little Hobble Creek	Stream	40.3476	-111.4028	8/18/2016 17:30	1	0	0	500				0.04
402037111243401	Upper Little Hobble	Stream	40.3435	-111.4093	9/19/2016 11:00	1	0	0	234	8.62	234	8.62	
402019111225001	Upper Main Creek	Stream	40.3387	-111.3807	9/19/2016 12:00	1	0	1	343	9.6		8.75	1.14
402100111230301	Maple Creek	Stream	40.3501	-111.3840	9/19/2016 12:13	1	0	0	330	11.1		8.9	0.91
402435111284301	Lower Main Creek	Stream	40.4097	-111.4787	9/19/2016 14:02	1	0	1	433	17.9		8.37	2.96
401836111243601	Upper Little Hobble	Stream	40.3100	-111.4099	9/21/2016 12:30	1	0	0	424	12		7.27	0.004
401938111244801	Upper Little Hobble	Stream	40.3273	-111.4132	9/21/2016 14:30	1	0	0	412	10.2		8.67	0.13
402023111244501	Little Hobble FS	Stream	40.3401	-111.4123	10/5/2016 12:00	1	0	1	417	6.8		8.75	0.58
402435111284301	Lower Main Creek	Stream	40.4097	-111.4787	10/5/2016 13:15	1	0	0	498	14.4		8.48	1.85
402425111281101	Batty Springs	Stream	40.4069	-111.4697	11/2/2016 13:44	1	0	0	667	11.8		7.39	0.072
402051111241001	Left Fork Little Hobble Creek	Stream	40.3475	-111.4027	11/3/2016 8:50	1	0	0	405	4.1		8.92	0.6
402216111251401	Little Hobble Creek	Stream	40.3710	-111.4206	11/3/2016 13:00	1	0	0	410	8.3		8.44	0.26
402129111233501	Maple Creek	Stream	40.3582	-111.3931	11/3/2016 13:45	1	0	0	402	9		9.18	0.75

Table 1. *Continued*

Station ID	Station Name	Type	Lat	Long	Site Visit Date & Time	Isotope Sample	General Chem Sample	Cont. Flow Gage	Specific Cond. (µS/cm)	Temp. (°C)	ORP (mV)[1]	pH	Q (cfs)[2]
402046111222501	Maple Creek	Stream	40.3461	-111.3736	11/3/2016 12:00	1	0	0	326	5.6		9.06	
402435111284301	Main Creek	Stream	40.4097	-111.4787	11/2/2016 9:00	1	0	0	627	8.3		8	5.45
402423111282101	Main Creek	Stream	40.4063	-111.4724	11/2/2016 12:06	1	0	0	717	9.2		8.4	1.62
402407111273301	Main Creek	Stream	40.4021	-111.4593	11/2/2016 14:11	1	0	0	570	12.2		8.54	0.35
402342111264301	Main Creek	Stream	40.3949	-111.4453	11/3/2016 9:30	1	0	0	489	3.8		7.84	0.05
402310111260601	Main Creek	Stream	40.3862	-111.4349	11/3/2016 11:30	1	0	0	512	7.6		7.56	0.08
401940111244401	Right Fork Little Hobble Creek	Stream	40.3278	-111.4121	11/2/2016 13:30	1	0	0	385	7.4		8.75	0.77
401946111244401	Right Fork Little Hobble Creek	Stream	40.3294	-111.4122	11/2/2016 14:00	1	0	0	449	6.6		8.76	0.68
402035111243401	Right Fork Little Hobble Creek	Stream	40.3431	-111.4094	11/3/2016 9:30	1	0	0	387	4.4		9.11	0.87
402411111273201	Spring Creek	Stream	40.4030	-111.4589	11/2/2016 15:16	1	0	0	735	11.5		8.5	1.01
402323111255401	Spring Creek	Stream	40.3898	-111.4317	11/3/2016 10:40	1	0	0	521	4.2		8.08	0.04
402311111252101	Spring Creek	Stream	40.3863	-111.4226	11/3/2016 10:30	1	0	0	528	12.2		7.7	1.61
402306111260801	Unnamed Canal	Stream	40.3851	-111.4356	11/3/2016 11:00	1	0	0	539	5.2		8.02	0.88
402018111225101	Upper Main Creek	Stream	40.3384	-111.3807	11/2/2016 11:30	1	0	0	375	5.7		9.06	1.15
401912111214501	Upper Main Creek	Stream	40.3199	-111.3625	11/3/2016 14:40	1	1	0	346	5.7		8.89	1.23
402115111241001	Unnamed Spring Right Fork	Stream	40.3541	-111.4027	11/3/2016 10:00	1	0	0	539	10.1		7.97	0.02
402136111234201	Tom Clark	Well	40.3602	-111.3950	8/16/2016 16:15	1	1	0	352	17	223	8.18	
402408111262701	Joyce Mecham	Well	40.4022	-111.4410	8/17/2016 12:15	1	0	0	500				
402313111262601	Burman Well	Well	40.3870	-111.4400	8/17/2016 14:00	1	1	0	332	12.7	216	7.47	
40224111251901	Raby	Well	40.3701	-111.4230	8/18/2016 13:30	1	1	0	304	14.2	204	7.91	
402208111241401	Coffman Well	Well	40.3688	-111.4040	8/18/2016 14:30	1	1	0	316	14.8	237	7.46	
402131111231601	Gibb	Well	40.3585	-111.3880	8/23/2016 11:30	1	1	0	327	12.1	152	7.74	

[1] Oxidation-reduction
[2] Discharge

Table 2. Summary of compiled water chemistry samples and stations. "G.W." is groundwater, "AWQMS" is for the UDEQ Ambient Water Quality Monitoring System, "SDWIS" is for the Utah Division of Drinking Water Safe Drinking Water Information System, and "WQP" is for the Water Quality Portal.

Data Source	All Samples	All Stations	G.W. Samples	G.W. Stations
AWQMS	922	8	9	1
SDWIS	127	4	127	4
WQP	2605	40	65	18
Loughlin	3	3	3	3

that evaluates the possible impact of proposed developments. Because nutrients are an important issue in Round Valley, the mass-balance approach was used for this study.

The mass-balance approach adds projected nitrogen mass from increasing septic density to the existing nitrogen mass, diluting the total mass with available groundwater flow and water added by the septic-tank systems themselves. The following equation was used to calculate the projected nitrate concentration (Wallace and Lowe, 1999):

$$N_P = \frac{[(ST_T - ST_C)Q_{ST}] \cdot N_L + [N_A(Q_M + [ST_T \cdot Q_{ST}])]}{[ST_T \cdot Q_{ST}] + Q_M} \quad (1)$$

where:

N_P = projected nitrate concentration (mg/L)

N_L = estimated average nitrate concentration from each septic tank (mg/L)

N_A = ambient (background) nitrate concentration (mg/L)

ST_T = total number of septic tanks in the system (variable, unitless)

ST_C = current number of septic tanks (constant, unitless)

QS_T = flow from each septic tank (L/s)

Q_M = groundwater flow computed from the model (L/s)

For the calculation, I assumed an average of three people per septic tank and used the basin fill area of 1813 acres, which is the area of the alluvium in the valley fill material (figure 3). I assumed indoor water use was 60 gallons (227 L) per person per day, and that nitrogen output was 17 grams per person per day, 15% of which was estimated to be ammonia. Groundwater flow is between 11 and 20 cfs (311–566 L/s), based on Darcy flux calculations and estimates provided in previous work (Roark and others, 1991).

Groundwater Levels

Depth to water in wells was measured in the field and the data were used to create a potentiometric surface map. Existing depth-to-water data were compiled from the USGS and the Utah Division of Water Rights (UDWRi) to examine seasonal and long-term groundwater-level fluctuations, as well as regional groundwater-level trends.

Local Analysis–UGS Data

Depth to water in 70 wells was measured from August 16, 2016 to August 25, 2016 (table 3). For each well, I measured the depth to water from the top of the well casing, the height of well stickup above (and in some cases below) ground surface, the type and diameter of well casing, and location information from a recreational-grade global positioning system unit (Garmin Oregon 450). A Slope brand slim-profile electric water-level indicator was used for all water-depth measurements. When possible and if available a well driller's report provided geologic descriptions and depth to screened intervals.

Groundwater-level measurements were conducted in late August to measure the base conditions of groundwater levels without the influence of precipitation. However, late August is a time when groundwater is pumped to water crops and yards. If the well was actively pumping, I either noted the pumping activity or asked the well owner to shut off the well and waited for the water level to stabilize. Groundwater levels from wells that were actively pumping were not used in the interpolation for the potentiometric surface maps but were measured and retained in case pumping influence needed to be accounted for in nearby non-pumping wells.

Field location data were verified using high-resolution aerial photography taken in 2016 and provided by Google^{TM}. The verified information provided locations for ground-surface elevation from the USGS 3DEP program (U.S. Geological Survey, 2015), which has 10-meter horizontal resolution in Utah and better than 6.6-foot (2 m) vertical accuracy in most low-relief areas (Gesch and others, 2014). To derive the water-level elevation, I subtracted the depth to water from the ground-surface elevation derived from the USGS dataset.

Groundwater elevations were interpolated using ArcGIS scripts to create a contour map of the potentiometric surface. Wells that were actively pumping at the time of measurement were not used. For the interpolation, unconsolidated material and underlying bedrock were assumed to be hydraulically connected, based on the fractured nature of the bedrock and lack of correlative and continuous confining layers in the unconsolidated sediments in the well drillers' records (table 3). This assumption is necessary because interpolating groundwater levels from two different aquifers would imply that the potentiometric surfaces from the two aquifers are the same, which is generally not the case.

Table 3. *Data for Round Valley wells used to construct the groundwater-elevation map (figure 21).*

ID	USGS Station ID	UTM X (m)	UTM Y (m)	Ground Elevation (ft)	Date Water Level Measured	Depth to Water from Ground Surface (ft)	Water Level Elevation (ft)	WIN[1]	Depth to Top of Screen (ft)	Open Interval Lithology	Well Depth (ft)	Level Date	Depth to Water (ft)	Link
1	402429111275000	460,594	4,473,121	5492	8/16/2016	40.2	5452	33042		Bedrock	150	6/15/1974	20	http://bit.ly/2fFNoed
2		464,280	4,470,522	5673	8/16/2016	14.6	5658			Bedrock	240	9/28/1994	14	http://bit.ly/2frJ84a
3		466,464	4,467,813	5964	8/16/2016	80.4	5884		275	Bedrock	305	7/15/1999	52	http://bit.ly/2ggdYdK
4		466,537	4,467,730	5974	8/16/2016	60.4	5914	11281	60	Valley Fill	180	11/16/1995	18	http://bit.ly/2gmjKM6
5	402151111233601	466,549	4,468,255	5960	8/16/2016	42.7	5918	33269	120	Bedrock	165	4/18/1974	30	http://bit.ly/2gmc6l1
6	402459111270501	461,633	4,474,058	5567	8/17/2016	29.7	5538							
7		462,608	4,472,749	5586	8/17/2016	16.8	5570	14422		Valley Fill	114	9/29/1990	20	http://bit.ly/2gBAbr1
8		462,606	4,472,494	5559	8/17/2016	<-2	>5561	30752	80	Valley Fill	100	2/12/1980		http://bit.ly/2ggbg7R
9	402356111260901	463,038	4,472,094	5581	8/17/2016	2.9	5578	25438	160	Bedrock	180	6/20/2002	15	http://bit.ly/2fFOLcU
10		462,021	4,472,901	5571	8/17/2016	26	5545							
11		462,277	4,472,869	5571	8/17/2016	26.1	5545		115			5/5/1977	24	http://bit.ly/2gBB2aU
12		462,617	4,470,803	5620	8/17/2016	83.5	5537	21320	250	Bedrock	290	1/21/2000	75	http://bit.ly/2fpi1DC
13		461,891	4,470,767	5719	8/17/2016	191.5	5528	438759	300	Bedrock	400	7/6/2015	194	http://bit.ly/2ghtvO0
14		461,647	4,471,061	5706	8/17/2016	178	5528	15954	150	Bedrock	183	6/10/1997	110	http://bit.ly/2fFXJXf
15	402342111263501	462,302	4,471,703	5548	8/17/2016	4.2	5543							
16		463,035	4,472,690	5619	8/17/2016	53.5	5565							
17		459,902	4,472,949	5451	8/18/2016	5.3	5446	33999		Valley Fill	92	5/16/1971	1	http://bit.ly/2fFWwzu
18	402416111265201	461,943	4,472,772	5558	8/18/2016	18.9	5539	24771	60	Valley Fill	102	1/25/2002	21	http://bit.ly/2frEQdd
19		464,217	4,469,808	5690	8/18/2016	86.2	5604	3400	200	Bedrock	220	7/12/1993	18	http://bit.ly/2fRHJ7H
20		463,972	4,469,605	5690	8/18/2016	10.1	5680		57	Valley Fill	71	7/15/1971	5	http://bit.ly/2gBvv46
21		463,579	4,469,005	5805	8/18/2016	33.5	5772	2592		Valley Fill	80	4/21/1993	31	http://bit.ly/2ggbqME
22		464,123	4,468,926	5761	8/18/2016	137.5	5624	9126	280	Valley Fill	321			http://bit.ly/2gmkKjv
23		465,677	4,468,406	5861	8/18/2016	41	5820	13120	220	Valley Fill	240	10/10/1996	17	http://bit.ly/2frGcoj
24		465,586	4,468,805	5831	8/18/2016	35.9	5795	33755		Valley Fill	169	3/23/1972	40	http://bit.ly/2fpg4qN
25		465,276	4,468,827	5808	8/18/2016	32.2	5775	31509	141	Valley Fill	153	5/5/1978	35	http://bit.ly/2ggiYir
26		464,870	4,469,057	5762	8/18/2016	25.1	5737	28941	200	Valley Fill	220	3/27/1986	35	http://bit.ly/2fFZPX6
27		467,078	4,467,617	6097	8/23/2016	86.5	6010	9724	80	Bedrock	108	7/15/1995	68	http://bit.ly/2fFYIac
28		467,456	4,466,581	6180	8/23/2016	27	6153		40	Valley Fill	105	11/14/1990	27	http://bit.ly/2fG2mAH
29		467,601	4,466,708	6214	8/23/2016	72.5	6141	16065	100	Valley Fill	150	6/30/1997	94	http://bit.ly/2ggbcVT
30		467,549	4,466,969	6201	8/23/2016	79.3	6122	14537	90	Valley Fill	140	12/1/1997	92	http://bit.ly/2g47tLR
31		467,552	4,466,842	6202	8/23/2016	70	6132	15973	100	Valley Fill	150	6/20/1997	92	http://bit.ly/2gBAx0t
32		467,465	4,466,217	6200	8/23/2016	14.5	6186	427134	65	Valley Fill	140	8/20/1970	15	http://bit.ly/2ggeZTd
33		465,742	4,466,400	6113	8/23/2016	99.4	6013	24211	255	Bedrock	360	4/22/2004	97	http://bit.ly/2ghqmxy
34		465,582	4,466,555	6130	8/23/2016	118.4	6012	7008	122	Bedrock	450	12/13/1994	135	http://bit.ly/2frNWXk
35		465,751	4,467,419	5974	8/23/2016	120.7	5853	9819	300	Bedrock	340	9/1/1995	160	http://bit.ly/2frPUqP
36		465,595	4,467,537	5931	8/23/2016	80.9	5850		150	Bedrock	190	5/30/1996	73	http://bit.ly/2gBxbuq
37		465,521	4,467,715	5901	8/23/2016	76.3	5825		110	Bedrock	266	6/27/1997	60	

Table 3. *Continued*

ID	USGS Station ID	UTM X (m)	UTM Y (m)	Ground Elevation (ft)	Date Water Level Measured	Depth to Water from Ground Surface (ft)	Water Level Elevation (ft)	WIN[1]	Depth to Top of Screen (ft)	Open Interval Lithology	Well Depth (ft)	Level Date	Depth to Water (ft)	Link
38		458,378	4,474,520	5544	8/23/2016	128.5	5415		189	Valley Fill	209	3/31/1998	120	http://bit.ly/2g44WkR
39		462,798	4,473,653	5687	8/24/2016	116.4	5571	30721	125	Bedrock	155	6/9/1980	105	http://bit.ly/2fFTD1t
40		465,175	4,471,905	6040	8/24/2016	90.8	5949	31330		Bedrock	125	7/6/1979	89	http://bit.ly/2gmofX6
41		466,441	4,467,280	6039	8/24/2016	9.3	6030	29660	50	Bedrock	110	10/10/1991	15	http://bit.ly/2gmoAsw
42		466,394	4,467,509	5986	8/24/2016	105.6	5880	434898	210	Bedrock	376	7/8/2011	119	http://bit.ly/2gBDEG3
43		467,628	4,469,458	6311	8/24/2016	138.4	6173	28277	160	Valley Fill	200	9/17/1987	108	http://bit.ly/2fphj9r
44		467,300	4,469,527	6210	8/24/2016	82.4	6128	28604	140	Valley Fill	200	11/13/1988	70	http://bit.ly/2fppgvs
45		466,421	4,468,645	5937	8/24/2016	72.3	5865	7639	270	Bedrock	290	10/24/1994	62	http://bit.ly/2ggh0yv
46		467,029	4,467,884	6080	8/24/2016	80.6	6000	10974	100	Valley Fill	227	12/4/1995	72	http://bit.ly/2g438Ip
47	402350111240001	466,280	4,471,919	6233	8/24/2016	174.3	6059	9708	165	Bedrock	240	7/17/1995	170	http://bit.ly/2g49pDW
48		466,486	4,470,460	6087	8/24/2016	69.1	6018	10963	120	Valley Fill	230	11/20/1995	70	http://bit.ly/2gghMf5
49	402301111240001	466,000	4,470,387	5967	8/24/2016	31.9	5935	431239	154	Bedrock	206	4/21/2008	25	http://bit.ly/2fRNkeg
50		466,054	4,470,467	5993	8/24/2016	8.1	5985	31634	125	Valley Fill	201	6/10/1978	1	http://bit.ly/2g4aI5E
51		465,763	4,469,926	5858	8/24/2016	130.6	5728	24831	134	Both	200	2/25/2002	130	http://bit.ly/2ggcVul
52		466,031	4,469,849	5911	8/24/2016	30.4	5881	11100	100	Valley Fill	207	12/18/1995	17	http://bit.ly/2gmjH2N
53		465,703	4,469,994	5849	8/24/2016	130.1	5719	25711		Bedrock	202	8/9/2002	131	http://bit.ly/2f74HZq
54		465,616	4,469,852	5826	8/24/2016	108.1	5718	430684	80	Bedrock	162	10/17/2007	116	http://bit.ly/2gghUev
55		465,858	4,468,246	5886	8/24/2016	66	5820	27590	100	Bedrock	340	7/3/2003	100	http://bit.ly/2frKH24
56		465,149	4,468,812	5797	8/24/2016	12.6	5784	27918	200	Valley Fill	123	9/9/2003	15	http://bit.ly/2fRREdn
57		463,330	4,469,247	5764	8/24/2016	105.5	5658	32823		Bedrock	123			http://bit.ly/2fRRTVF
58		460,815	4,473,209	5502	8/25/2016	32.1	5470	16643		Valley Fill	80	11/15/1997	24	http://bit.ly/2fG2pfK
59		460,720	4,473,070	5491	8/25/2016	35.2	5455				65			
60		460,851	4,473,170	5499	8/25/2016	32.5	5466	32412	98	Bedrock	122	10/15/1974	22	http://bit.ly/2frQ7tY
61		465,526	4,469,749	5805	8/25/2016	75	5730		140	Bedrock	170	9/20/1988	67	http://bit.ly/2fRYFe2
62	402129111242001	465,501	4,467,616	5943	8/25/2016	89	5854	15964		Bedrock	230	6/27/1997	60	http://bit.ly/2fRSiYj
63	402235111252000	464,053	4,469,590	5694	8/25/2016	24.5	5670	16173	190	Bedrock	220	7/28/1997	9	http://bit.ly/2f7aPkm
64		464,369	4,469,044	5737	8/25/2016	26.3	5711	10097				9/11/1995	9	http://bit.ly/2ghtE3S
65		465,161	4,468,167	5839	8/25/2016	35.4	5804	428812	70	Bedrock	120	11/16/2006	21	http://bit.ly/2gghzse
66		466,232	4,468,494	5906	8/25/2016	66.3	5840	16571	198	Bedrock	238	11/8/1997	20	http://bit.ly/2f7auhz
67		465,235	4,468,014	5870	8/25/2016	42.9	5827	10105	50	Valley Fill	90	11/8/1995	20	http://bit.ly/2fG0NmB
68		462,205	4,470,943	5631	8/25/2016	99	5532	431954	231	Bedrock	470	2/2/2009	93	http://bit.ly/2gmoKAx
69		464,872	4,469,333	5751	8/25/2016	49.7	5701	30961	80	Valley Fill	100	6/25/1980	15	http://bit.ly/2fpiXYL
70		457,153	4,473,445	5601	8/23/2016	181	5420		205	Bedrock	250	10/22/1974	195	http://bit.ly/2ggiLvt

[1] *Utah Division of Water Rights Well Identification Number*

Interpolation of groundwater elevations assumes that the water measured in wells is connected between the wells, and the wells are not tapping separate, disconnected aquifer systems. Hydraulic connection between the fractured underlying bedrock and overlying unconsolidated material is supported by the observation that adjacent wells screened in different hydrogeologic materials have similar groundwater elevations.

Empirical Bayesian kriging (EBK) was applied to interpolate groundwater-level elevations. The EBK interpolation technique is a robust geostatistical technique that is appropriate for interpolating relatively small datasets. Kriging is a geostatistical technique that assumes that variables have spatial relations that can be modeled, that objects nearer to each other have properties with greater correlation than objects farther apart, and that the relation between correlation and distance can be modeled. The model can be used to create a more accurate interpolation. The relation of correlation with distance can be plotted using a semivariogram, which is created by plotting distance between each point (i.e., wells) on the horizontal axis and the difference squared of the spatially relatable variable (i.e., water levels) between every point in the dataset on the vertical axis. Kriging models a curve that is fit to the semivariogram to model spatial variation over distance. Geostatistical techniques allow the estimation of a standard error of an interpolated prediction raster (Webster and Oliver, 2001; Hengl, 2007). Geostatistical techniques are more effective if the interpolated data follow a normal distribution and have a defined semivariogram. Kriging generally requires data having a known statistical distribution to properly interpolate the data, requiring transformation of the interpolated data to match known distributions (Hengl, 2007). EBK is a kriging technique that automatically builds the geostatistical model by subsetting the interpolated dataset and generating hundreds of simulations (Clayton and Kaldor, 1987; Hengl, 2007). The Round Valley groundwater level data are appropriate for this technique because they have a normal distribution and groundwater levels are spatially correlateable.

The EBK interpolation produced a raster (gridded cells) of the potentiometric surface and a raster of standard error. I contoured the potentiometric surface raster and smoothed the resulting contours using the ArcGIS default line-smoothing tool and then clipped the contours to the areal extent of the measured wells. The settings used for the EBK tool include a K-Bessel detrended semivariogram model and log empirical transformation, which were used because they are the most robust settings for interpolating input. The drawback to K-Bessel detrended modeling is that it is the most processor-intensive settings for the tool. The first-order trend in the case of the water levels is the general east-west gradient of topography and groundwater gradient in the region. Cokriging and simple kriging (other geostatistical techniques) produced similar interpolation trends as EBK, but with larger error.

Aspect and slope analyses were conducted on the resulting EBK potentiometric surface raster. The aspect quantifies the compass direction of greatest curvature of a surface. The slope indicates the magnitude of the hydraulic gradient. The slope and aspect of the potentiometric surface raster can imply the magnitude and direction of groundwater flow, specifically Darcy velocity, assuming homogeneous and isotropic hydraulic conductivity throughout the study area.

Temporal Analysis–USGS Data

Trends in the USGS water-level data (U.S. Geological Survey, 2019) were examined to determine how groundwater levels have varied seasonally since the 1950s. Because long-term data for Round Valley are sparse, I examined groundwater variations in the greater region of the Provo River watershed (HUC 16020203) (figure 7) which has areas with similar development, groundwater, and climate settings as Round Valley (Baker and Peterson, 1970). To visualize the regional water-level variations, all water-level measurements in the Provo River watershed were standardized and then aggregated by taking their average and median values. Standardization removes the arbitrary datum using the mean depth to water from a well's time series, putting the focus on the average changes in depth to groundwater. Water levels in each well were standardized by subtracting the mean depth to water of the period of record for that well from each depth-to-water measurement of that well. I then averaged all the standardized water levels from all the wells for specific time bins.

To plot standardized seasonal variations in groundwater level, all groundwater-level data (U.S. Geological Survey, 2019) for the Provo River watershed were downloaded, which consisted of 6153 measurements from 442 wells. Next, the depth-to-water level in each well was standardized. From the 442 wells, 138 wells were used in the analysis, 16 wells had only 2 measurements and 45 wells had more than 30 measurements; the remaining 77 wells had 2 to 30 measurements. I subtracted each depth-to-water measurement from each well's mean depth to water to determine the difference from mean depth to water of each well. I then averaged the difference of mean depth to water for all the wells for each month and plotted the data to display the average monthly difference from mean depth to water.

For long-term data, I further filtered the data by analyzing only wells having measurements spanning more than four years. Using the same standardization techniques as the monthly plots, I lumped standard water levels into yearly bins and plotted long-term changes in water levels for the Provo River watershed.

Only nine wells in Round Valley had more than one measurement. I plotted the water-level data in the valley by well for visual assessment. No standardization was applied to these water levels for the plots. The USGS recorded all the measurements in the late 1980s.

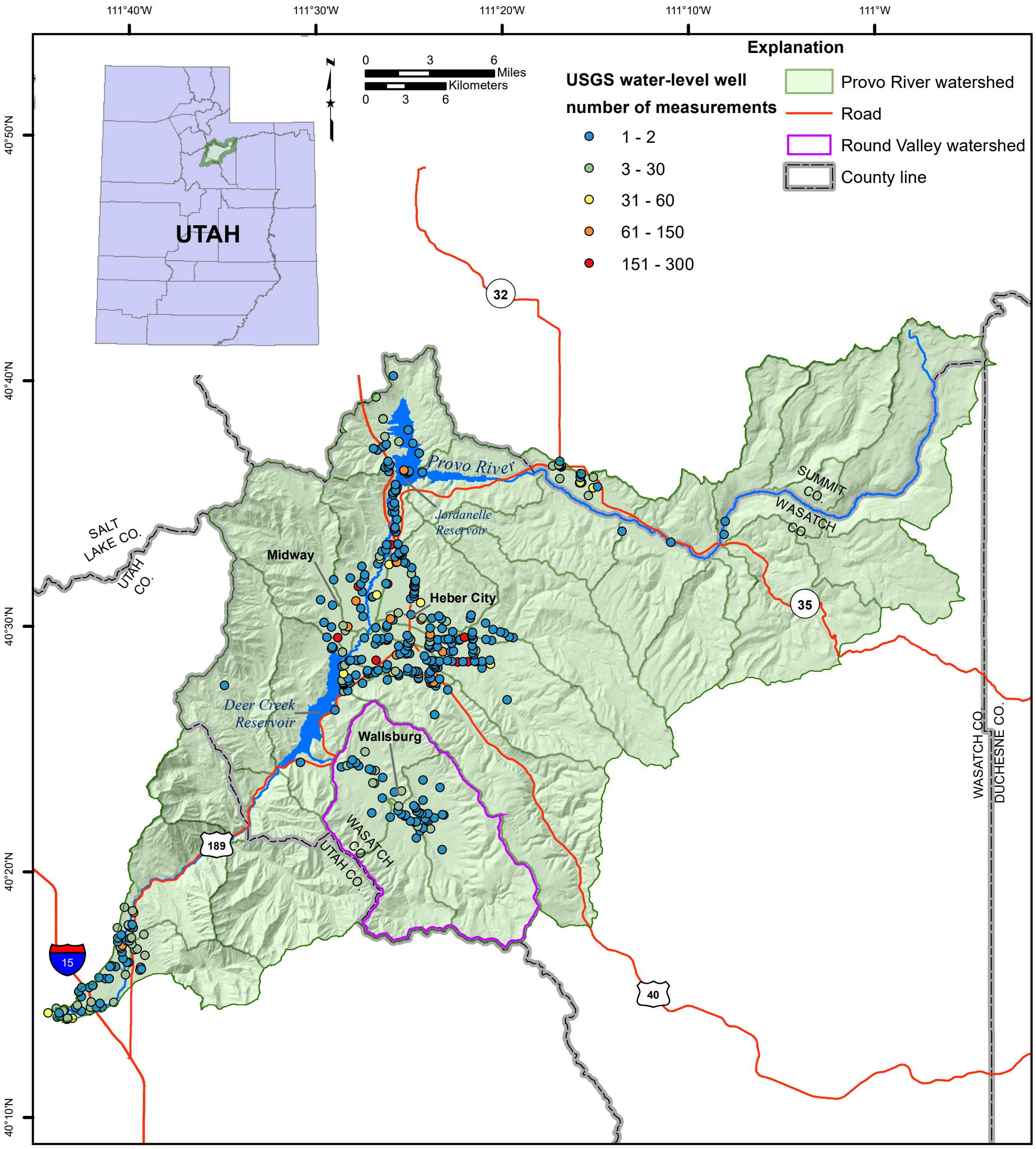

Figure 7. Extent and location of Provo River watershed and USGS wells used for regional groundwater-level statistics.

Regional Analysis–Utah Division of Water Rights Data

To better understand the general groundwater-flow directions between surrounding valleys, groundwater-level elevations from well drillers' records obtained from the UDWRi were compiled and interpolated. I tabulated data for 772 wells in the region using scanned well drillers' logs accessed from the UDWRi webpage. The tabulated depth-to-water data from the drillers' records were joined to the geographic information system point file, named "wrpod," that shows all the UDWRi points of diversion (Utah Division of Water Rights, 2018). The depth to water and the "wrpod" tables were joined using each well identification number (WIN). Elevation was assigned to each well using the data from the USGS 3DEP program, which provides elevation data that have 33-foot (10 m) horizontal resolution and a vertical root mean square error of 5 feet (1.55 m) (Gesch and others, 2014; U.S. Geological Survey, 2015). I determined water-level elevation by subtracting the depth to water reported on the well drillers' reports from the ground-surface elevation derived from the USGS elevation data.

The data were filtered for outliers before I interpolated the groundwater-level elevations. I plotted the wells on a normal quantile-quantile (Q-Q) plot and used a semivariogram to remove spatial outliers. Outliers deviated from the quantile-quantile line (figure 8) or fell outside of the semivariogram cluster (figure 9). Of the 772 water-level elevations, 45 were considered outliers and removed from the dataset. Most of the measurements considered outliers were higher water-level elevations, which could indicate a separate or perched aquifer system for these wells.

The data were interpolated after tabulating and filtering. Similar to the UGS data, I interpolated the UDWRi data using the EBK geostatistical interpolation technique. The interpolation assumes that groundwater levels near each other are more similar than those separated by greater distances, which implies that the wells are in the same or hydraulically connected aquifer(s). The resulting interpolation is a representation of the average groundwater levels from 1959 to 2012, which is the range of years for available groundwater-level measurements.

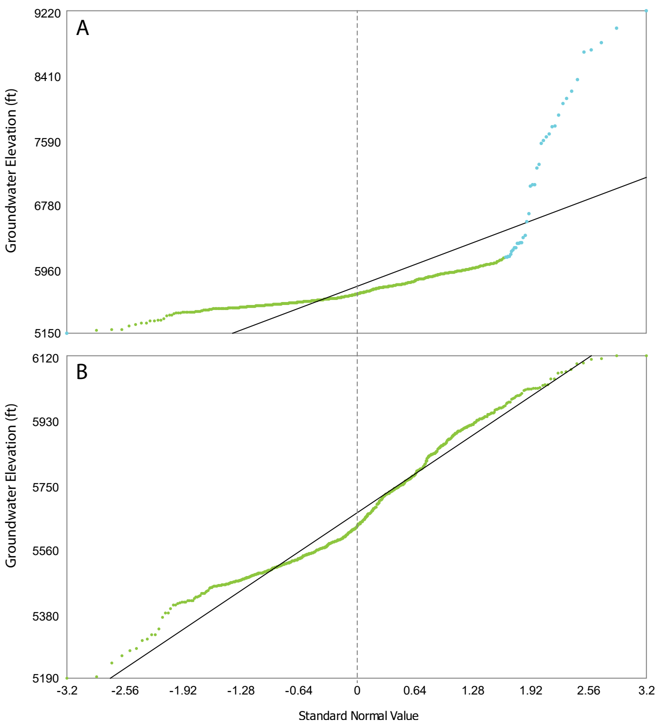

***Figure 8**. Normal Q-Q plots for the regional groundwater-elevation data **A.** prior to outlier (blue dots) removal, and **B.** after outlier removal. Note that normally-distributed data will follow the line closely and are required for kriging.*

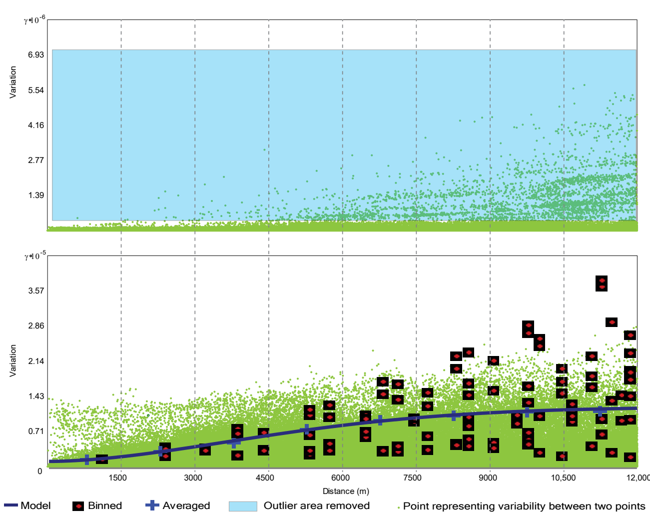

***Figure 9**. Semivariograms before (top) and after (bottom) removal of outliers (blue box). The bottom semivariogram shows the binned and averaged values of the data, as well as a simple kriging model fit to the data.*

Stream and Spring Discharge

Historical Data

I compiled historical stream discharge data from the USGS, a consultant's report (Allred Restoration and Bio-West, 2013), and the UDEQ. From October 1, 1938, to September 29, 1950, prior to the filling of Deer Creek Reservoir, the USGS operated stream gage 10158500 on Main Creek near the intersection with Highway 189 at the mouth of Round Valley. I examined the 0.50, 0.05, and 0.95 quantiles of discharge by day of year. An Eckhardt (2005) baseflow separation was conducted on the discharge data using an alpha (recession) value of 0.997 and a base flow index (BFI) of 0.80.

Existing UDEQ data were also compiled. The UDEQ collected hourly stage data on Main Creek about 0.25 miles (0.4 km) upstream from the old USGS gage from April 2015 to June 2016. UDEQ also periodically measured discharge of Main Creek at or near the location of the stage measurements.

The UDEQ stage measurements used a nonvented transducer submerged in the creek at a bridge. Because the transducer was nonvented, its readings include both the height of water above the transducer's reference point and the local barometric pressure. Using barometric pressure data from the Heber Airport weather station (KHCR), I removed the barometric component from the total pressure measurements of the nonvented transducers. Barometric pressure was removed by determining the linear relationship between the transducer readings and the barometric pressure readings and then subtracting that relationship from the transducer readings. I used the robust fitting of linear models algorithm (rlm) to determine the relationship between the two datasets, which ignored large outliers (Ronchetti, 2009) to produce a slope of 0.71 feet (0.22 m) of water head change per foot (0.3 m) of water change at the barometer and an offset of 8 feet (2.4 m) of water.

A stage-discharge relationship was established by matching manual discharge measurements to the closest recorded stage measurement of the transducer. To determine the stage-discharge value, I used an optimization script to fit an exponential equation to the stage measurements:

$$Q = ax^b + c \qquad (2)$$

where:

Q = discharge (cfs)

a, b, c = parameters varied to fit the equation x = stage (ft)

The stage data were converted to estimated discharge using the parameters from the optimization.

The estimated discharge data provided the means to estimate baseflow contribution to streamflow. Baseflow represents the groundwater component of streamflow and is generally assumed to be the local minima of the discharge hydrograph curve. I removed discharge spikes that were concurrent with temperatures that fell below freezing. Finally, the data were smoothed using a daily mean and the baseflow was found using the Eckhardt (2005) technique, an alpha of 0.997 and a BFI of 0.90.

UGS Data

Four non-vented transducers were deployed throughout Round Valley to determine various streamflow contributions over time (figure 10). One transducer was installed on the main trunk of Main Creek (MC1), one on Little Hobble Creek (RF2), one on upper Main Creek (UM5), and one on Spring Creek (SC3) near the spring head. At each site, the transducer was secured in a consistent location that limited lateral and vertical movement. Periodic manual discharge measurements were recorded using transects across the profile of the stream with a Hach stream velocity meter. For Little Hobble Creek, a method as described for the UDEQ data was applied. For Spring Creek, the parameters in the equation were optimized for flow in a culvert to the stage data to match manual measurements (Isenmann and others, 2016):

$$Q = 0.5^{h} \cdot h^{2.175} \cdot 0.716 \cdot \sqrt{32.2 \cdot \left(\frac{d}{12}\right)^{6}} \tag{3}$$

where:

Q = culvert discharge (cfs)

h = depth of water (feet)

d = diameter of culvert (in)

Upper Main Creek (UM5) was in a diversion that became clogged and unclogged over several instances, causing the geometry of the measured section to change frequently and making the transducer data useless.

Lower Main Creek (MC1) manual measurements were limited to low-discharge events. To correct the stage data, I correlated USGS gage data at Daniels Creek (10157500) to manual discharge measurements recorded by the UDEQ and the UGS at the mouth of Main Creek (figure 11A and B). Daniels Creek is the adjacent watershed immediately to the north of the Main Creek watershed and has a similar drainage area and similar characteristics. Using that relationship, I modeled discharge of Main Creek (MC1) and determined the relationship between the modeled discharge and the measured stage values (figure 11C and D). That relationship was used to adjust the stage readings to better estimate the high discharges of Main

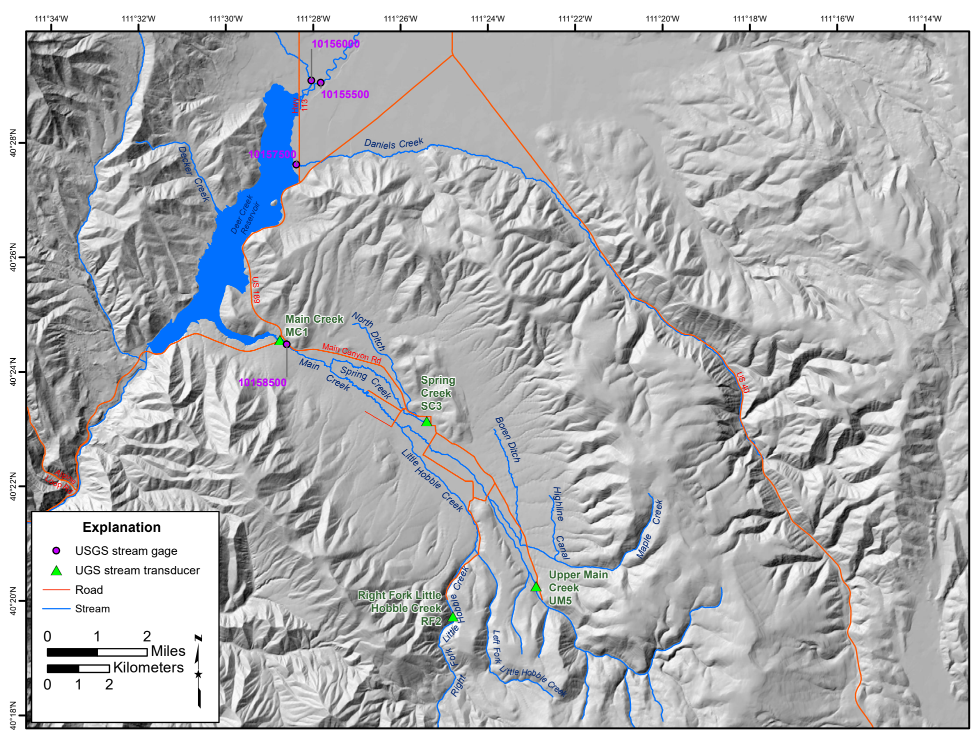

Figure 10. Location of continuous discharge monitoring points. The numbers are USGS station identification numbers. Hillshade base map and street data from the Utah Automated Geographic Reference Center (2019).

Creek (figure 11E).

The UGS Wetlands group conducted a spring survey of mountain springs within the U.S. Forest Service boundaries of the Round Valley watershed during this study. They verified existing Utah Division of Water Rights points of diversion, measuring flow and updating locations where possible. They verified a total of 71 streams, ponds, and springs in the watershed.

Well Data

Detailed information was collected for 211 wells in Round Valley and along Deer Creek Reservoir where Main Creek enters. Data were compiled from the UDWRi and included well screen depth, depth to water, casing material and extent, lithology, construction information, and specific capacity information. Because some wells were drilled prior to the establishment of record keeping by the UDWRi, there likely are wells in the valley that have not been accounted for by these records. I used the information I tabulated to create cross sections, check depth to water, and estimate aquifer transmissivity (see below).

Cross Sections and Basin Depth

Five cross sections across the unconsolidated sediments of Round Valley were created using a combination of well logs (Utah Division of Water Rights, 2018), digital elevation data (U.S. Geological Survey, 2015), and geologic maps (Biek and Lowe, 2009; Constenius and others, 2011). I produced cross sections by connecting locations of wells on a map of available well logs, going point to point, so the cross sections do not follow exact straight-line paths (plate 1). Elevation and coordinates were assigned to points at 33-foot (10 m) intervals along each line.

Subsurface information came from 211 well logs compiled from the UDWRi (2018). For each well log, I assigned the driller's interpretation of geologic material to one of six categories: bedrock, clay, clay with boulders, gravels and sand, sand-cobbles-boulders, and soil. The simplified geology was added to each cross section, as well as well construction information if available. Geologic units from mapping (Biek and Lowe, 2009; Constenius and others, 2011) were also simplified into five different units: coarse stream alluvium (Qal), clay-rich stream deposits (Qal–Clay), alluvial-fan de-

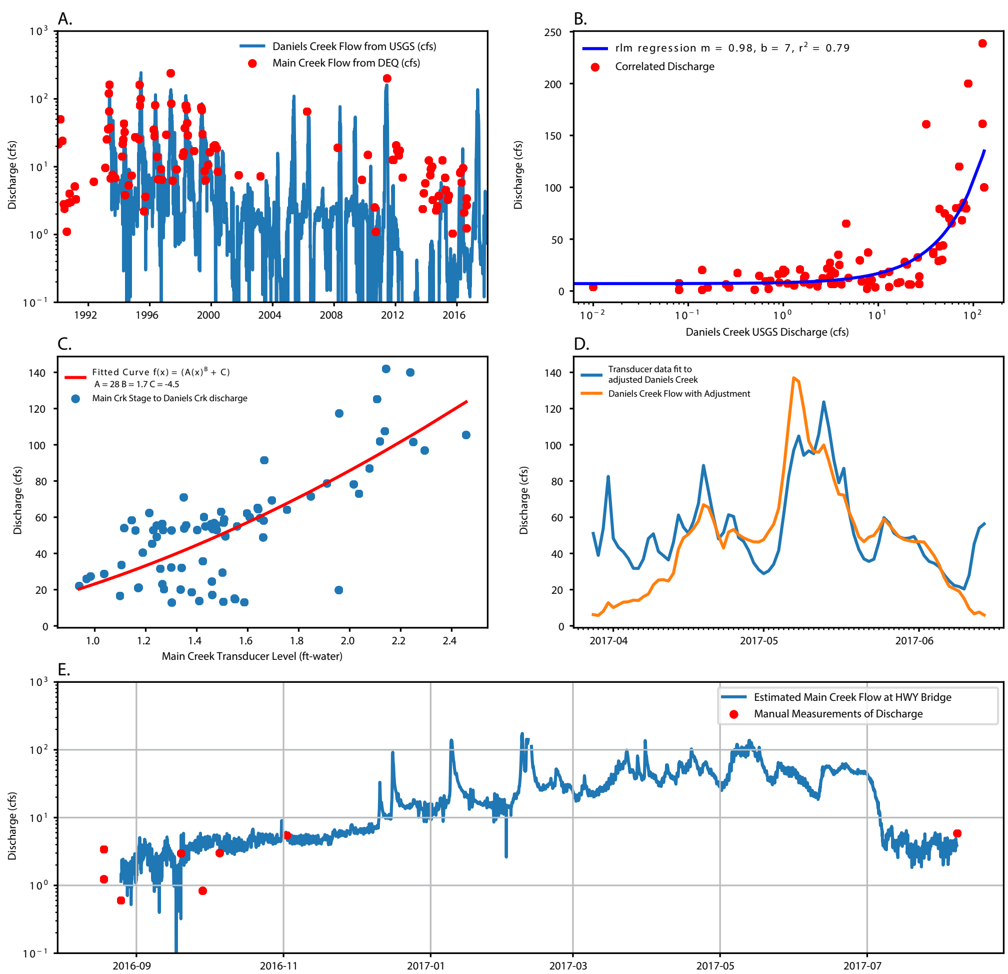

***Figure 11.** Process to estimate flow at Main Creek. Plots **A.** and **B.** define the relationship between Main Creek discharge and Daniels Creek discharge. Plots **C.** and **D.** define the relationship between Main Creek discharge and transducer readings; plot **E.** is the resulting output.*

posits (Qaf), the Granger Mountain Member of the Oquirrh Formation (Pogm), and the Wallsburg Ridge Member of the Oquirrh Formation (IPowr). Wells with descriptors containing the words *fractured*, *hardpan*, and *quartzite* were commonly grouped into bedrock depending on the context of the log. Next, I interpreted and correlated the grouped units between the well logs to the contacts on the map.

A depth-to-bedrock map was also created by interpreting depth to bedrock from each of the 98 logs of wells that reportedly penetrated bedrock. To constrain where the basin fill thins and bedrock is exposed at the surface, I added points to the contacts between the unconsolidated material and bedrock on the geologic maps, assigning land surface elevations at these points. The points were interpolated using similar methods as described in the water level section.

Hydrologic Budget Estimates

The UGS's Utah Basin Model (UBM) was the primary means for estimating large water budget components of the Round Valley watershed. The UGS created the UBM using conceptual and analytical techniques derived from the USGS Basin Characterization Method (BCM), which has been applied to most of the western parts of Utah (Flint and others, 2004; Flint and Flint, 2007; Heilweil and Brooks, 2011; Thorne and others, 2012). The UGS created the UBM because the USGS did not provide the script framework for the BCM and did not publish results from the BCM for areas outside of the Great Basin. The UBM uses a monthly water-soil-balance model to determine evapotranspiration, runoff, recharge, and soil water. This method is presently untested and uncalibrated but produces a first-pass estimate of major budget components.

Soil-Water Balance

A soil-water balance model was created for the Round Valley basin for the years 2001 to 2017. This model, the UBM, is preliminary and still being tested, but is appropriate for the scale of this study. The UBM is a decision tree-based soil-water-balance model that uses a series of nested "if-then" statements to determine how water is apportioned through the soil system and calculates the amount of recharge or runoff for a given month. The UBM integrates spatial data from ArcMap (ESRI, 2017) with programming written in Python (vanRossum, 2014) and follows the logic and soil water budget accounting used by the BCM as presented by Flint and others (2004), Flint and Flint (2007), Heilweil and Brooks (2011), and Thorne and others (2012). For explanations of the language and terms referenced in this section, please review these publications.

Monthly precipitation (as rain and snowmelt) and potential evapotranspiration are the temporally variable inputs to the model. Temporally static input to the model includes soil property grids of total soil water, field capacity, wilting point, and geologic permeability. The monthly precipitation, snowmelt, and evapotranspiration grids' inputs are summed with the estimate of existing soil moisture from the previous month's calculation to yield a monthly available soil-water volume. For the first model iteration, soil water was set to field capacity. For each subsequent iteration, water is routed to actual evapotranspiration, runoff, or recharge via four nested "if-then" statements (figure 12) based on the amount of available soil water calculated for a given month. If total available water is greater than total soil water, water is directed to groundwater recharge as limited by vertical hydraulic conductivity between the soil and the aquifer. Water beyond the limit of infiltration to the aquifer is directed to runoff, the next month's soil moisture, and actual evapotranspiration. When the soil moisture is greater than wilting point, actual evapotranspiration is equivalent to potential evapotranspiration. Actual evapotranspiration is an estimate of the evapotranspiration happening in the area, whereas the potential evapotranspiration is the amount of evapotranspiration that could happen given the energy available. If the available water is greater than field capacity and less than total soil water, but it is limited by hydraulic conductivity from entering the aquifer, it becomes runoff. Recharge is the amount of available water greater than the field capacity up to the limit of hydraulic conductivity. If the available water is between field capacity and wilting point, it becomes actual evapotranspiration up to the value of potential evapotranspiration. Available water greater than potential evapotranspiration is retained as the following month's soil moisture. Potential evapotranspiration may become actual evapotranspiration for available water values as low as the wilting point. If available water is less than wilting point, no water is available for actual evapotranspiration, runoff, or recharge, and all available water is carried forward to the next month's soil moisture. The resulting rasters were averaged to determine the monthly and yearly average soil water, actual evapotranspiration, runoff, and recharge.

The UBM uses soil properties from the U.S. Department of Agriculture State Soil Geographic (STATSGO2) data (Natural Resources Conservation Service, 2016). Soil data from STATSGO2 are provided as polygons separated by the Mapping Unit Identifier, which is the unique identifier to connect each polygon to the associated tables in the STATSGO2 database. I used a weighted average to summarize the soil properties for a given Mapping Unit Identifier and then output values for soil thickness (depth to bedrock restrictive layer in meters), bulk density (in g/cm^3), field capacity (in percent), and wilting point (in percent). Wilting point, total soil water, and field capacity were derived from the STATSGO2 output, and the units are in meters of water. Total soil water equals the soil thickness multiplied by porosity. Porosity (percent) is calculated as:

$$100 \times \frac{1 - \rho_b}{\rho_p} \qquad (4)$$

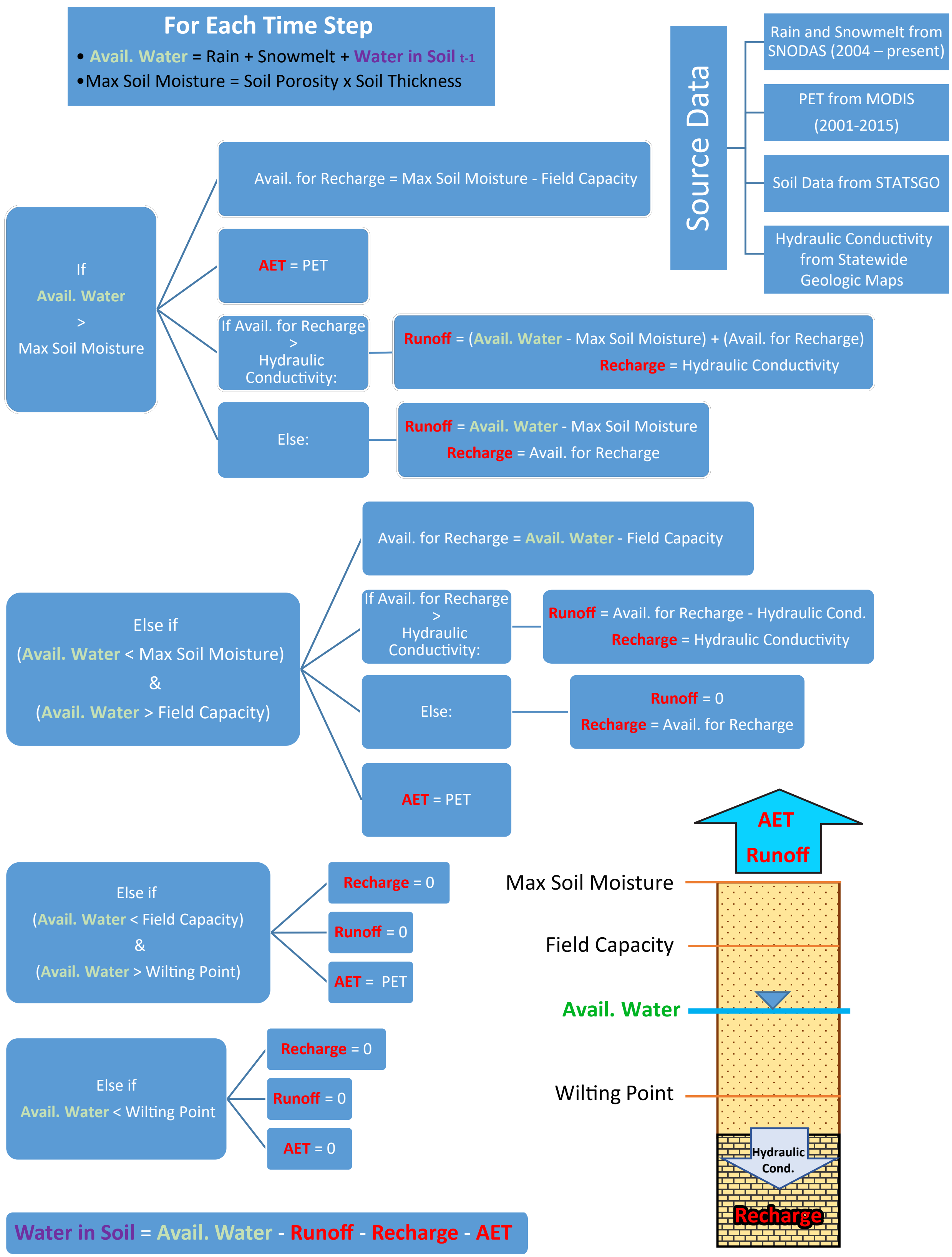

Figure 12. *Utah Basin Model (UBM) conceptual flow chart. PET is the potential evapotranspiration and AET is the actual evapotranspiration.*

where:

ρ_b = bulk density (g/cm^3)

ρ_p = particle density (2.65 g/cm^3)

If valley fill is dominant, the UBM uses a modified soil thickness of 20 feet (6 m), following the conceptualization of Flint and Flint (2007), to accommodate for the additional thickness of the unconsolidated material. The total soil-water, field-capacity, and wilting-point grids were then rasterized to match the grid dimension of the inputs for precipitation, snowmelt, and potential evapotranspiration.

Geologic permeability is required for the UBM calculation of runoff and recharge. The geologic unit in a given area is based on the digital geologic map of Utah (Hintze and others, 2000). For each geologic unit a value of permeability in meters per month was assigned following the assumed unit permeabilities presented in Heilweil and Brooks (2011, table A3-1). The geologic permeabilities were then rasterized to match the grid dimension of the inputs for precipitation, snowmelt, and potential evapotranspiration.

Evapotranspiration Data

Evapotranspiration estimates are based on MODIS16 rasters (Mu and others, 2011; Mu and others, 2013). MODIS16 is 500-meter-square (5382ft^2) horizontal resolution absolute and potential evapotranspiration grid derived from NASA's Moderate Resolution Imaging Spectroradiometer (MODIS) satellite input and the modified Penman-Monteith algorithm (Mu and others, 2013). Eight-day raster data from 2001 to 2014 were downloaded as tiles, re-projected to Albers Conic Equal Area (USGS) projection, and mosaiced into consistent monthly data. The evapotranspiration and potential evapotranspiration layers were then scaled by a factor of 10,000 so that the reported units were in meters of water. I then filled missing cell data in each raster dataset using focal statistics in ArcGIS (ESRI, 2017) with a radius of 18 kilometers (11 miles), which averages surrounding cells to produce the value of the missing cells. The resulting grids were used to calculate areal evapotranspiration for the study area.

Precipitation Data

Parameter-elevation Regressions on Independent Slopes Model (PRISM) provided the input for precipitation (PRISM Climate Group, 2018). The monthly raster data were scaled to meters and then projected into Albers Conic Equal Area. I then downsampled the precipitation rasters from 4-kilometer (2.5 mile) horizontal resolution to 250-meter (820 ft) horizontal resolution using the cubic convolution downsampling technique in ArcMap (ESRI, 2017).

Stream Loss and Gain

Seepage runs are near-concurrent measurements of stream discharge at various points along the stream to ascertain the amount of water lost or diverted over the path of the stream. A seepage run was conducted on Main, Little Hobble, and Spring Creeks (figure 13). Discharge and chemical field parameters were measured (table 1) at a total of 33 sites (figure 13).

Using the stream data compiled for discharge estimates in combination with seepage run data from Brigham Young University and collected for this study, I estimated seepage loss along Little Hobble Creek, Spring Creek, and Main Creek. Continuous measurements for stream discharge along different segments provided by a consultant's report allowed for the estimation of Main Creek seepage loss for most of 2013. Allred Restoration and BIO-WEST (2013) continuously measured three different locations along Main Creek (figure 13).

Aquifer Properties

Transmissivity from Specific Capacity

Specific capacity is a well's discharge divided by the drawdown that the discharge produces. If the well's radius and the pumping duration are known, the transmissivity of the aquifer at the well can be estimated with the following equation (Theis and others, 1963):

$$T = \frac{S_c}{4\pi} \ln\left(\frac{2.25\, T\, t_p}{r^2 S}\right) \tag{5}$$

where:

T = transmissivity ($distance^2/time$)

S_c = specific capacity ($distance^2/time$)

t_p = duration of pumping (time)

r = well radius (distance)

S = estimated storativity (dimensionless; generally 0.001 is used)

Because transmissivity is on both sides of the equation, this is an iteratively solved equation, where an estimate for transmissivity is put into the equation for the first iteration, and then the resulting transmissivity is put into the equation for every subsequent iteration, until the transmissivity entered is equal to the transmissivity returned.

The UDWRi does not require a specific capacity test for private wells, but the well log form accommodates information from the driller. I compiled specific capacity data from 28 well logs, including the well operated by Wallsburg (WIN 13759).

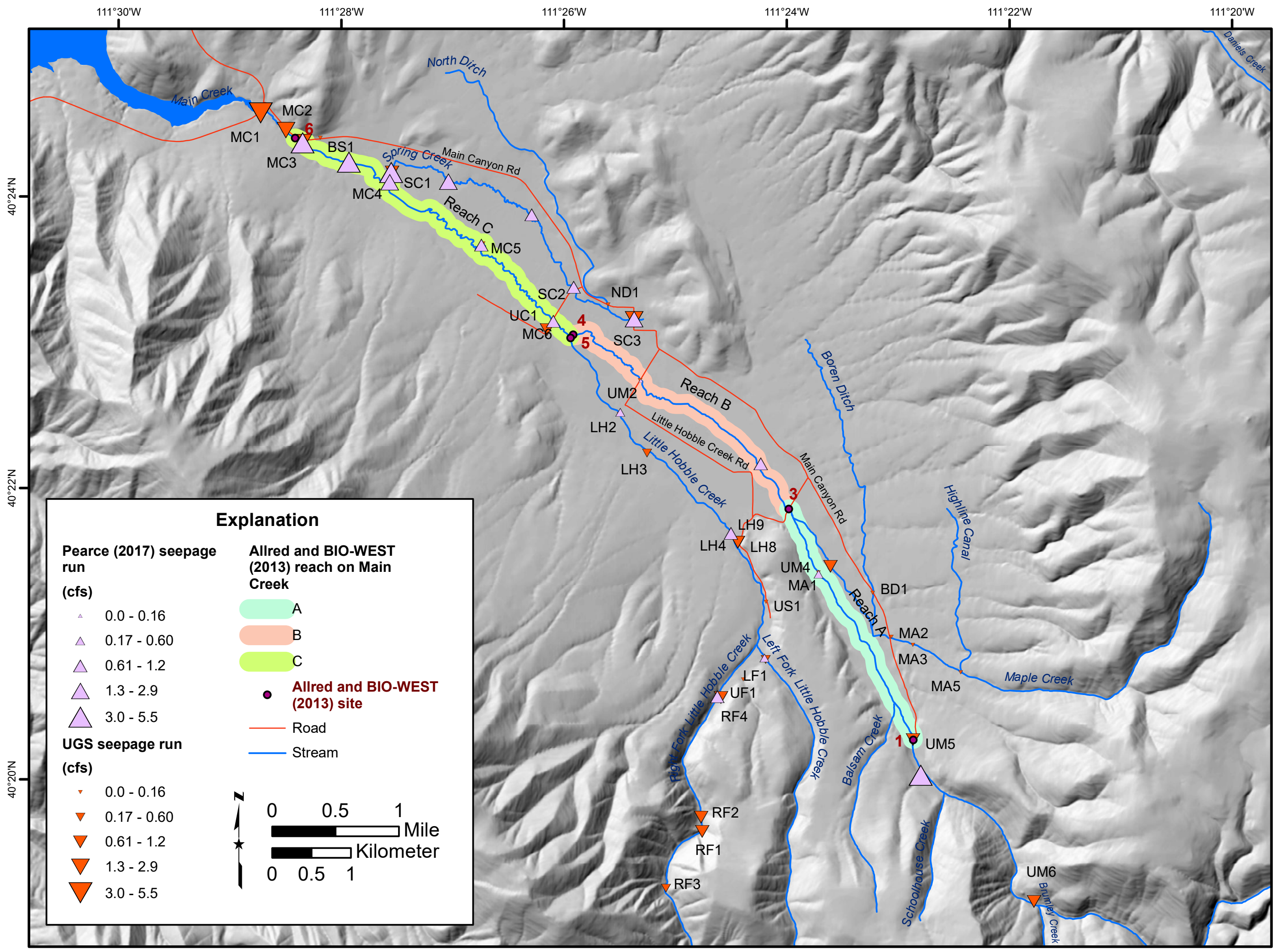

Figure 13. *Monitoring locations and segments for the seepage runs conducted in Round Valley.*

Aquifer Test

Loughlin Water Associates (2017) provided aquifer test data from two wells in the center part of Round Valley (figure 14). This aquifer test used wells at WIN 16173 (Cabin well) and WIN 10097 (Nelson #1 well), where Nelson #1 well is the larger-diameter pumping well and the Cabin well was the observation well. Depth to water measurements were obtained for both wells (table 3).

The aquifer test consisted of hourly step-wise pumping rate increases of 20 gallons per minute (gpm) (1.3 L/s) from 20 to 80 gpm (1.3-5 L/s). Total pumping duration was 240 minutes, and the maximum displacement was 54.25 feet (16.5 m). Loughlin Water Associates (2017) measured recovery for 56 minutes after pumping concluded. The step-drawdown data allowed for the application of a Hantush-Jacob (Hantush and Jacob, 1955; Hantush, 1961) step-drawdown technique to determine well loss, wellbore skin factor, and well efficiency. Based on this technique, well loss (drop in water level in the well caused by inefficiencies of the well) is estimated using the following equation (Hantush and Jacob, 1955; Hantush, 1961):

$$well\ loss = CQ^{P} \tag{6}$$

where:

C = well loss coefficient ($time^2/distance^5$)

Q = discharge (volume/time)

P = well loss coefficient (dimensionless)

The step-drawdown test determined the aquifer transmissivity to be 225 ft^2/day (21 m^2/day), with a well skin factor of -0.43 and well loss factors of 0.04 min^2/ft^5 (C) and 2.297 (P), resulting in a drawdown of 9.25 feet (2.8 m) at a pumping rate of 80 gpm (5 L/s).

Well parameters derived from the step-drawdown test were used to better estimate the Round Valley aquifer parameters. I examined aquifer data from a test conducted in 1995 and data from a test conducted by Loughlin Water Associates (2017) in 2016, both using the Nelson #1 well as the pumping well. The

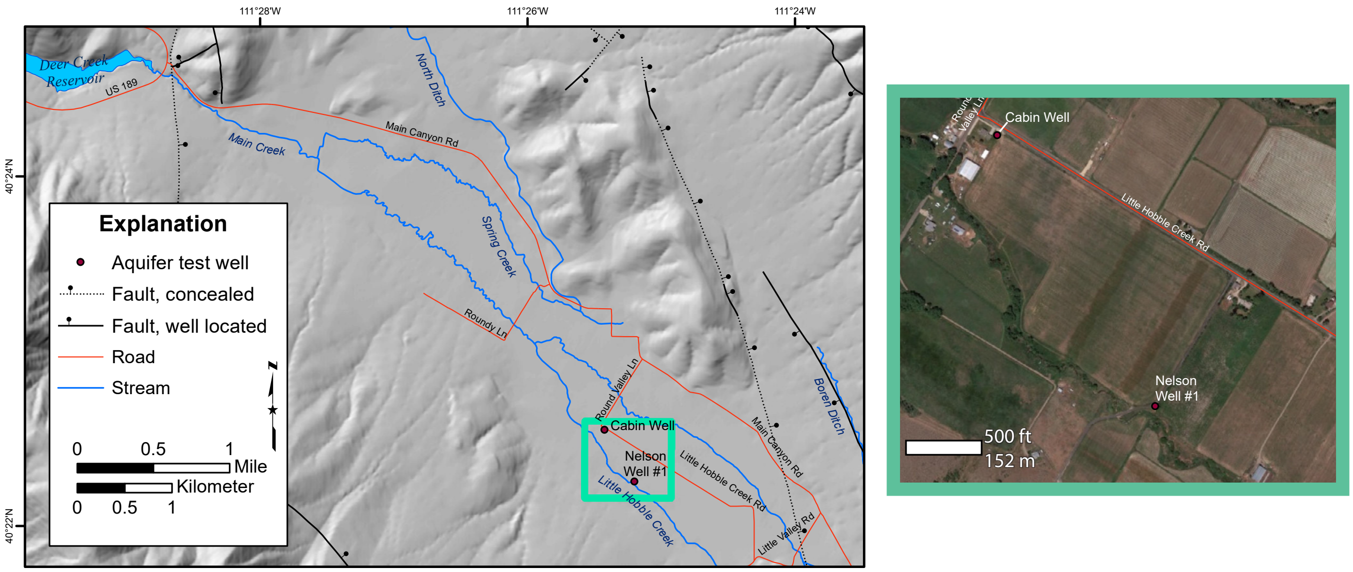

Figure 14. Location of aquifer test examined for this study. Hillshade base map and street data from the Utah Automated Geographic Reference Center (2019). Aerial photo from Google (copyright 2019).

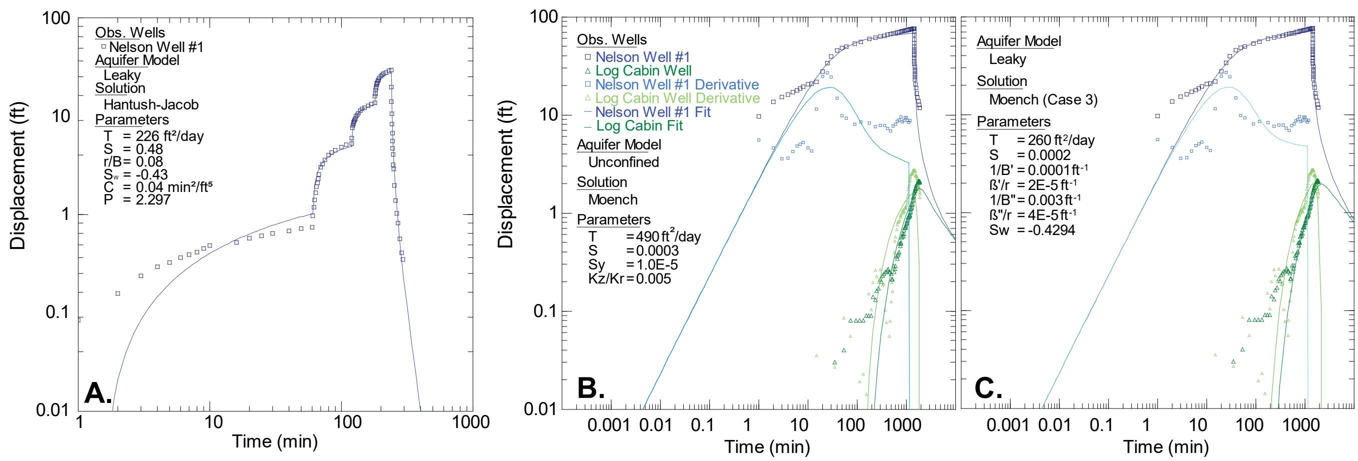

*Figure 15. Aquifer test analyses. **A.** Step-drawdown, **B.** unconfined, and **C.** analysis of the aquifer test data from Loughlin Water Associates (2017).*

2016 data included water-level measurements from both the pumping well and an observation well (Cabin well) 2075 feet away from and northwest (azimuth = 330 degrees) of the pumping well (Nelson #1 well). The pumping well is within 100 feet of Little Hobble Creek, and the observation well is within 500 feet of Little Hobble Creek. Unfortunately, discharge data of the creek were not provided with the pumping test data.

Based on the relatively shallow depth to water of the wells observed in the aquifer test and the interpreted hydrogeology of the area, two types of aquifer test type curves were selected to analyze the pumping test data: Moench (1997) unconfined aquifer and Moench (1985) leaky confined aquifer. I also attempted to match a fractured, dual-porosity type curve to the data, but was unsuccessful in producing a reliable match to the observed data in both wells. AQTESOLV™ aquifer test analysis software was used to conduct all curve matching (Duffield, 2007).

Both wells were assumed to penetrate part of the fractured bedrock aquifer. Available lithology information from the Nelson #1 well included reference to a tight boulder and clay layer at 170 feet (52 m), as well as a tight conglomerate at 262 feet (80 m), both of which could describe the fractured bedrock layer in the valley. The Log Cabin well log describes a fractured yellow conglomerate at a depth of 24 feet (7.3 m), which likely represents the bedrock of the valley.

Both the 1995 and 2016 datasets showed an inflection point within the first 100 minutes of pumping, which commonly represents wellbore storage. However, a similar trend of drawdown was also observed in the observation well, which could indicate that the early-time drawdown observed in the wells could be influenced by a nearly constant-head line source, like Little Hobble Creek. Deviation from the type curves is likely due to wellbore storage or a line source.

Analytic Element Model

To estimate the hydraulic conductivity of the system and better understand the groundwater system, the valley was modeled using an analytic element model. I used the TimML (Bakker, 2004, 2006a, 2006b) Python library to create and run the model. The library allows for modeling the potentiometric surface of multiple layers of the aquifer system, as well as the addition of recharge and pumping. The model also allows for modeling inhomogeneities because the hydraulic conductivity can be set to a different value in each zone.

The model consists of two layers of differing hydraulic conductivities. The unconsolidated material is surrounded by an area representing the bedrock and mountainous region of Round Valley and is modeled as an area of lower hydraulic conductivity and higher recharge. Recharge was set to between 0.004 and 0.016 inches (0.1–0.4 mm) per day (Roark and others, 1991). Wells were also included in the model. Specific details on the parameters of the model are summarized by Inkenbrandt (2018).

Analytic element models require the input of specified heads and defined head gradients (Bakker, 2006a, 2006b). For this model, I used the gradient derived from the potentiometric surface map and specified the head of Deer Creek Reservoir level as 5417 feet (1651 m). I defined the head along the rivers, which were treated as line sinks in this model, as the same as the ground elevation.

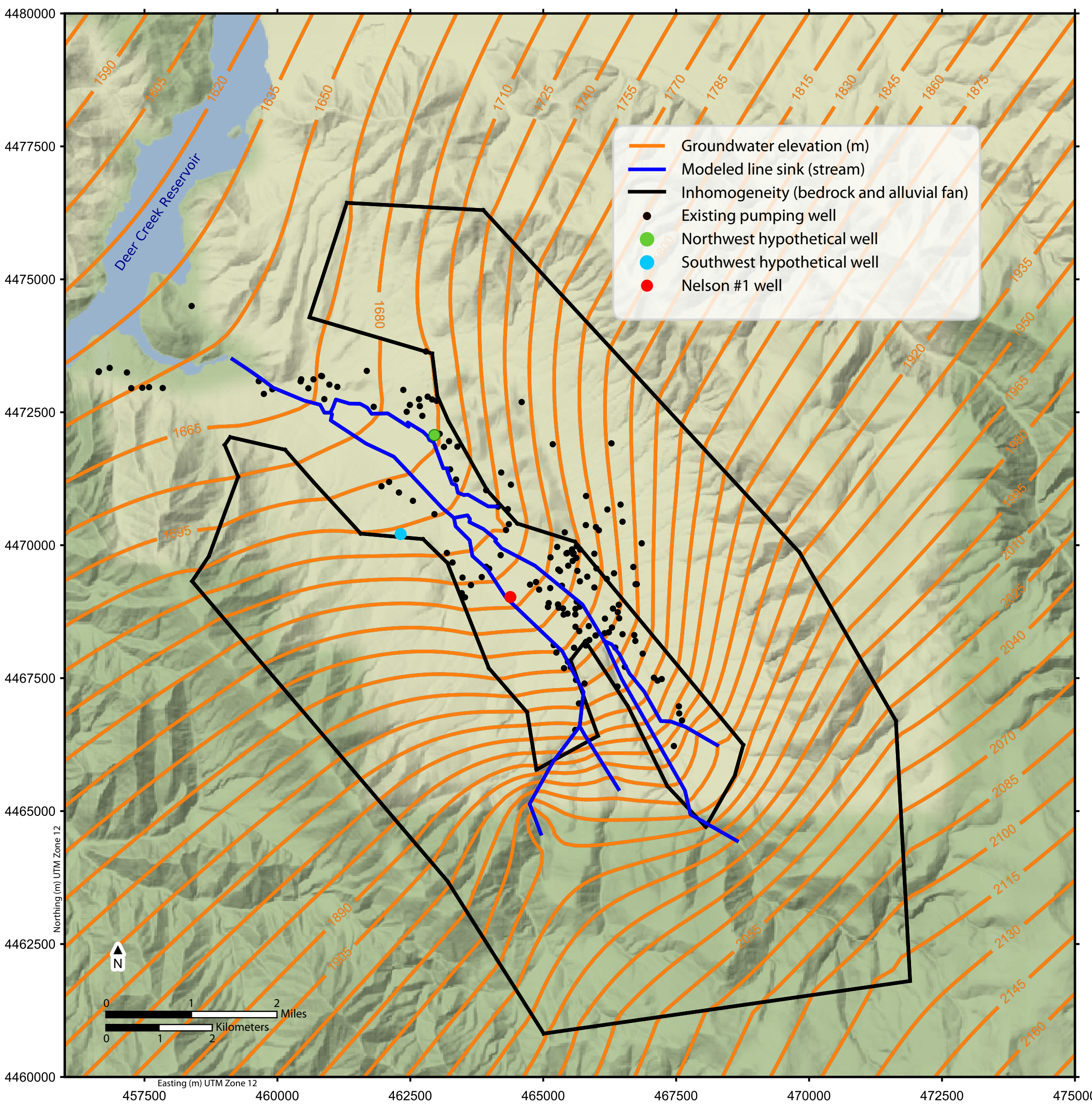

__Figure 16.__ Layout of analytic element model used for this study, including line sinks (streams) and an inhomogeneity (bedrock and alluvial fan). Hillshade base map and street data from the Utah Automated Geographic Reference Center (2019).

I calibrated the model using data from the aquifer test and modeled the "static" potentiometric surface of the valley by adding the ambient continuous pumping of the dominant wells in the valley. Pumping values were set to 5 gpm (30 m^3/day) by default, unless additional information was available. The static water level did not include pumping of the Nelson #1 or the Cabin wells. I then calculated an initial "pumping" water level, adding the Nelson well's pumping and creating an output of the Cabin well's nonpumping level. Using SPOTPY (Houska and others, 2015), I chose the hydraulic conductivities of the unconsolidated sediment and the underlying fractured sandstone as parameters, as well as a leakage factor between the two units. The model estimated parameters using a Simulated Annealing (Houska and others, 2015) optimization technique, running over 40 iterations to minimize error to below 0.017 meters.

Using the calibrated model, forward models were run for different pumping scenarios, keeping all other variables constant. The pumping scenarios consisted of three different potential large-pumping well locations: the northwest portion of the valley (figure 16, green dot), the southeast portion of the valley at the current Nelson #1 well location (figure 16, red dot), and the hills to the south of the alluvial valley-fill material (figure 16, blue dot). A pumping rate of 80 gpm (436 m^3/day) was assigned to each production well. In the scenarios where all wells were pumped, I assumed an arbitrary pumping rate of 30 gpm (164 m^3/day) and a higher rate of 55 gpm (300 m^3/day) for each well.

RESULTS

Water Chemistry

Water chemistry analyses can provide clues to the provenance of water and allow for comparison of water types. Water samples having significantly different chemistry are typically from different sources, and water samples that have geochemically similar characteristics are typically derived from a similar geochemical setting. However, when provided with an informed understanding of the hydrogeology, including interpreted cross sections and potentiometric readings, water chemistry can support a conceptual model of a system. All but two water samples from this study are calcium bicarbonate type water, and they cluster closely on piper (figure 17) and stable isotope plots (figure 18).

Two samples appear to be outliers on the piper diagrams (figure 17). The station labeled "1" on the piper diagrams (figure 17) is well USGS-402219111254401, a well at the south end of Round Valley Lane. The chemistry of this well is calcium bicarbonate type having a specific conductance comparable to those of the other samples at 419 µS/cm, but it has a relatively high charge balance error (table 4). Nearby samples appear to have a different chemistry. Because there is only one sample for this station, it is difficult to determine why this sample is different, but it is not sufficiently different to

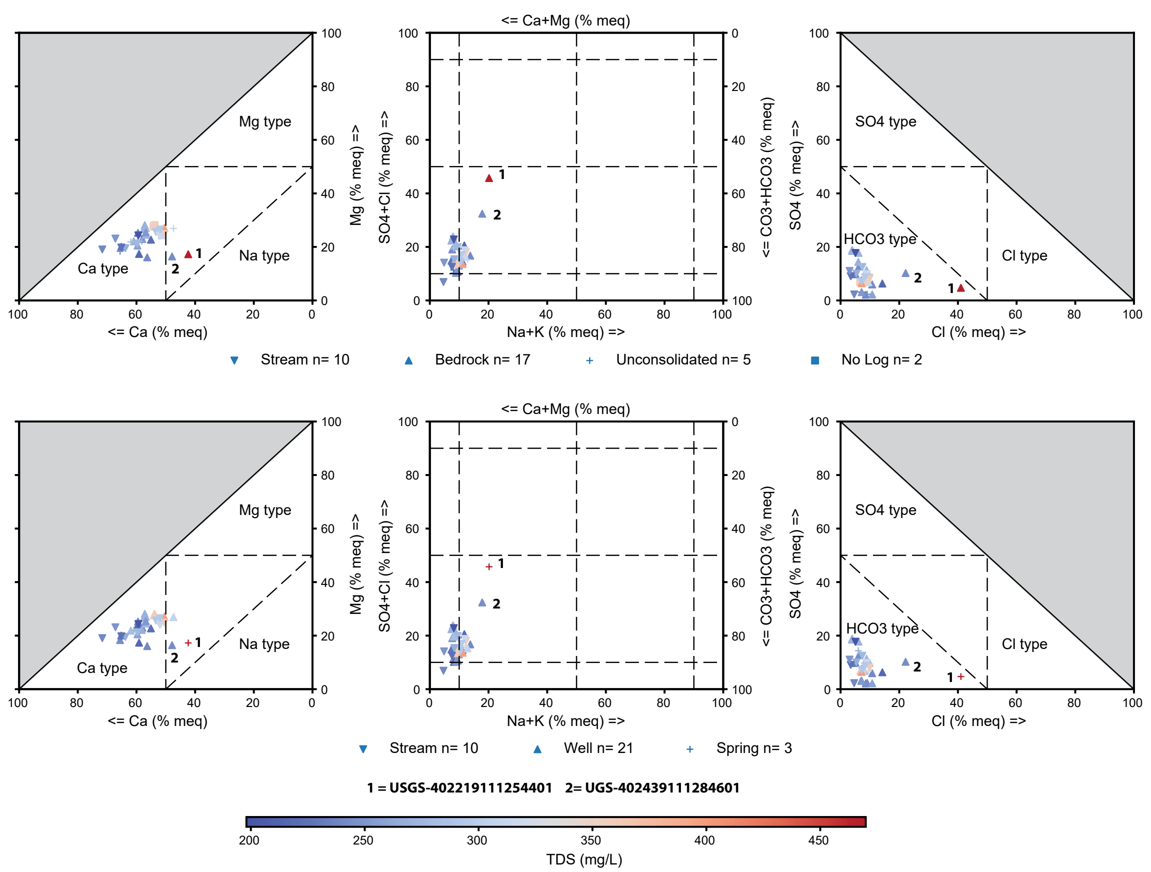

Figure 17. *Piper diagram of water chemistry compiled for this study. Sample points labeled 1 and 2 are outliers from the other samples.*

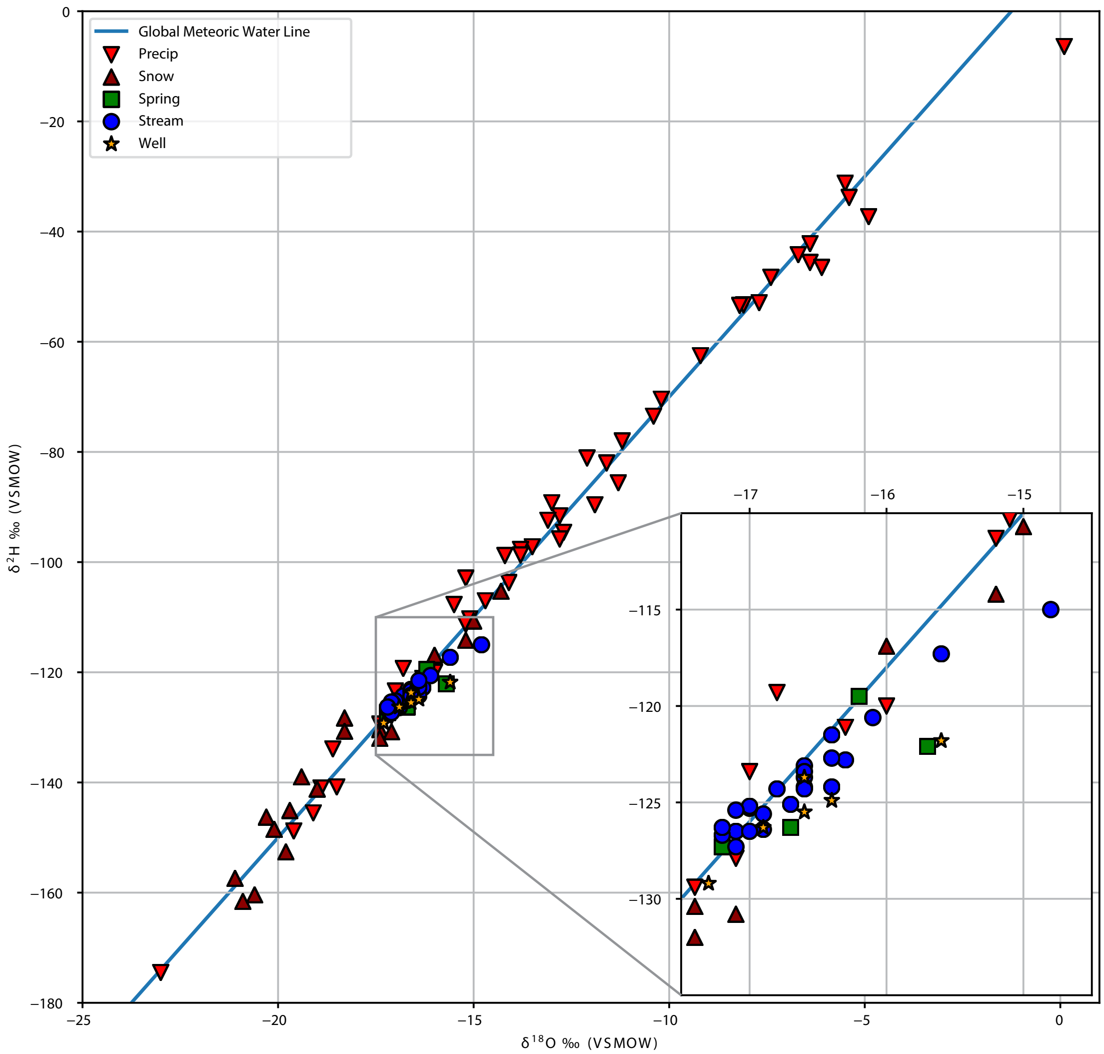

Figure 18. *Stable isotope analysis of samples collected for this study.*

suspect a different aquifer system. The other outlying sample, labeled "2" on the piper diagrams (figure 17), is from station UGS-402439111284601, which is a spring located on the shore of Deer Creek Reservoir near the mouth of Main Creek. This sample is also a calcium bicarbonate water type and has specific conductance of less than 1000 µS/cm. The sample was collected from a spring box after a long period of no use, which could have influenced the quality of the sample. Also, this sample is somewhat outside the area of study and may be from an aquifer system more influenced by Deer Creek Reservoir.

The stable isotope data did not show significant differences between the stream and groundwater samples (figure 18). All samples plotted within the range of the snow samples collected for this study. The snow and rain isotope values had considerably more spread than the groundwater and stream samples. All isotope values were near the Global Meteoric Water Line, though there was a slight evaporative signature in one well near upper Main Creek, which likely represented evaporated surface water influence.

Groundwater

Based on the available compiled data and the UDWQ groundwater classification system (https://deq.utah.gov/water-quality/classes-utah-ground-water-quality-protection-program), groundwater in Round Valley (including the bedrock) classifies as Class IA, which is pristine quality. Compiled total-dissolved-solids concentration ranges from 216 to 470 mg/L. Specific conductance ranges between 374 and 847 µS/cm. None of the compiled inorganic constituents exceed the standards set by the UDWQ (https://deq.utah.gov/water-quality/standards-utah-ground-water-quality-protection-program).

Dissolved inorganic nitrogen in groundwater ranges from < 0.1 mg/L (below detection limit) to 2.76 mg/L, with an average nitrogen concentration of 1.6 mg/L as nitrogen. Nitrogen concentrations are generally higher in the northeast part of the valley, near Wallsburg, which is in the downgradient part of the valley.

Table 4. *Compiled chemistry used for piper diagrams.*

Station Id	Easting	Northing	Elev (m)	Data Source	Station Type	Material	WIN[1]	pH	Temp (°C)	TDS (mg/L)	Calc. TDS (mg/L)	Spec. Cond. (µS/cm)	Ca (mg/L)	Mg (mg/L)	K (mg/L)	Na (mg/L)	NaK (mg/L)	SO_4 (mg/L)	Cl (mg/L)	HCO_3 (mg/L)	CO_3 (mg/L)	CO_2 (mg/L)
402023111244501	464980	4465588	1921	UGS	Stream	Stream		8.55	11.7	240.0	324	402	68.2	11.0	0.0	5.1	5.1	4.3	6.6	228.5	0.0	6.2
402131111231601	467054	4467617	1856	UGS	Well	Bedrock	9724	7.74	12.1	240.0	338	427	62.9	15.1	0.0	11.8	11.8	4.3	12.9	231.0	0.0	29.8
402136111234201	466461	4467813	1818	UGS	Well	Bedrock		8.18	17.0	272.0	377	461	64.3	18.1	1.7	9.1	10.8	42.4	10.8	231.0	0.0	10.7
402208111241401	465701	4468769	1781	UGS	Well	Bedrock	151	7.46	14.8	244.0	339	417	59.8	15.4	1.1	8.1	9.3	27.0	9.8	217.5	0.0	206.0
402216111251101	464369	4469044	1749	UGS	Well	Bedrock	10097	6.50		216.0	297	379	52.2	9.3	1.2	11.2	12.4	12.0	20.0	190.0	1.0	
40224111251901	464089	4468926	1756	UGS	Well	Unconsolidated	9126	7.91	14.2	244.0	312	400	63.1	10.7	1.3	8.1	9.4	4.3	12.6	211.5	0.0	58.2
402313111262601	462655	4470803	1712	UGS	Well	Bedrock	21320	7.47	12.7	258.0	327	433	63.4	13.2	1.2	11.4	12.6	4.3	15.7	218.0	0.0	115.0
402439111284601	459334	4473477	1659	UGS	Spring	Bedrock		7.44	16.0	470.0	587	847	98.7	24.4	2.8	52.3	55.1	18.5	119.0	271.0	0.0	14.9
9290	467840	4464992	1948	UGS	Well	Bedrock	32864	7.30		270.0	384	487	64.0	19.1	1.6	8.5	10.1	45.0	7.0	238.0	1.0	
SDWIS-1612-004916	464308	4470298	1731	SDWIS	Well	Bedrock	13759			275.0	384	483	63.0	16.5	1.0	11.4	12.5	27.8	16.0	248.0	0.0	6.0
SDWIS-1756-009290	467840	4464992	1948	SDWIS	Well	Bedrock	32864	6.90		271.0	369	461	56.2	16.2	1.3	8.4	9.7	45.4	7.0	234.0	1.0	181.0
USGS-402041111230901	467179	4466063	1889	WQP	Spring	Bedrock		7.60		269.8	384	470	63.7	14.0	1.0	9.6	11.0	35.5	11.0	249.3	0.0	6.0
USGS-402045111225701	467453	4466208	1890	WQP	Well	Unconsolidated	427134	7.60	10.0	283.0	390	489	70.0	15.0	1.7	9.5	11.2	24.0	18.0	251.4	0.0	10.0
USGS-402213111234803	466262	4468927	1797	WQP	Well	Bedrock	28591	7.80	12.0	222.0	298	378	48.0	12.0	1.9	10.0	11.9	14.0	9.8	202.8	0.0	5.3
USGS-402219111254401	463527	4469124	1760	WQP	Well	Bedrock	16757	6.80	11.0	243.0	298	419	48.0	10.0	0.9	20.0	20.9	20.0	32.0	167.5	0.0	43.0
USGS-402222111245801	464612	4469212	1749	WQP	Well	Bedrock	28933	7.20	10.5	228.0	327	401	59.0	11.0	1.1	7.0	8.1	20.0	7.7	221.0	0.0	22.0
USGS-402226111225701	467466	4469322	1908	WQP	Well	Unconsolidated	28277	7.70	12.5	219.0	309	385	53.0	13.0	1.0	7.8	8.8	6.0	10.0	218.6	0.0	7.1
USGS-402231111241201	465698	4469484	1776	WQP	Well	Unconsolidated	427130	7.50	11.5	267.0	376	465	65.0	15.0	1.1	12.0	13.1	16.0	14.0	252.6	0.0	13.0
USGS-402306111260901	462944	4470576	1716	WQP	Well	Bedrock	33624	7.30	12.0	241.0	322	420	56.0	9.7	1.2	15.0	16.2	12.0	16.0	212.5	0.0	17.0
USGS-402311111251401	464242	4470724	1727	WQP	Spring	Bedrock		7.36	11.0	317.8	447	547	72.2	20.7	1.8	18.4	20.2	19.2	20.2	294.0	1.0	18.7
USGS-402312111233901	466482	4470745	1866	WQP	Well	Bedrock	21089	7.40	12.0	251.0	363	449	59.0	16.0	1.0	10.0	11.0	7.0	12.0	257.5	0.0	16.0
USGS-402342111263501	462337	4471690	1691	WQP	Well	No Log		7.30	9.5	362.0	518	623	82.0	26.0	3.0	14.0	17.0	22.0	16.0	354.8	0.0	29.0
USGS-402343111264001	462219	4471721	1690	WQP	Well	No Log		7.20	9.0	357.0	510	618	81.0	25.0	2.8	14.0	16.8	22.0	18.0	347.5	0.0	35.0
USGS-402408111262201	462647	4472490	1695	WQP	Well	Unconsolidated	30752	7.80	11.5	308.0	403	531	61.0	21.0	1.7	18.0	19.7	19.0	14.0	268.5	0.0	7.4
USGS-402423111275001	460575	4472963	1671	WQP	Well	Bedrock	427366	7.50	12.0	400.0	567	686	83.0	27.0	3.6	19.0	22.6	23.0	19.0	392.5	0.0	20.0
USGS-402435111282900	459658	4473338	1672	WQP	Stream	Stream		7.88	11.8	292.7	419	491	64.7	18.8	2.5	13.1	15.6	19.0	14.0	287.3	0.0	6.3
UTAHDWQ-4996895	462955	4471860	1695	WQP	Stream	Stream		7.00	13.8	362.7	496	665	79.1	23.6	2.7	20.5	23.2	25.6	22.9	316.0	6.0	2.0
UTAHDWQ-4996900	463371	4471099	1707	WQP	Stream	Stream		8.03	9.9	316.6	456	544	72.5	20.4	2.2	17.7	20.0	27.5	19.9	292.6	2.9	4.7
UTAHDWQ-4996905	463094	4470704	1709	WQP	Stream	Stream		7.73	9.6	276.2	405	470	69.1	14.9	1.1	12.0	13.4	31.9	14.7	257.8	3.1	6.8
UTAHDWQ-4996910	463953	4469523	1736	WQP	Stream	Stream		8.23	7.8	278.5	357	403	65.6	12.2	1.1	9.2	10.4	22.2	9.3	233.5	3.5	4.3
UTAHDWQ-4996915	465171	4465813	1904	WQP	Stream	Stream		8.10	7.2	223.0	337	378	71.5	13.2	1.0	8.9	9.9	18.7	5.3	215.0	3.2	3.4
UTAHDWQ-4996917	464656	4465046	2027	WQP	Stream	Stream		8.26	11.6	248.2	360	449	67.4	14.1	1.1	4.9	6.1	24.6	6.1	235.4	6.2	1.7
UTAHDWQ-4996920	464238	4469954	1733	WQP	Stream	Stream		8.04	7.0	195.5	265	324	43.3	10.9	1.3	6.1	8.1	26.8	6.7	168.8	0.4	6.6
UTAHDWQ-5913460	459399	4473337	1653	WQP	Stream	Stream		8.04	10.9	291.4	404	478	62.1	19.3	2.3	13.2	15.5	22.4	14.9	266.8	3.1	20.8

[1]*Utah Division of Water Rights Well Identification Number*
[2]*Discharge*
[3]*Total suspended solids*
[4]*Turbitity*
[5]*Dissolved oxygen*

Table 4. *Continued*

Station Id2	Alk (mg/L)	NO_3+NO_2-N (mg/L)	NH_3-N (mg/L)	P (mg/L)	Al (mg/L)	B (mg/L)	Ba (mg/L)	Cd (mg/L)	Cr (mg/L)	Cu (mg/L)	F (mg/L)	Fe (mg/L)	Ni (mg/L)	P (mg/L)[3]	Si (mg/L)	Mn (mg/L)	Zn (mg/L)	Q (cfs)[2]	TSS (mg/L)[3]	Turb (TU)[4]	DO (mg/L)[5]	Charge Balance Error	Water Type
402023111244501	198.0	0.43	0.02	0.01		0.001						0.002		0.011	10.5			0.47	1.69	0.55		-8%	Ca-HCO_3
402131111231601	190.0	0.59		0.01		0.001						0.002		0.015	16.4				1.69	0.22		-12%	Ca-HCO_3
402136111234201	186.0	0.28	0.02	0.02		0.001						0.002		0.022	12.7				1.69	0.55		-6%	Ca-HCO_3
402208111241401	182.0	0.01	0.02	0.01		0.001						0.002		0.008	13.8				7.20	3.97		-7%	Ca-HCO_3
402216111251101	156.0	0.40										0.040				0.007						-5%	Ca-HCO_3
40224111251901	181.0	0.28	0.02	0.07		0.001						0.047		0.066	23.8				10.80	16.60		-10%	Ca-HCO_3
402313111262601	183.0	1.55	0.02	0.03		0.001						0.030		0.029	17.8				9.60	17.70		-13%	Ca-HCO_3
402439111284601	222.0	1.66		0.06		0.051						0.058		0.059	24.8				1.69	0.90		-17%	Ca-HCO_3
9290	195.0	0.30		0.01								0.020		0.010		0.001	0.02					-5%	Ca-HCO_3
SDWIS-1612-004916	203.0	1.11	0.10	0.02		0.035	0.06	0.0006	0.003	0.012	0.13	0.140	0.006	0.020	18.0	0.005	0.03			0.41		-4%	Ca-HCO_3
SDWIS-1756-009290		0.26	0.20	0.01		0.050	0.05	0.0005	0.005	0.004	0.10	0.020	0.005	0.010	12.3	0.005	0.09			0.35		1%	Ca-HCO_3
USGS-402041111230901	204.3	0.42	0.10	0.02		0.050	0.06	0.0016	0.005	0.011	0.13	0.070	0.008	0.023	15.5	0.008	0.04			1.07		-1%	Ca-HCO_3
USGS-402045111225701	207.0	0.38		0.12		0.020					0.10	0.016		0.123	17.0	0.002						-5%	Ca-HCO_3
USGS-402213111234803	167.0	0.36				0.030					0.20	0.005			21.0	0.017						-6%	Ca-HCO_3
USGS-402219111254401	138.0			0.03		0.020					0.10	0.087		0.031	28.0	0.009						-10%	Ca-HCO_3
USGS-402222111245801	182.0	0.19		0.06		0.010					0.20	0.011		0.061	13.0	0.001						-3%	Ca-HCO_3
USGS-402226111225701	180.0	0.68				0.020					0.10	0.007			16.0	0.002						-5%	Ca-HCO_3
USGS-402231111241201	208.0	0.55				0.020					0.10	0.008			17.0	0.003						-7%	Ca-HCO_3
USGS-402306111260901	175.0	1.40		0.12		0.020					0.10	0.014		0.123	19.0							-8%	Ca-HCO_3
USGS-402311111251401	241.3	1.83	0.04	0.07	0.01	0.042	0.13	0.0001	0.003	0.001	0.10	0.019	0.005	0.070	19.0	0.005	0.02	1.91	4.12		10.09	-9%	Ca-HCO_3
USGS-402312111233901	212.0	0.73		0.03		0.020					0.10	0.007		0.031	17.0							-5%	Ca-HCO_3
USGS-402342111263501	292.0					0.050					0.20	2.000			21.0	0.470						-6%	Ca-HCO_3
USGS-402343111264001	286.0					0.030					0.20	0.690			20.0	0.200						-6%	Ca-HCO_3
USGS-402408111262201	221.0	2.00		0.06		0.030					0.10			0.061	20.0							-11%	Ca-HCO_3
USGS-402423111275001	323.0	0.91		0.52		0.050					0.10	0.008		0.521	26.0							-5%	Ca-HCO_3
USGS-402435111282900		0.56		0.25		0.020					0.45			0.245	18.2			15.00				-5%	Ca-HCO_3
UTAHDWQ-4996895	264.0	0.85	0.04	0.09	0.01	0.052	0.17	0.0001	0.004	0.001		0.022	0.005	0.087		0.009	0.02	0.20	33.60		6.69	-9%	Ca-HCO_3
UTAHDWQ-4996900	241.3	1.45	0.04	0.10	0.01	0.037	0.12	0.0001	0.003	0.004		0.060	0.005	0.103		0.011	0.01	1.25	14.62		11.17	-7%	Ca-HCO_3
UTAHDWQ-4996905	212.5	0.19	0.04	0.06	0.01	0.030	0.11	0.0001	0.003	0.001		0.022	0.005	0.062		0.020	0.01	2.60	16.73		11.92	-3%	Ca-HCO_3
UTAHDWQ-4996910	193.1	0.17	0.06	0.10	0.01	0.031	0.10	0.0001	0.003	0.006		0.073	0.005	0.097		0.013	0.01	4.64	25.22	1.30	10.90	-5%	Ca-HCO_3
UTAHDWQ-4996915	177.6	0.26	0.04	0.03	0.01	0.030	0.10	0.0001	0.002	0.001		0.020	0.005	0.032		0.005	0.01	2.11	6.36		10.01	-14%	Ca-HCO_3
UTAHDWQ-4996917	202.3	0.15	0.03	0.04	0.02	0.030	0.10	0.0001	0.003	0.001		0.040	0.005	0.044		0.015	0.01	2.66	11.54	5.50	10.30	-3%	Ca-HCO_3
UTAHDWQ-4996920	151.5	0.34	0.05	0.05	0.09	0.030	0.09	0.0006	0.004	0.012		0.074	0.005	0.048		0.009	0.02	5.52	12.61	6.57	11.38	-2%	Ca-HCO_3
UTAHDWQ-5913460	231.8	0.49	0.06	0.10	0.04	0.067	0.10	0.0010	0.004	0.011	0.46	0.265	0.009	0.097	15.9	0.039	0.02	25.66	35.18	9.74	9.49	-5%	Ca-HCO_3

[1]*Utah Division of Water Rights Well Identification Number*
[2]*Discharge*
[3]*Total suspended solids*
[4]*Turbitity*
[5]*Dissolved oxygen*

Surface Water

Long-term monitoring data from the Utah DEQ indicate surface water trends in Round Valley have shown an overall decrease in the loading of nutrients and dissolved solids (figure 19), most likely due to restoration work along the lower parts of Main Creek (Wasatch Conservation District, 2012). However, the loading of these constituents is closely correlated to discharge, and discharge since the restoration has been lower than the past average discharge (figure 19); further monitoring should be conducted to verify this trend.

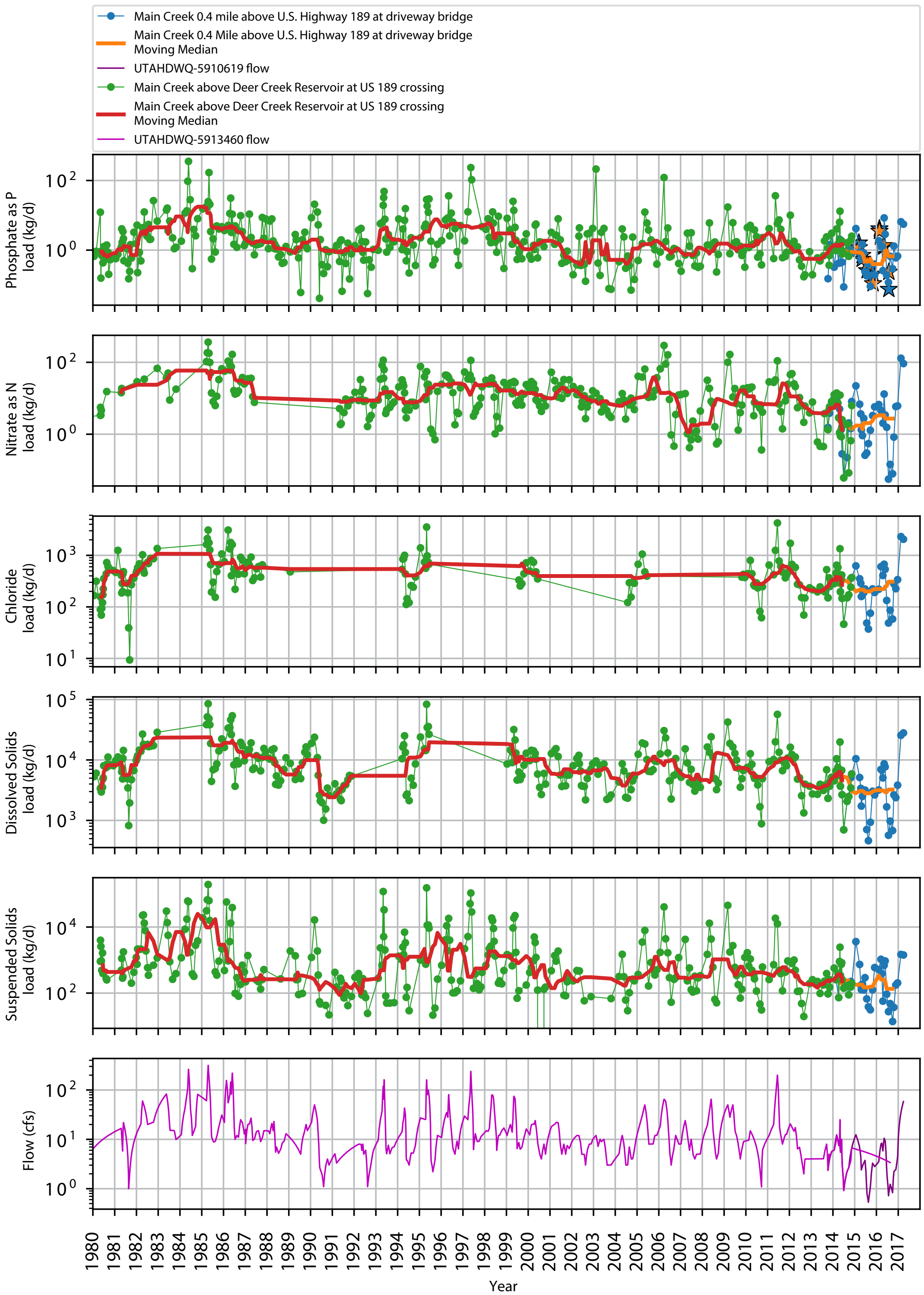

Figure 19. *Loading over time of different constituents in Main Creek near Deer Creek Reservoir. Source data from UDEQ (Utah Department of Environmental Quality, 2019).*

Septic Tank Density

Estimates from the mass-loading technique provide a first pass of how increased residential density might influence nutrient loads in the groundwater. Based on the parameters used in the model, there will be a 1 mg/L valley-wide nitrate (NO_3 as nitrogen) valley-wide concentration increase above current levels if lot size (per tank) is 2 acres (figure 20). If the estimated groundwater flow is higher (15 cfs), then a density of one tank per 1.3 acres would increase nitrate by 1 mg/L. Greater density of septic systems will result in increased nitrate in the groundwater. Based on this model, if lot sizes are 0.3 acres or smaller, the maximum contaminant limit for nitrate in drinking water (10 mg/L) will be exceeded (figure 20). Adding about 500 septic systems to the valley will likely result in an increase in the average valley-wide nitrate concentration of 0.5 mg/L, where the areas with higher concentrations of septic systems would have higher concentrations of nitrate.

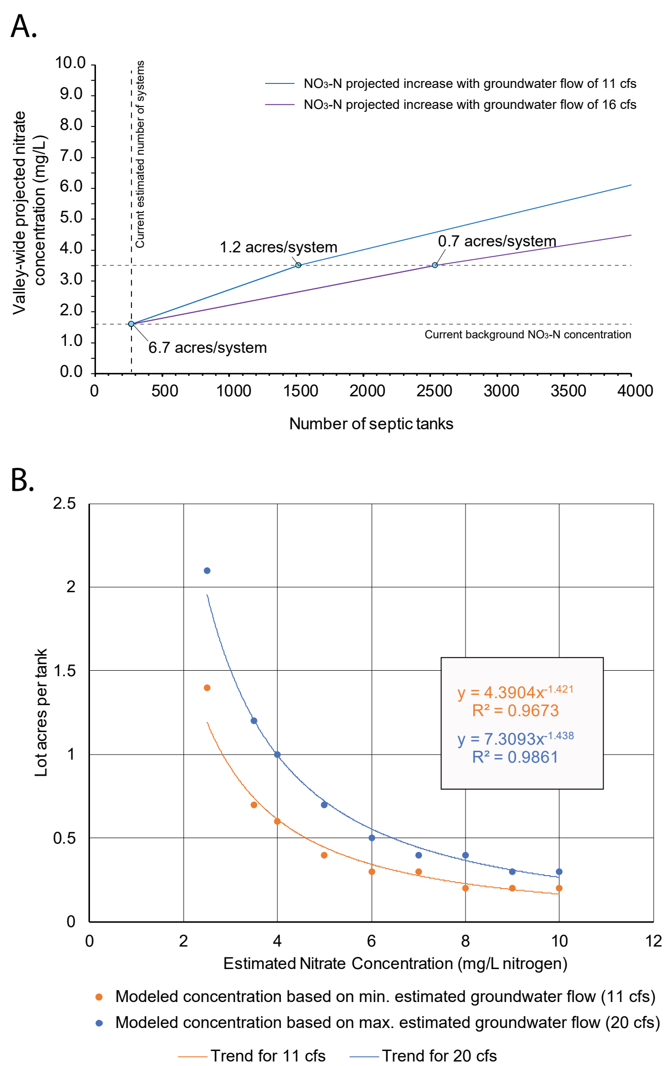

***Figure 20.** Nitrate concentration projection for different septic-tank densities. A) Projected nitrate concentrations with increased septic density, showing a nitrate threshold of 3.5 mg/L reached at septic tank densities between 0.7 and 1.2 acres per system. B) Modeled relationship between septic tank density and projected nitrate concentration.*

Note that this method did not consider the current septic-tank density of Wallsburg and only used the average density of the valley-fill material. The model also is only based on the available nitrate data, which is limited. I used a small area for the mass balance calculation because the projected septic-tank densities are the average for the entire area, and a development would likely be a high-density area surrounded by lower density plots. Much of the valley-fill area will not be developed because of land suitability and ownership, so a smaller area is more representative of potential development in the valley. Also, most of the wells having nitrate data are clustered within the alluvium (figure 3).

Potentiometric Surface Maps

The goal of examining groundwater levels is to (1) establish a baseline of groundwater levels for the valley (figure 21), (2) determine direction and magnitude of local and regional groundwater flow (figure 22), and (3) characterize long-term and seasonal groundwater-level changes.

Measured depth to water ranged from flowing (above ground surface) to 195 feet below ground surface. General groundwater gradient is to the west, toward Deer Creek Reservoir (figure 22). Based on the regional groundwater map, groundwater divides approximately follow the topographic divides, limiting groundwater flow between Round Valley and adjacent valleys (figure 23).

One of Round Valley's intra-basin faults likely compartmentalizes water or restricts groundwater flow across its plane. Evidence for compartmentalization is a groundwater elevation difference of 153 feet over a lateral distance of 925 feet between wells 51 and 52 (figure 21). Wells 53 and 49 substantiate water levels recorded in wells 51 and 52, respectively. The inferred fault crosses between wells 51 and 52, suggesting that the drastic difference in water levels could be due to hydraulically disconnected fault blocks. Wells 41 and 42, which are 780 feet apart, show a groundwater elevation difference of 150 feet (figure 21). While they do not straddle the inferred fault as depicted by Biek and Lowe (2009), the steep potentiometric gradient implies that the fault passes between and hydraulically segregates the two wells.

Adjacent wells not separated by a fault, where one is screened in fractured Oquirrh Formation and the other is screened in the valley alluvium, have comparable groundwater elevations, suggesting that the units are hydraulically connected. Potentiometric surface contours project without deflection from overlying unconsolidated sediments to underlying bedrock (figure 21), implying strong hydraulic connection and similar hydraulic conductivity.

Based on the aspect of the slope of the potentiometric surface, average azimuthal groundwater-flow direction over the entire interpolated area of Round Valley is 267° (near due west), having a standard deviation of 55°. The average hydraulic gra-

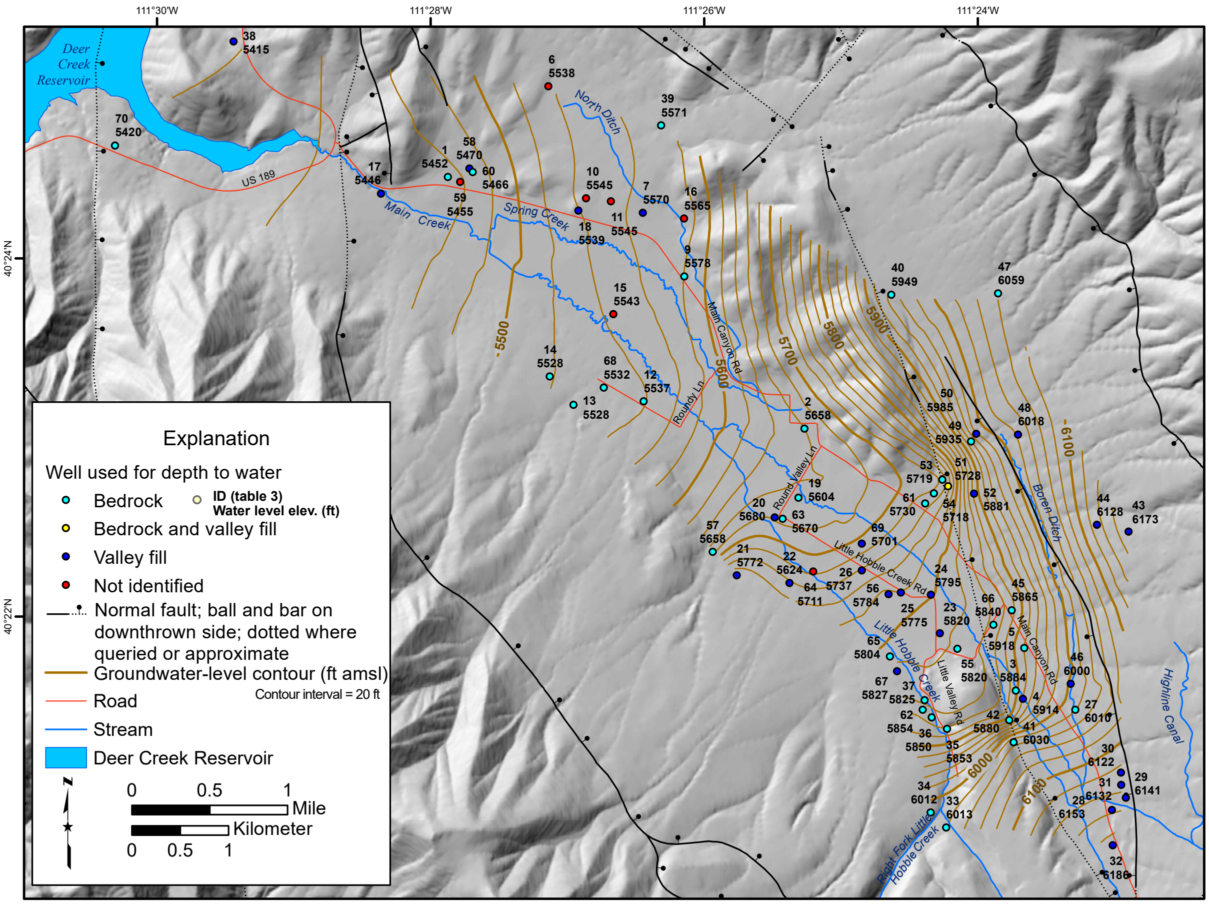

Figure 21. Groundwater-level elevation of Round Valley. See table 3 for details and links to well records for each well. Hillshade base map and street data from the Utah Automated Geographic Reference Center (2019).

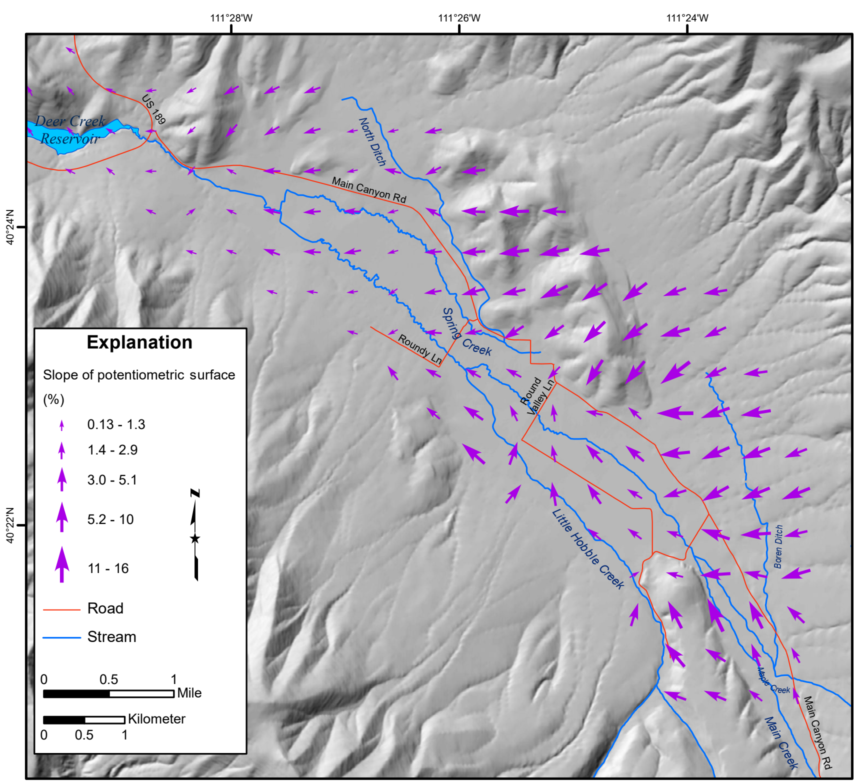

Figure 22. Direction and magnitude of groundwater gradient (derived from figure 21). Hillshade base map and street data from the Utah Automated Geographic Reference Center (2019).

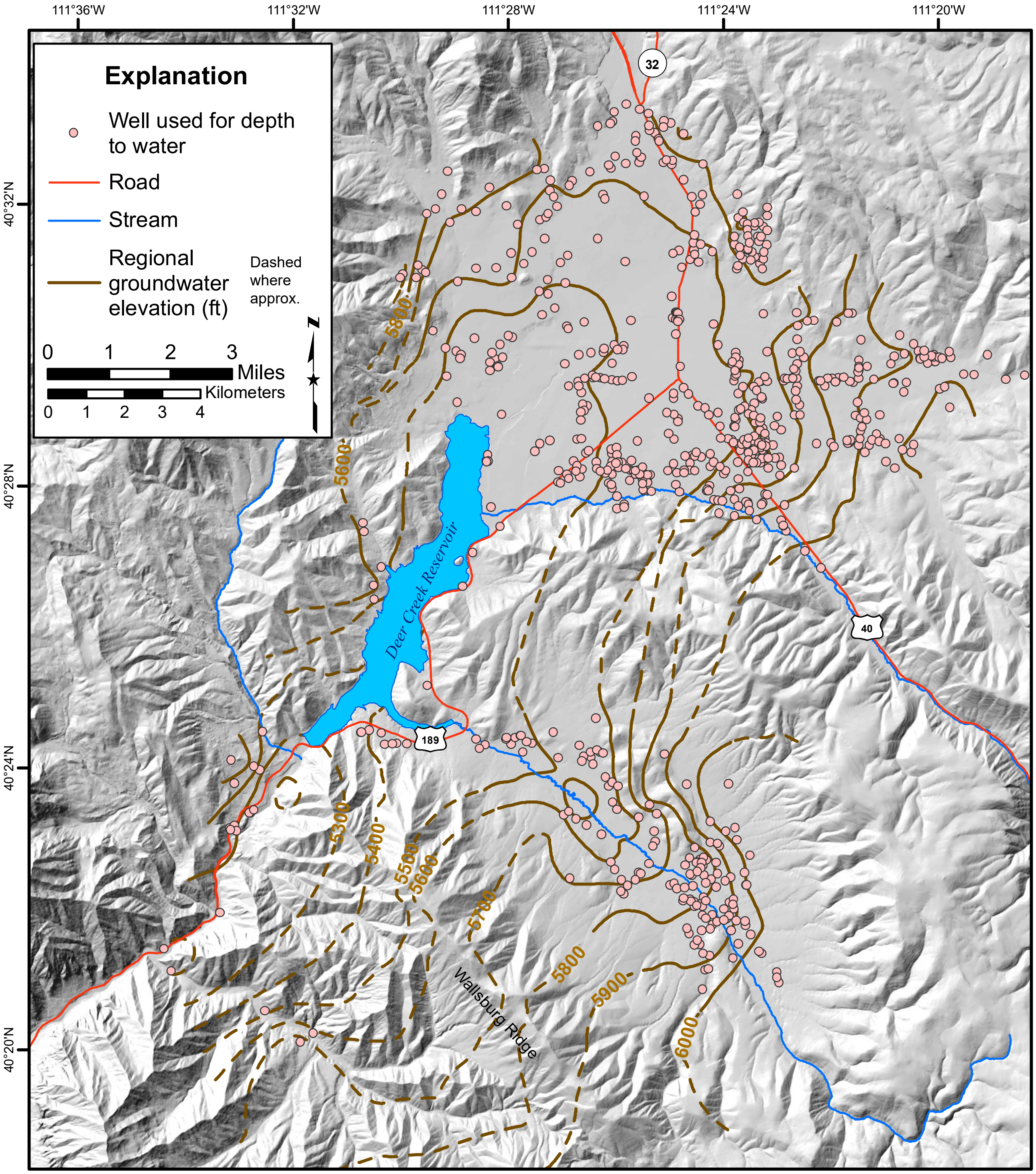

Figure 23. Regional groundwater depth derived from Utah Division of Water Rights data (Utah Division of Water Rights, 2019). Hillshade base map and street data from the Utah Automated Geographic Reference Center (2019). Note that dashed contours are not supported with data and may not support groundwater elevations in bedrock.

dient of the interpolated area is 0.03, where highest gradients are in the east and lowest near Dear Creek Reservoir (figure 21). The average gradient in the east may be greater due to the deflection of the potentiometric surface across the mapped faults, which, as discussed above, likely locally compartmentalize groundwater in the valley.

In some areas of the valley, the potentiometric surface intersects the ground surface (figure 24) within the uncertainty of the land-surface elevation (about 5 ft [1.55 m]). Evidence of shallow groundwater in these areas includes seeps and springs, hydrophilic (wetland-type) plants, and gaining sections of creeks. Flowing wells near well 18 and land owners'

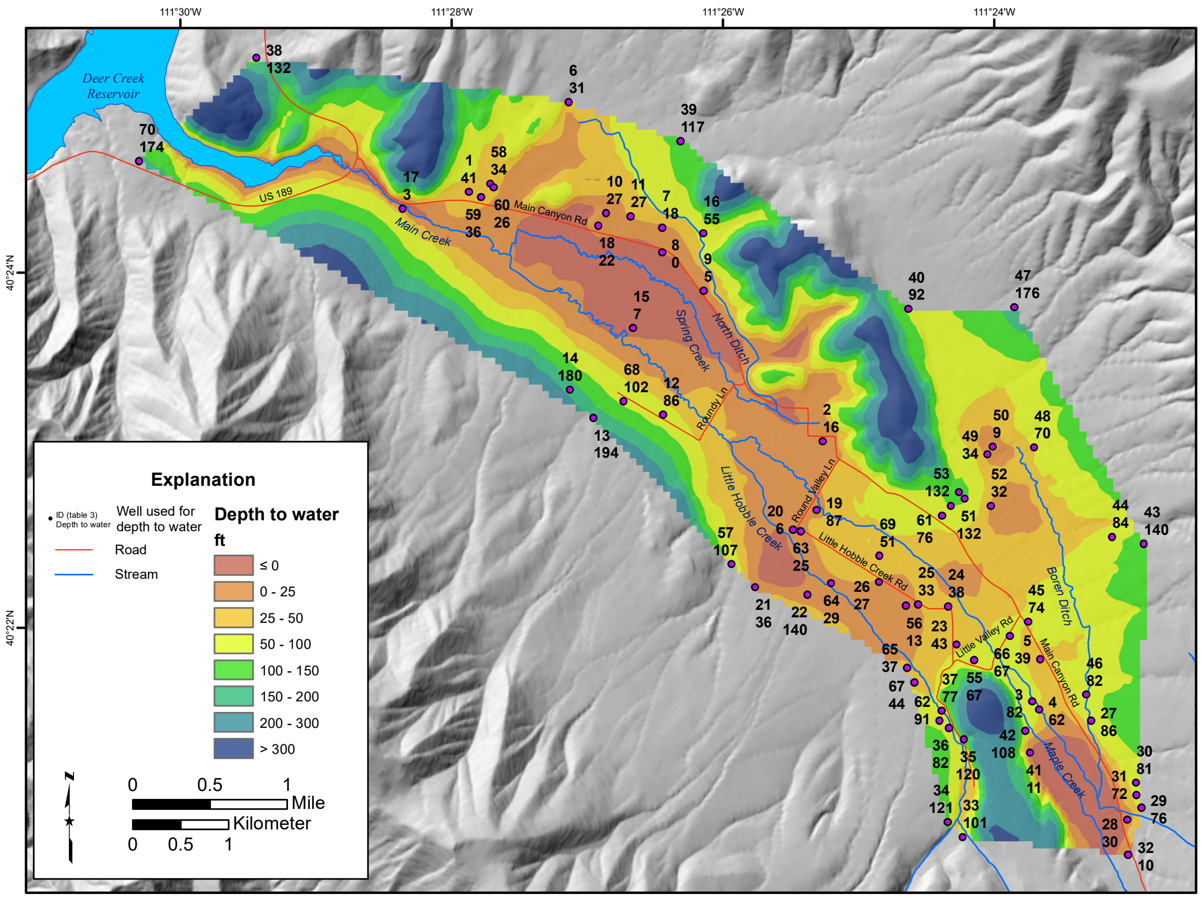

Figure 24. *Depth to water in Round Valley derived from groundwater-level contours on figure 21 and land-surface elevation (U.S. Geological Survey, 2015).*

reports of recently installed septic tanks rising to the land surface near well 22 indicate shallow groundwater just north of well 18. The flowing wells indicate that groundwater is likely locally confined in some parts of the valley, but lack of correlatable clay layers in the available well logs suggests that the confinement is not widespread.

Regional groundwater elevations indicate that groundwater divides generally follow topographic divides (figure 23). Significant amounts of groundwater do not likely flow from adjacent Heber Valley to Round Valley, nor does water enter or leave the watershed to the south or east. However, these groundwater divides are based on limited data and the assumption that the various aquifers are hydraulically connected.

Groundwater Hydrographs

The monthly USGS data (figure 25A) show that regional water levels are generally highest in June and lowest in January. This trend could be explained by a rapid response to spring snowmelt and lack of precipitation as rain in other months. The seasonal measurements collected by the USGS in the late 1980s do not show this general trend (figure 26).

There is no visually discernable trend in long-term regional variations in water level (figure 25B). There are spikes in the data, including one in 1951–53, one in the mid-1980s, and one in the late 1990s, as well as dips in the water levels in the mid-to late 1950s, early 1990s, and early and late (not mid-) 2000s. However, I did not apply tests to determine if these variations are statistically significant. The average deviation from mean water levels did not exceed 10 feet over the period of examination, which supports the validity of the regional groundwater elevation map made from water levels recorded on different dates (figure 23).

Surface Water Hydrographs

Flow measurements of streams and springs are essential to understanding a basin-wide hydrologic budget. Hydrologic data from several other studies were combined with measurements from this study. Each set of measurements provides valuable estimates of the amount of water leaving the Round Valley basin.

The most comprehensive discharge record is from USGS gage 10158500 at the mouth of Round Valley. The average discharge from 1938 to 1950 was 9626 acre-feet per year (ac-ft/yr) (13.3 cfs; 377 L/s); the maximum discharge was 19,384 ac-ft/yr (26.8 cfs; 758 L/s) and the minimum discharge was 3369

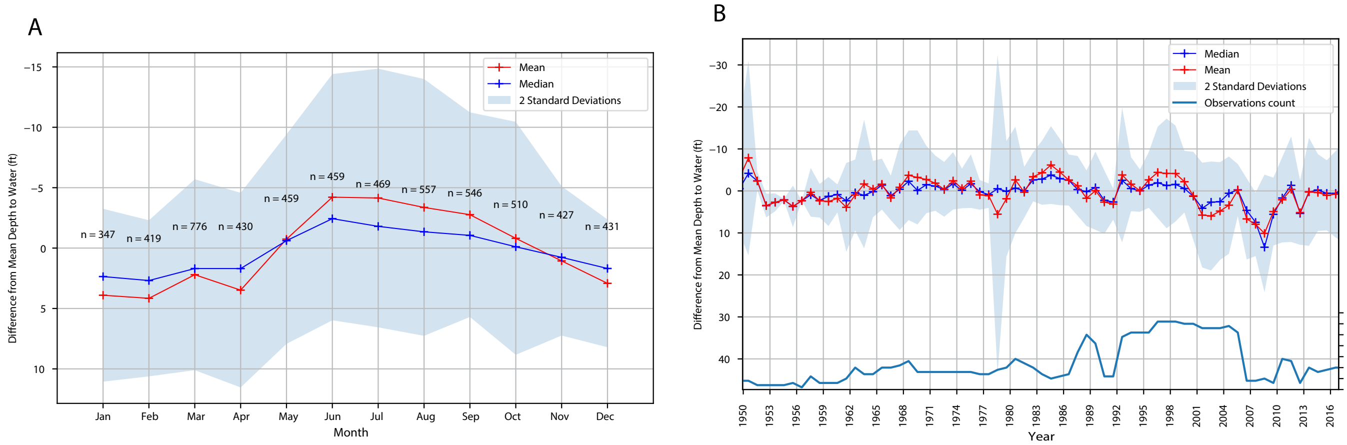

Figure 25. A. *Monthly regional trend of groundwater levels in the Provo River watershed (n = number of observations) and* ***B.*** *long-term regional trend for all USGS wells in the Provo River watershed (U.S. Geological Survey, 2019).*

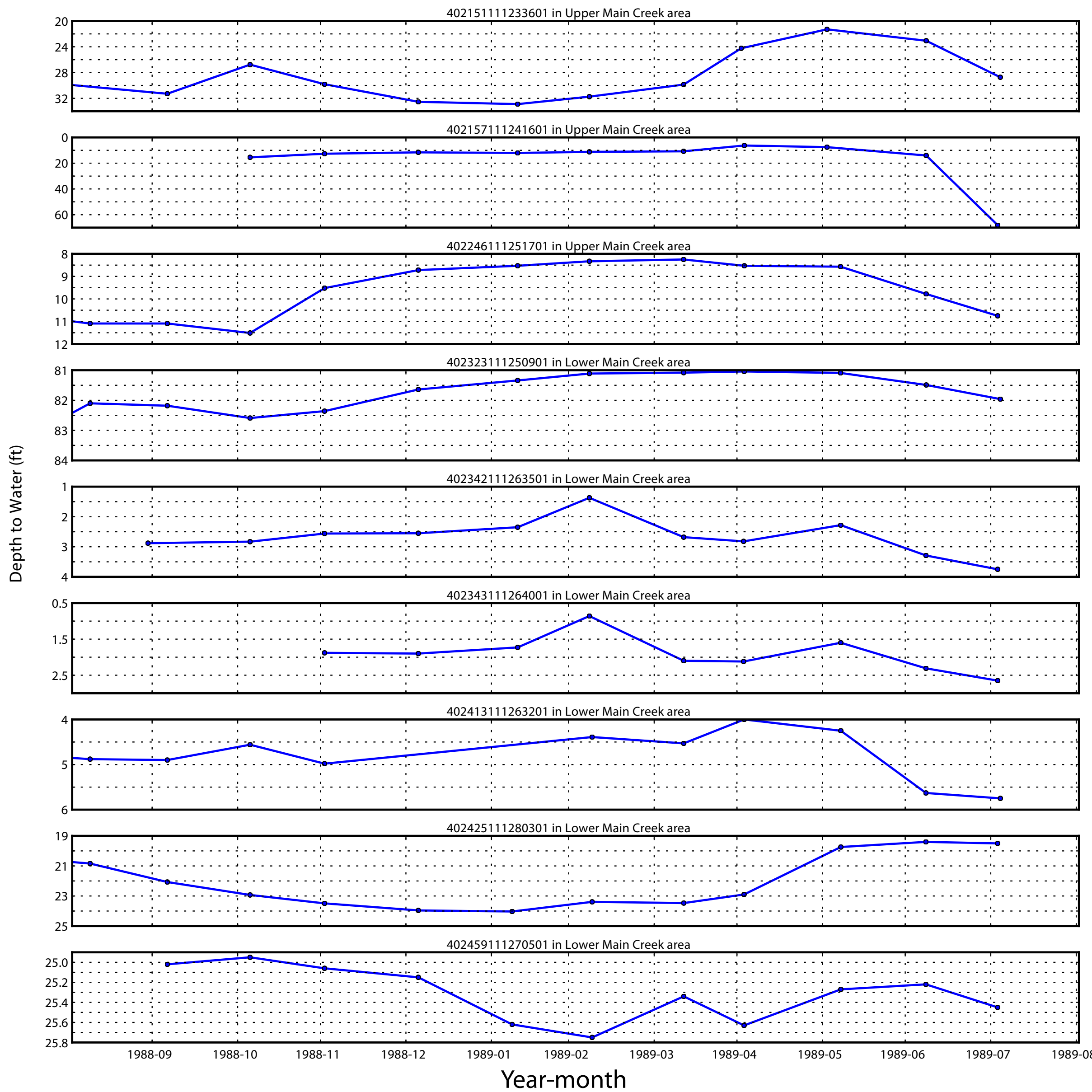

Figure 26. *Hydrographs of monthly groundwater levels measured in wells in Round Valley by the USGS from 1988 to 1989.*

ac-ft/yr (4.65 cfs; 132 L/s) (figure 5). Based on the Eckhardt (2005) method, average baseflow for this period was 2000 ac-ft/yr (2.76 cfs; 78.2 L/s), about 50% of the average discharge. The USGS measurements were recorded prior to the filling of Deer Creek Reservoir, which is immediately downstream of the gage. Changes in the local base level of Main Creek could have impacted the hydrologic system in a way that makes the USGS measurements unrepresentative of the current system.

The Utah DEQ also provided semi-continuous records for sites near the mouth of Round Valley (figure 27). Average volume leaving Main Creek for water year 2015 is 4600 ac-ft/yr (6.35 cfs; 180 L/s), with an estimated baseflow of 2900 ac-ft/yr (4 cfs; 113 L/s) (figure 28). Their discharge measurements show no prominent spring runoff, which is comparable to low-precipitation years measured by the USGS (i.e., 1940 and 1944). Their data also show multiple discharge spikes, which are assumed to be erroneous spikes introduced by ice forming on the creek, but which could potentially represent actual high-flow events.

Allred and Bio-West (2013) provided discharge data along Main Creek for part of 2013 (figure 13). From March to November of 2013, Main Creek released 1154 ac-ft (0.0014 km^3) of water. Assuming January and February discharges for that year were comparable to March (100 ac-ft/mo [1.66 cfs; 47 L/s]), the total discharge for Main Creek in 2013 was about 1400 ac-ft/yr (1.9 cfs; 55 L/s). However, there are several gaps in these data, especially for site 6 (figure 29). Allred and Bio-West (2013) measured higher flows at site 1 in upper Main Creek than at site 6 at lower Main Creek (figure 29A; figure 13) during peak runoff, which can be attributed to diversion of the creek to irrigation as well as loss in the stream to recharge in the aquifer. While some of the water loss could be attributed to evapotranspiration from crop use, the recharged water should reappear as discharge at the mouth of Main Creek, assuming that negligible groundwater is leaving the valley to Deer Creek Reservoir. The total loss between these points for the months of May and June is 720 acre-feet. During other months (during baseflow), site 6 has higher discharge.

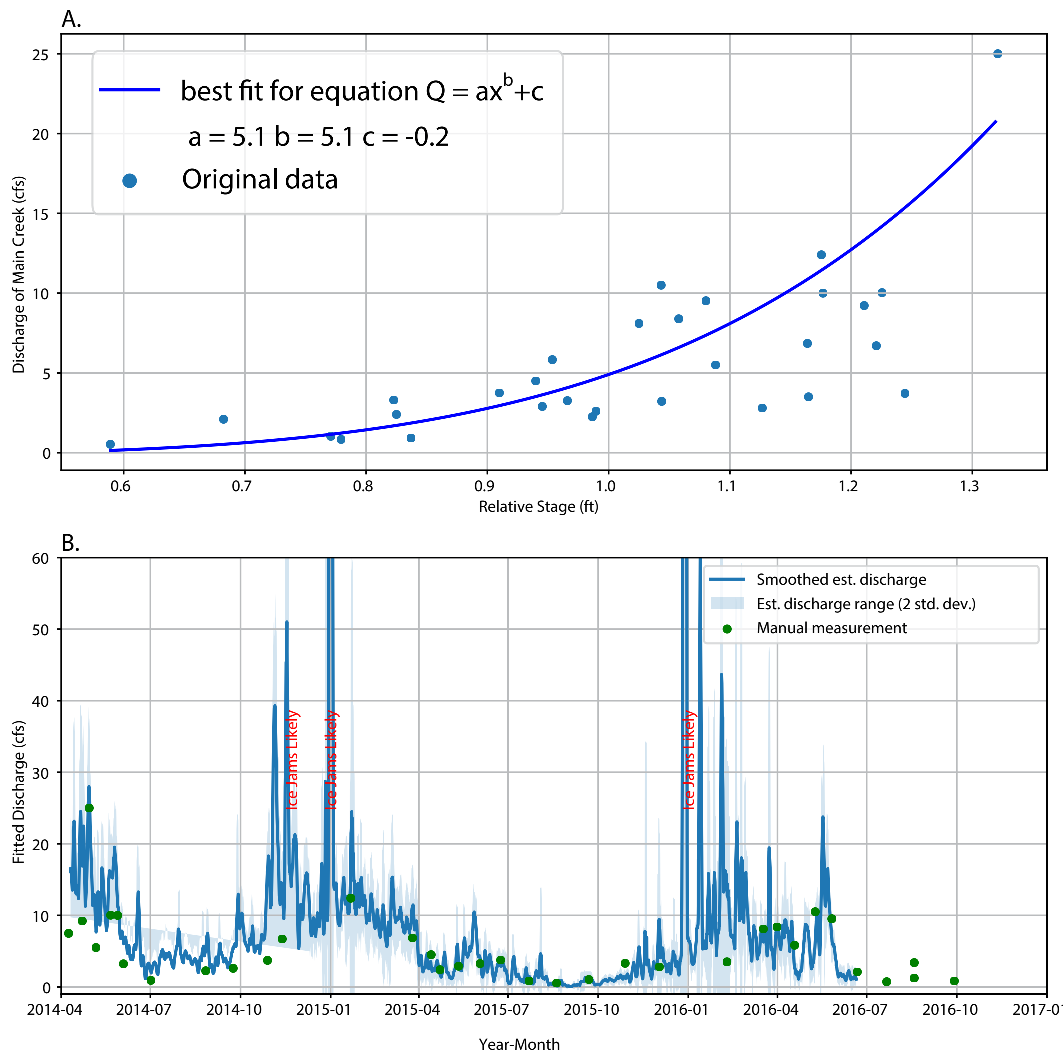

Figure 27. A. *Stage-discharge relationship at UDEQ site 5910619 (Main Creek 0.4 mile above U.S. Highway 189 at driveway bridge). The stage-discharge relationship was established using manual measurements and concurrent transducer readings.* ***B.*** *Estimate of discharge over time (bottom) on Main Creek near Deer Creek Reservoir from UDEQ raw data.*

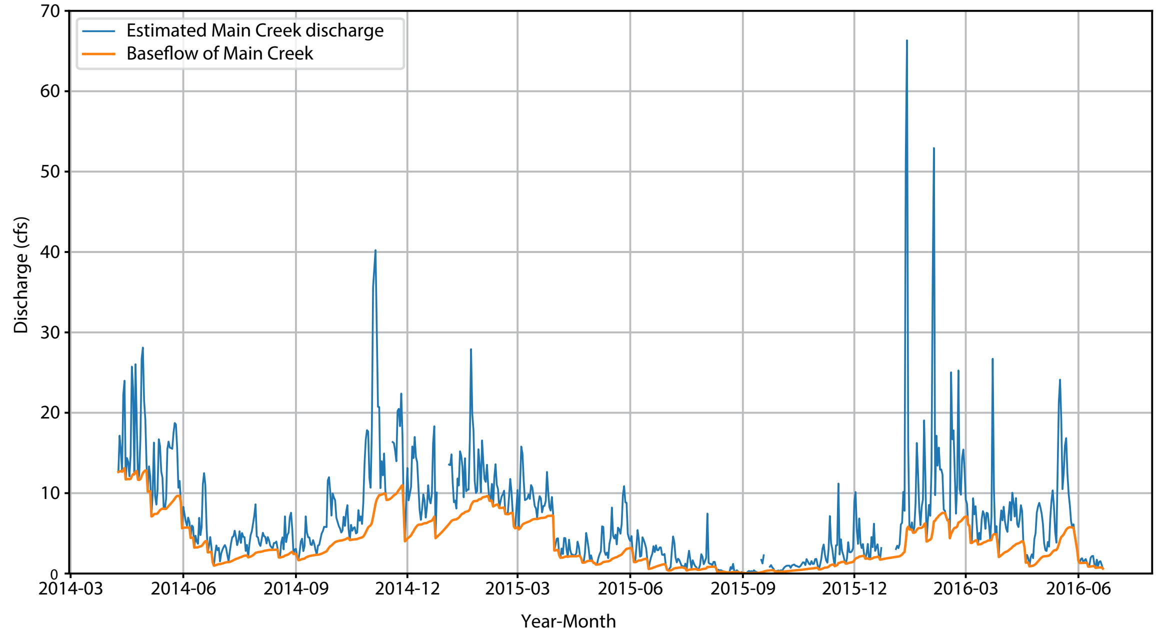

Figure 28. *Estimated discharge and baseflow of lower Main Creek based on UDEQ transducer readings.*

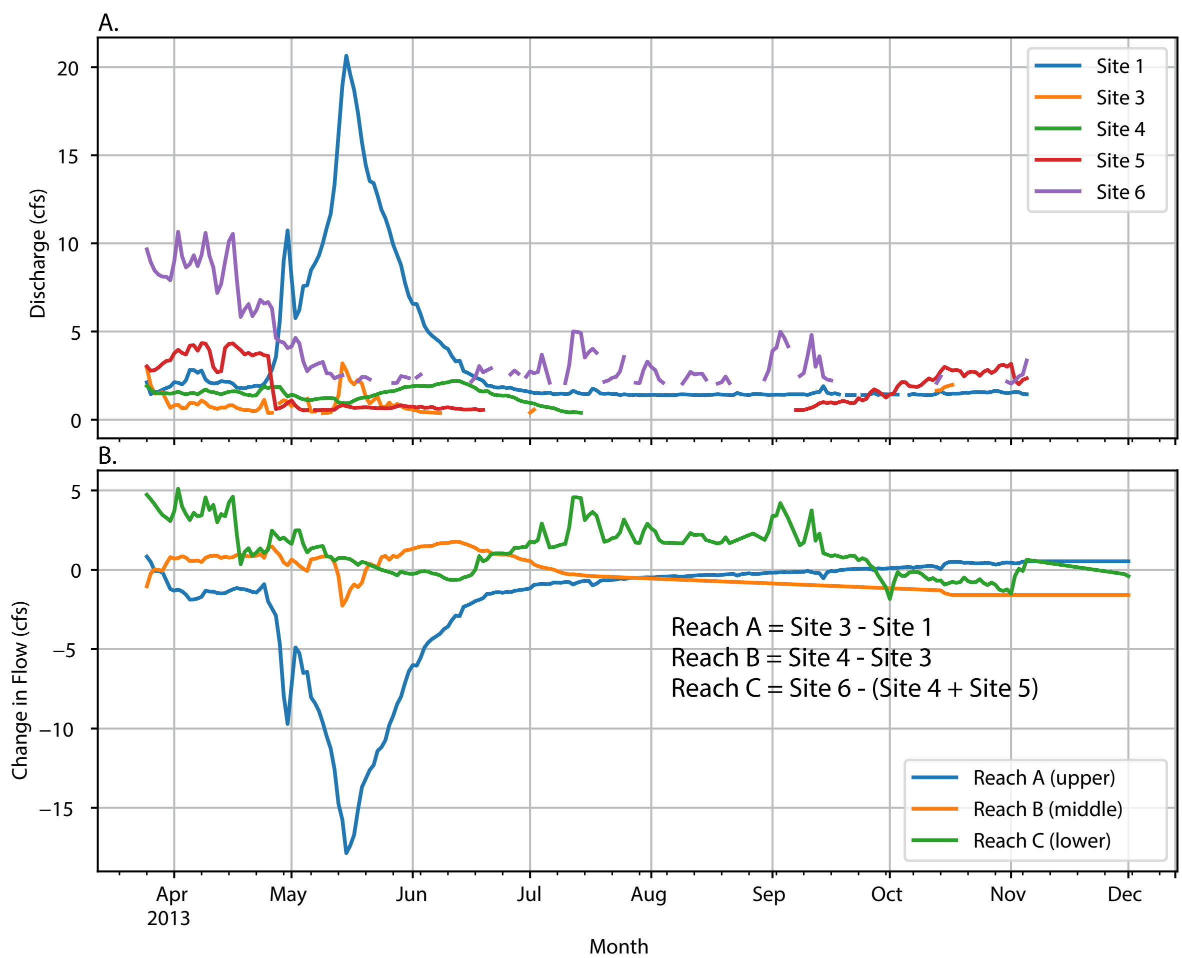

Figure 29. *Seepage loss hydrograph for different segments of Main Creek from Allred and Bio-West (2013).* ***A.*** *Discharge along Main Creek in 2013 and* ***B.*** *change in flow along Main Creek 2013.*

This study also produced discharge data for streams in Round Valley (table 5). Of the four sites I measured for this study, three produced semi-reliable discharge estimates. Estimated discharge for the mouth of Main Creek from August 2016 to August 2017 is 15,000 ac-ft/yr (587 L/s), with an estimated baseflow of 7000 ac-ft/yr (9.7 cfs; 274 L/s). Little Hobble and Spring Creek contributed 3100 and 1500 ac-ft/yr, respectively. Unfortunately, data from Upper Main Creek were compromised by an unreliable discharge measurement site. Lack of high-discharge manual measurements for the stage-discharge relationships makes the estimates for the higher discharges less reliable than the estimates for the lower discharges.

Spring Creek was measured at the discharge point for the spring that feeds it. Based on my measurements, the discharge for this spring is relatively stable over time. This could imply that the spring comes from a bedrock source where seasonality is attenuated. However, more chemistry data and flow data should be collected to better constrain the sources of Spring Creek spring.

Table 5. *Estimated discharge data measured by the UGS for three stream sites in Round Valley.*

Year	Month	Little Hobble (ac-ft)	Spring Creek (ac-ft)	Lower Main (ac-ft)	Lower Main baseflow (ac-ft)
2016	Aug	10	58	32	30
2016	Sep	29	112	177	127
2016	Oct	36	107	233	144
2016	Nov	27	92	250	158
2016	Dec	35	75	607	229
2017	Jan	67	113	1055	429
2017	Feb	2	129	1922	673
2017	Mar	780	150	1968	925
2017	Apr	944	212	2369	1251
2017	May	763	143	3575	1608
2017	Jun	314	155	2022	1093
2017	Jul	47	159	394	332
2017	Aug	16	24	47	40
Total		3070	1529	14,651	7036

Flow duration curves for Main Creek show that the recent flow measurements by the Utah DEQ and Allred and Bio-West (2013) are lower than the USGS historical averages (figure 30). UGS flow measurements are higher than historical flows, reflecting that precipitation for 2017 was much higher than averages over the past 80 years (figure 31). Low flow (<3 cfs) measurements by the UGS are also lower than the USGS values, despite the higher than normal precipitation during the UGS measurement period. The older USGS data may not be entirely representative of the system because Deer Creek Reservoir was filling during the measurement interval.

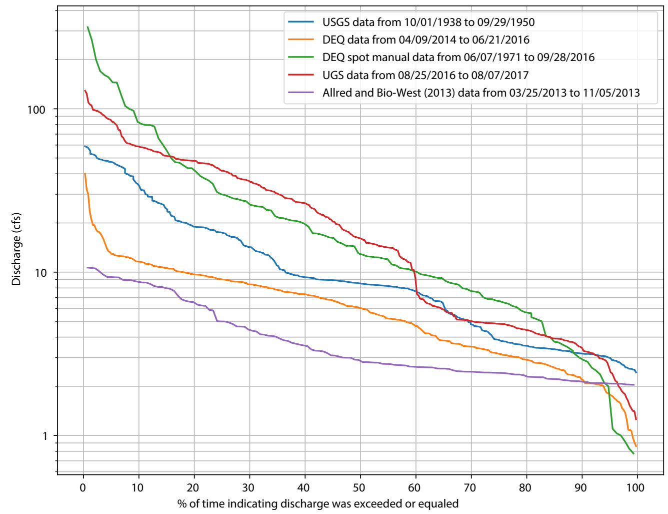

Figure 30. *Flow duration curves for data collected near the mouth of Main Creek.*

Hydrologic Budget

A preliminary hydrologic budget was created to better understand the amount of water available in Round Valley. The hydrologic budget calculated for this study produced similar estimates of inflows and outflows as the Roark and others (1991) study. However, this study also provides surface-water values, and used different methods to estimate some of the components of the groundwater budget. This study produced a total basin budget and a more specific groundwater budget. Most results for both budgets are derived from the UBM but checked and supported by other measured data like the stream discharge measurements and remotely-sensed (satellite-based) evapotranspiration.

Precipitation and Evapotranspiration

The two biggest components of a basin budget are precipitation and evapotranspiration. Precipitation is the driving factor in the hydrologic budget of Round Valley. From 2000 to 2017, the compiled PRISM Climate Group (2018) data (table 6) indicate that the amount of precipitation in Round Valley averaged 88,000 ac-ft/yr (122 cfs; 3442 L/s), ranging from 65,000 (2001) to 145,000 (2011) ac-ft/yr (90-200 cfs; 2542-5671 L/s). The standard deviation of the data is 22,000 ac-ft/yr. The variation in precipitation can result in widely different average annual discharges of Main Creek, as observed in the compiled hydrographs (figure 31). The accuracy of UBM hinges on the reliability of the available water input, which is the PRISM data. However, the precipitation results must be taken with some caution, as there is no physical precipitation gage in Round Valley, only gages in Heber Valley, Deer Creek Reservoir, and a SNOTEL station (435: Daniels-Strawberry) immediately east of the headwaters of Main Creek. Data for the basin were interpolated between stations and adjusted for elevation based on a regression equation by the data provider, the PRISM Climate Group.

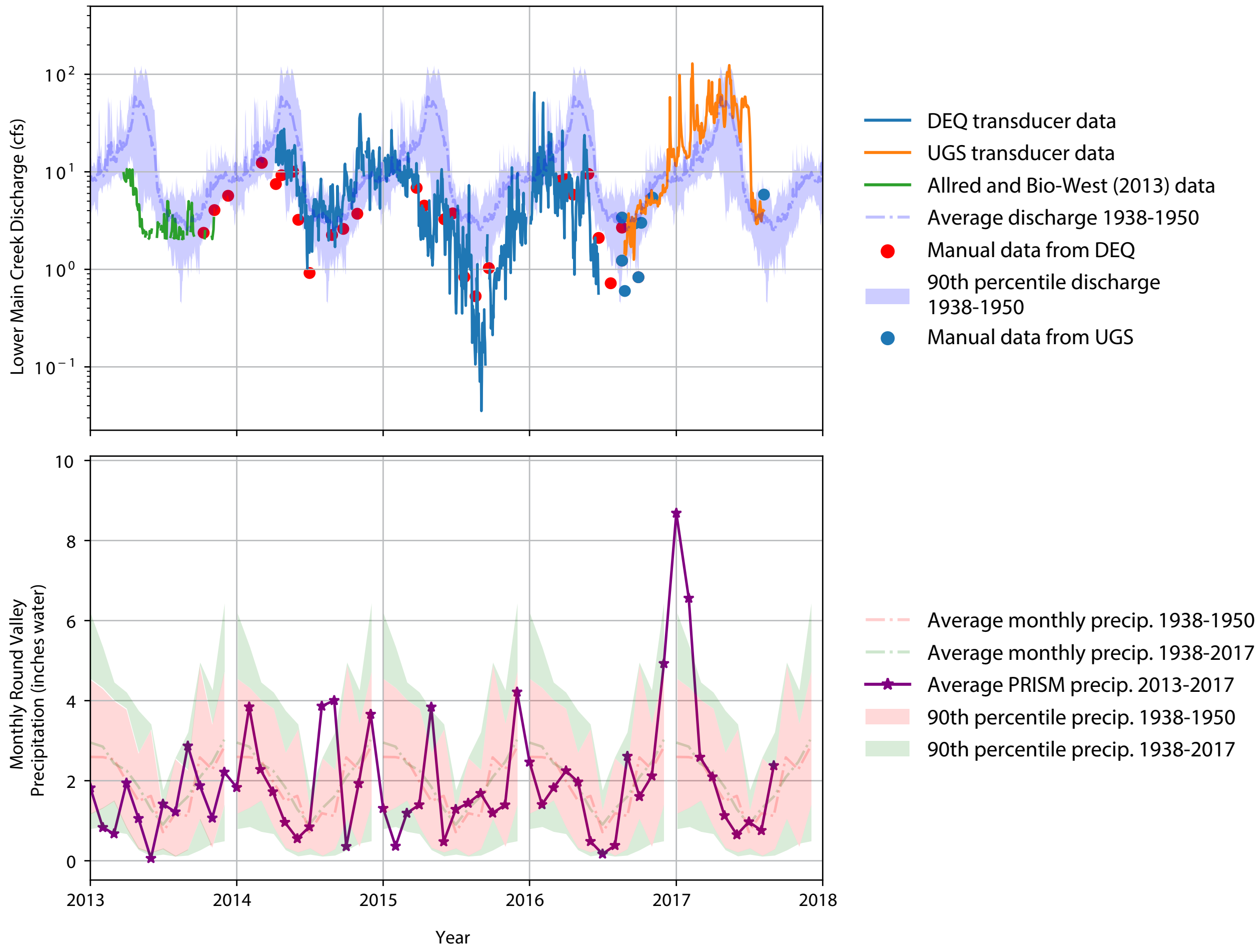

Figure 31. *Compiled discharge (top) and precipitation (bottom) compared to the historical 1938 to 1950 data.*

Table 6. *Precipitation estimates from the PRISM Climate Group (2018) from 2000 to 2017.*

Water Year	Watershed (HUC 12[1])			Bedrock Area	Valley Fill Area	Valley Total
	Little Hobble Creek (160202030402)	Upper Main Creek (160202030403)	Main and Spring Creek (160202030404)			
	ac-ft/yr	ac-ft/yr	ac-ft/yr	ac-ft/yr	ac-ft/yr	ac-ft/yr
2000	15,251	32,000	17,074	46,984	18,261	65,245
2001	14,865	33,161	16,180	47,435	17,587	65,021
2002	16,767	35,885	18,484	52,418	19,674	72,092
2003	16,267	34,613	18,622	50,575	19,885	70,460
2004	18,583	40,289	20,510	58,293	22,128	80,421
2005	28,785	58,949	32,923	87,774	34,669	122,444
2006	23,182	48,914	26,303	71,925	27,902	99,827
2007	16,342	35,412	17,806	51,246	19,231	70,477
2008	19,397	42,483	21,938	61,597	23,399	84,996
2009	23,129	48,671	26,308	71,627	27,866	99,493
2010	17,957	39,404	19,477	56,833	20,991	77,824
2011	33,603	69,993	38,910	103,242	41,332	144,574
2012	14,992	31,828	16,976	46,612	18,092	64,704
2013	16,223	34,692	18,457	50,630	19,692	70,321
2014	21,383	45,013	23,387	65,720	25,250	90,971
2015	16,182	33,578	18,389	49,521	19,535	69,056
2016	16,896	36,371	19,105	53,027	20,327	73,354
2017	24,544	52,779	29,086	77,055	30,911	107,966

[1]*Hydrologic Unit Code - defines a stream drainage area*

Evapotranspiration, the other large component of the basin-wide budget, does not have as much relative variation as precipitation. The standard deviation of the UBM output is 13,000 ac-ft/yr (18 cfs; 508 L/s), whereas the standard deviation of the MODIS16 data from 2004 to 2017 is 6200 ac-ft/yr (8.6 cfs; 243 L/s). The average estimated actual evapotranspiration from the UBM is 77,000 ac-ft/yr (106 cfs; 3012 L/s) (table 7). The MODIS16 estimate for average basin-wide actual evapotranspiration from 2004 to 2017 is 84,000 ac-ft/yr (116 cfs; 3286 L/s).

Runoff

Average runoff for the basin is assumed to be equivalent to the discharge of Main Creek where it leaves the valley. The UBM estimated the basin average runoff for water years 2001 to 2017 to be 9400 ac-ft/yr (13 cfs; 368 L/s), which is about twice that of the 2015 Utah DEQ estimate of 4600 ac-ft/yr (6.4 cfs; 180 L/s) and compares favorably to the average discharge measured at USGS station 10158500 of 8515 ac-ft/yr (12 cfs; 333 L/s). The UGS measurement for 2017 was 15,000 ac-ft/yr (21 cfs; 587 L/s) (table 7), but was for a water year with above-average precipitation (table 6). Also, the ratio of discharge between Little Hobble Creek and the mouth of Main Creek is favorable at 21% for the UGS flow measurements and 23% for the UBM.

Although more than half of the flow is supplied by groundwater baseflow, surface water supplies are heavily dependent on the yearly availability of incoming precipitation. Years having lower than average precipitation result in many of the segments of Little Hobble and Main Creek being dry, especially near the center of Round Valley. This modeled output implies that the recharge-to-baseflow flow is relatively fast.

Table 7. *Output of hydrologic components from the Utah Basin Model (UBM) for calendar years 2004 through 2017.*

	Watershed (HUC 12[1])					
	Little Hobble Creek (160202030402)	Upper Main Creek (160202030403)	Main and Spring Creek (160202030404)	Bedrock	Valley Fill	Valley Total
	ac-ft/yr	ac-ft/yr	ac-ft/yr	ac-ft/yr	ac-ft/yr	ac-ft/yr
Actual Evapo-transpiration	17,954	38,020	20,449	56,250	21,191	77,441
Available Soil Water	29,597	65,727	21,652	105,591	11,808	117,399
Precipitation	19,686	41,891	22,219	61,251	23,707	84,958
Recharge	1868	3484	1736	5461	1745	7206
Runoff	377	1506	623	1253	1306	2559
Recharge and Runoff	2245	4990	2358	6714	3051	9765

[1]Hydrologic Unit Code - defines a stream drainage area

Groundwater

Due to the limited scope of this study, not all groundwater budget components were estimated at high precision for Round Valley. However, I did produce a groundwater budget for comparison to the Roark and others (1991) budget (table 8). My estimated infiltration from precipitation (based on the UBM) is lower than that estimated by Roark and others (1991) due to the difference in how precipitation is calculated. For the entire basin, the UBM shows that recharge is highest during times of spring runoff and increased precipitation, and that the recharge is focused in the mountains (figure 32).

Well Data

Well Statistics

Well development has increased significantly since Roark and others (1991) conducted their study. From 1970 to 1980, the number of registered identifiable wells in Round Valley increased from 5 to about 65 (figure 33). From 1980 to 1992, the number of registered wells did not increase significantly. From 1992 to present, the number of registered wells has increased logarithmically, increasing quickly at first in the 1990s and appearing to taper off more recently. Currently, there are 196 well logs with well completion dates. There are more than 196 wells in Round Valley, as some of the wells do not have well logs or are not identified in the Utah Division of Water Rights Records.

Well construction statistics show the median reported depth to water and screen bottom depth in Round Valley are 35 and 192 feet (11 and 58.5 m), respectively, signifying that most wells in Round Valley derive their water from this interval (figure 34). Cones of depression that intersect this interval have a higher probability of impacting wells in the valley, depending on the shape of the cone of depression.

Table 8. *Groundwater budget for Round Valley.*

		Roark & Others (1991)	This Study
		ac-ft/yr	ac-ft/yr
Recharge	Precipitation	2172	1740
	Stream Infiltration	3620	4100
	Unconsumed Irr. Water	1448	600
	Subusurface Inflow	724	539
	Total	**7964**	**6979**
Discharge	Evapotranspiration	1303	1059
	Springs and gaining streams	6516	5340
	Wells	145	500
	Subsurface Outflow to consolidated rocks	0	80
	Total	**7964**	**6979**

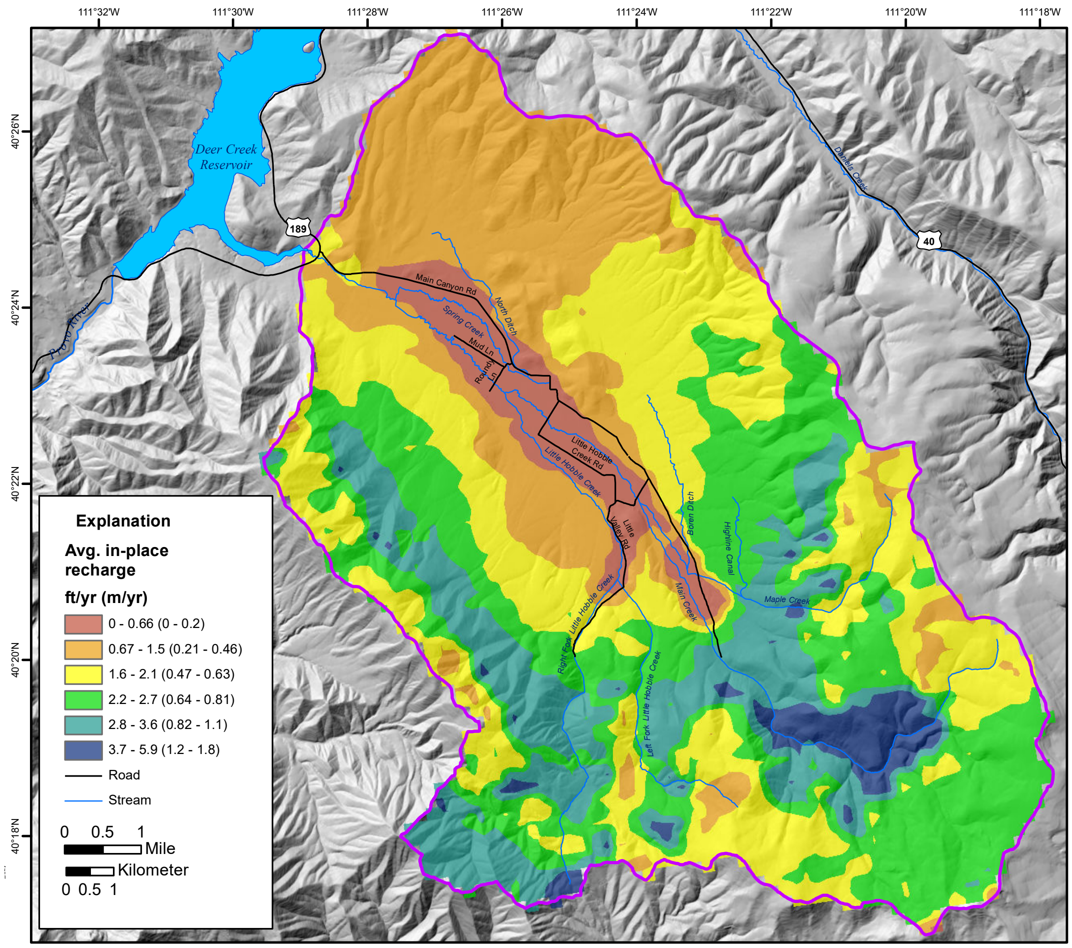

***Figure 32.** Distribution of average annual recharge for Round Valley from the Utah Basin Model (UBM) from 2004 to 2017. Hillshade base map and street data from the Utah Automated Geographic Reference Center (2019).*

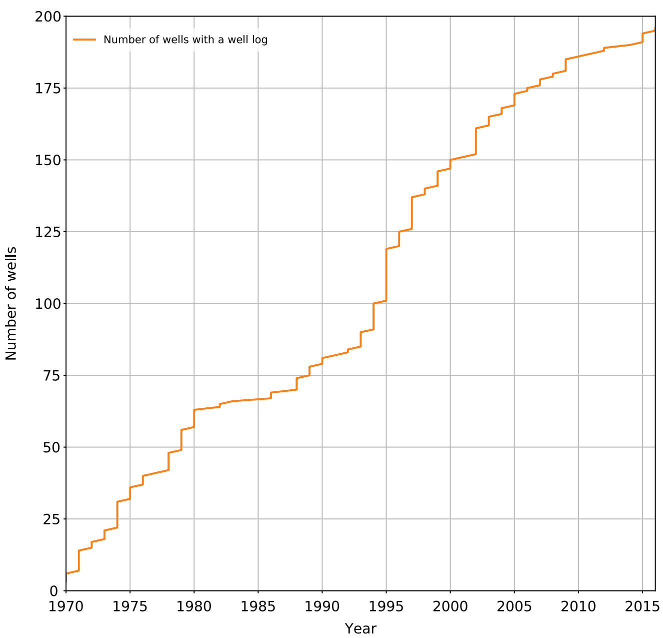

***Figure 33.** Number of recorded wells in Round Valley from 1970 to 2016.*

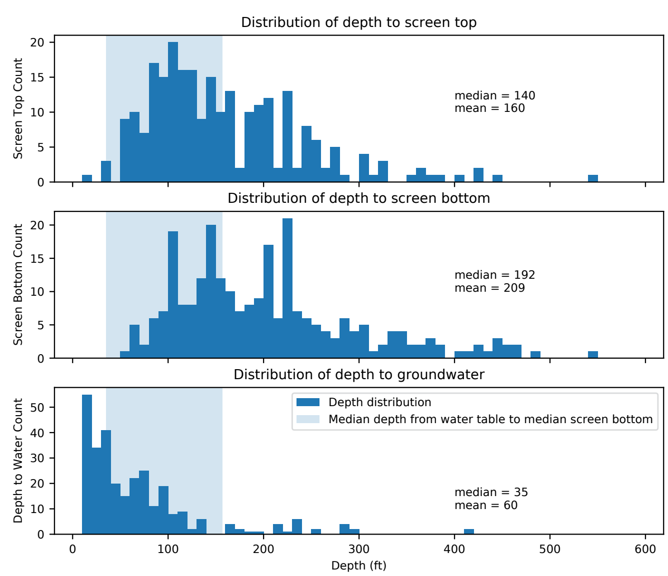

***Figure 34.** Statistics on well construction.*

Basin Depth

Unconsolidated valley-fill thickness varies significantly over the area of Round Valley. The thickest unconsolidated material is in the southeast part of the valley (figure 35; plate 1). Normal faults in this region create a graben and half graben having very deep depths to bedrock. One well log in this area (WIN 433315) indicates a depth to bedrock of 800 feet (245 m), but the description may be suspect due to the expected nature of the material in the alluvial fan. Total thickness of valley fill in the east part of the valley is very difficult to know due to limited well information. Near the northeast valley-bounding fault, the alluvial fan material is likely deeper than 500 feet (152 m). The unconsolidated valley fill in the northeast part of the valley is likely compartmentalized based on the presence of springs and steep gradients observed in water levels. The lack of surface water on the alluvial-fan deposits in the eastern part of the valley could be explained by the thicker and vertically conductive basin material there, which allows precipitation and runoff to percolate down to the water table instead of running off as surface flow.

The depth to bedrock map (figure 35) indicates that there may be another fault that follows the west side of the hill near Wallsburg, which could explain the presence of the large spring that sources Spring Creek and relatively large depths to bedrock near the exposures. Near the paths of Main and Little Hobble Creek, the depths to bedrock are much shallower, about 100 to 200 feet (30–60 m). These depths wedge out to the southeast and near the mouth of the valley.

Due to the heavily fractured nature of the bedrock and the boulder-rich alluvial fans, which are themselves composed of eroded bedrock, it was difficult for me (and I assume drillers) to interpret where the alluvial-fan material ended and the fractured bedrock began. Ambiguous descriptions and similar geology made well-log interpretation challenging. The similar density of the alluvial-fan material to the fractured bedrock makes gravity surveys an ineffective tool to delineate basin-fill thickness.

Aquifer Properties

Transmissivity from specific capacity estimates (figure 36) ranged from 38 ft^2/day to 33,000 ft^2/day (3.5 to 3100 m^2/day). The step-drawdown test (figure 15A) and leaky type curve (figure 15C) showed the aquifer transmissivity to be about 200 ft^2/day (19 m^2/day) and 300 ft^2/day (28 m^2/day), respectively, while the unconfined analysis (figure 15B) produced a transmissivity estimate of 500 ft^2/day (46 m^2/day). The calibrated analytic element model produced an estimate of hydraulic conductivity of 0.6 ft/day (0.2 m/day) for the unconsolidated material and 0.06 ft/day (0.02 m/day) for the bedrock, with only 0.5 days of lag in between the bedrock and unconsolidated sediment layers.

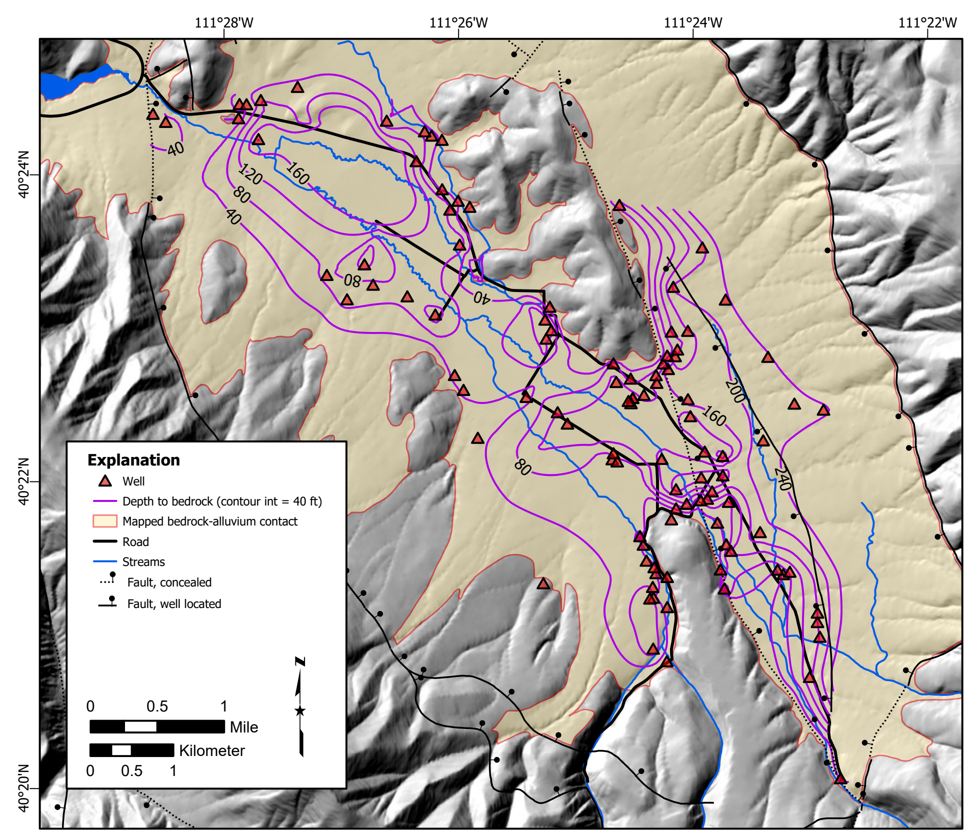

Figure 35. Depth to bedrock in the unconsolidated deposits of Round Valley. Contours are in feet below ground surface. Hillshade base map and street data from the Utah Automated Geographic Reference Center (2019).

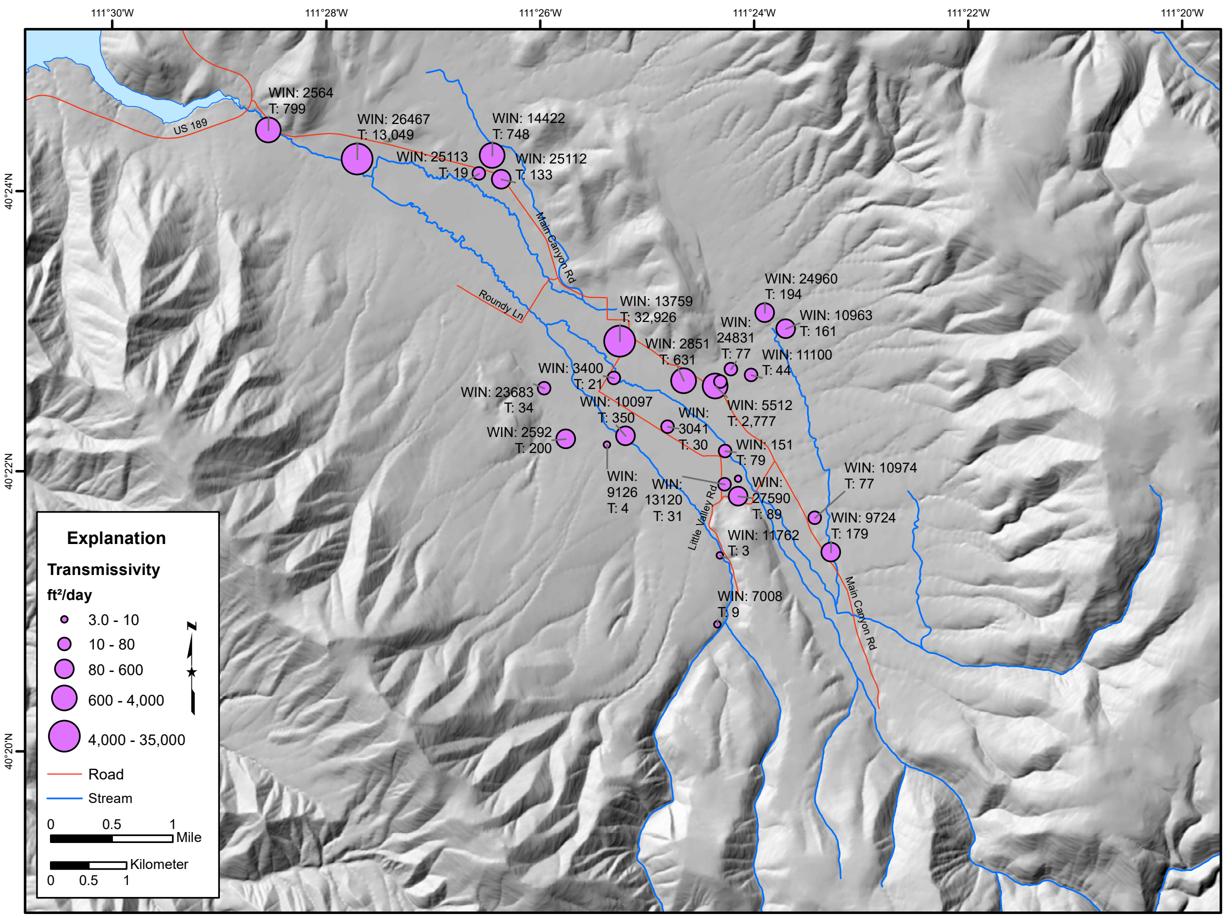

Figure 36. *Estimates of transmissivity from specific capacity.*

Forward Modeling Results

Forward modeling using the analytic element model allowed for first-pass estimates of the effects of additional pumping on the Round Valley aquifer system. Based on the model, drawdown responds proportionately (figure 37) to pumping increases. Adding more wells results in a cumulative effect of the drawdown-to-pumping slope. Adding a large pumping well to the valley results in an average of about 0.01 feet (1 mm) of decline in existing wells per gallon per minute of pumping increase. Removing or reducing recharge in the model drastically increases drawdown, shifting the intercept of the linear relationship. Based on the model, most potential and existing pumping locations appear to have similar impacts on the average drawdown observed in wells, although the hypothetical southeast valley well has a much smaller overall average impact than the other locations. It is worth noting that in every scenario, drawdown is highest near the pumping well and decreases exponentially with radial distance from the well. The input of infiltration from streams and surface water decreases the amount of drawdown, buffering the effects of well pumping on groundwater levels. This effect is due to capture of the stream or surface water by the pumping (assuming a hydraulic connection to the aquifer) and would result in reduced stream flow or surface-water levels, respectively.

DISCUSSION AND SUMMARY

Flow of groundwater in Round Valley is generally from east to west toward Deer Creek Reservoir. The alluvial fill and the Oquirrh Formation in Round Valley are hydrologically connected. Based on contrasting adjacent water levels, at least one fault in the valley likely compartmentalizes the aquifer system. General regional groundwater levels are highest in June and lowest in December but can vary locally. Long-term groundwater levels in the Provo watershed do not show a significant upward or downward trend over the past six decades.

Based on geochemical data, well log examination, cross sections, and aquifer tests, the groundwater and surface water systems appear to be closely connected, so that additional pumping from either the alluvial or fractured bedrock aquifer units would affect the surface water supply. While there are localized confined areas in the valley, there is connection between the aquifer system and the streams. The groundwater budget is currently poorly constrained, but an imbalance in the budget due to low precipitation or increased groundwater pumping will lower the water table, which will reduce stream flow of Main and Little Hobble Creeks. As the local irrigators have transitioned from flood irrigation to pivot irrigation and from unlined streams and canals to piped and lined systems, losses from evaporation of

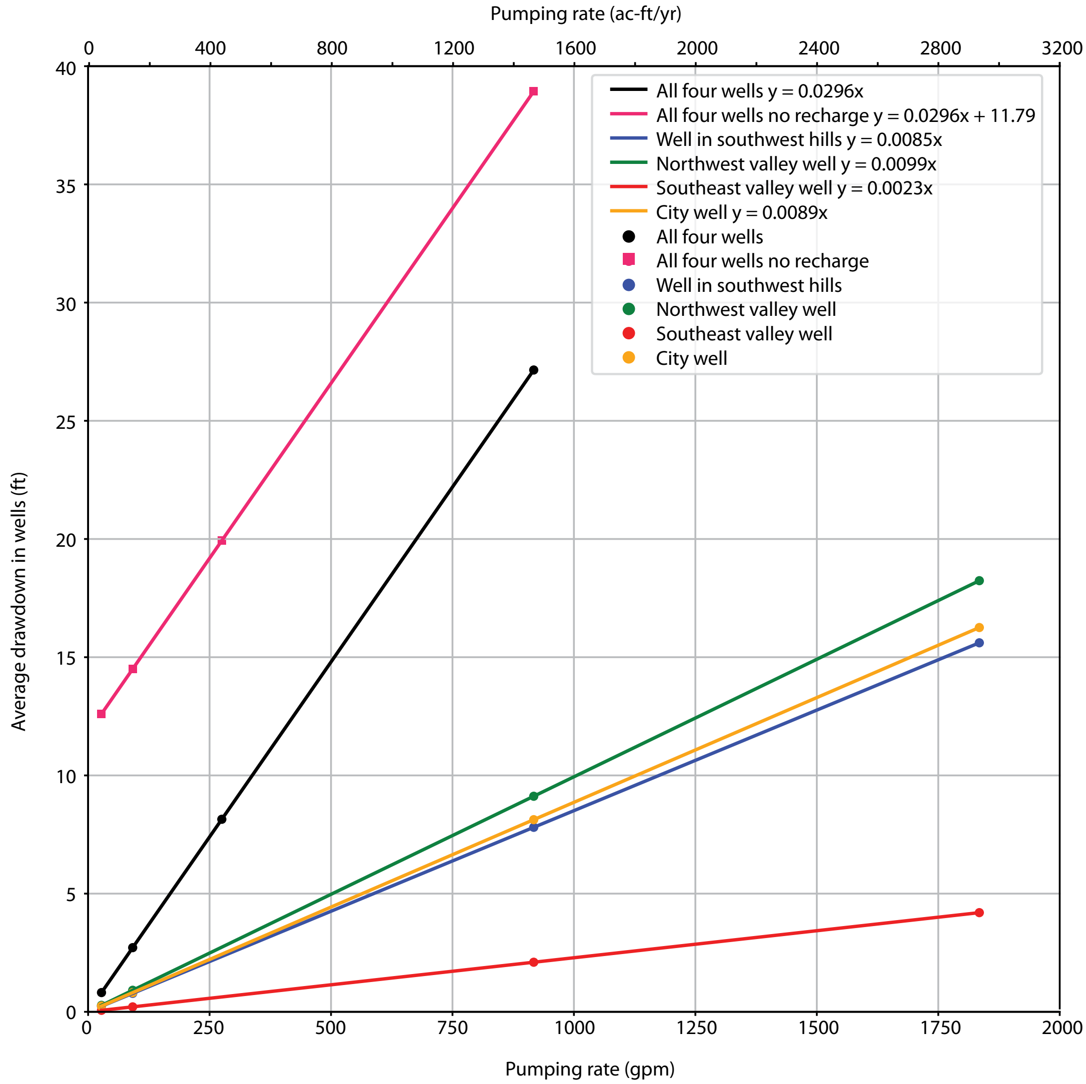

Figure 37. *Results of analytic element forward model with varying pumping scenarios.*

those surface applications have slightly decreased. However, recharge to the groundwater system from irrigation losses and stream and canal seepage have also decreased. With increases in population, groundwater use has also increased, although some of that use is returned to the aquifer by septic systems.

Significant variations in precipitation over time are driving storage fluxes in the Round Valley hydrologic system. Flow hydrographs at the mouth of Main Creek show almost no spring runoff effect during dry years, likely due to less available water and higher diversion demand during drier years. Based on the soil water storage value in the UBM, the soil-water budget appears to be in deficit during dry years and in surplus during wet years, indicating that most of the groundwater recharge to the system occurs during wetter years. While no evidence exists for the mouth of Main Creek going completely dry (though upstream segments have gone dry), the condition is possible if there are several drier-than-average years in combination with the current rate of extraction and diversion.

The fractured sandstone and limestone bedrock beneath the unconsolidated sediments and in the mountain blocks of Round Valley is an important aquifer for the basin. Water stored in this aquifer drives the discharge of the springs and gaining reaches of the headwaters of Main and Little Hobble creeks. More than one-third of the wells examined in this study are screened to the fractured bedrock, which are more wells than thought by previous authors (Roark and others, 1991). The vertical extent of this aquifer is not well defined, as there are not many deep wells in the valley. Because this aquifer is laterally and vertically extensive and is nearly as transmissive as the overlying alluvial aquifer, it will likely be the preferred target for future development. A fractured bedrock aquifer system can be more susceptible to contamination and have less storage than an alluvial aquifer (Franciss, 2010).

ACKNOWLEDGMENTS

Thanks to Wasatch County for providing matching funding for this study. I am especially grateful to Glen Shepherd for helping me access and measure many of the privately-owned wells in Round Valley. Thanks to all the well owners who allowed me to measure depth to water in their wells. Edwin Gibbs provided access to wells at Deer Creek State Park and measurements from his own well. I thank Daniel Gunnell for the tour of the valley and assistance with access to private property. Thanks to Bill Loughlin and Mike Nelson for aquiring the aquifer test data. Thanks to Stan Smith for help with the chemical analyses. Bill Lund and Steven Emerman assisted with reviews of the groundwater level portions of this publication. I appreciate the careful reviews from Bill Loughlin and Janae Wallace, as well as additional review from my colleagues Stephanie Carney, Kimm Harty, Mike Lowe, Hugh Hurlow, Mike Hylland, and Peter Nielsen.

REFERENCES

Allred Restoration and Bio-West, 2013, Main Creek instream flow recommendations report: Unpublished consultant's report prepared for the Utah Reclamation Mitigation and Conservation Commission, 77 p.

Baker, A.A., 1976, Geologic map of the west half of the Strawberry Valley quadrangle, Utah: United States Geological Survey IMAP 931, 11 p.

Baker, C.H., Jr., and Peterson, D.L., 1970, Water resources of the Heber-Kamas-Park City area, north-central Utah: Utah Department of Natural Resources Technical Publication 27, 91 p.

Bakker, M., 2004, Transient analytic elements for periodic Dupuit–Forchheimer flow: Advances in Water Resources, v. 27, no. 1, p. 3–12.

Bakker, M., 2006a, Analytic element modeling of embedded multiaquifer domains: Ground Water, v. 44, no. 1, p. 81–85.

Bakker, M., 2006b, An analytic element approach for modeling polygonal inhomogeneities in multi-aquifer systems: Advances in Water Resources, v. 29, no. 10, p. 1546–1555.

Berg Engineering, 2015, Wallsburg overlay zone: Berg Engineering, Midway Utah, 62 p.

Biek, R.F., and Lowe, M.V., 2009, Geologic map of the Charleston quadrangle, Wasatch County, Utah: Utah Geological Survey Map 236, scale 1:24,000.

Clayton, D., and Kaldor, J., 1987, Empirical Bayes estimates of age-standardized relative risks for use in disease mapping: Biometrics, v. 43, no. 3, p. 671–681.

Constenius, K.N., Clark, D.L., King, J.K., and Ehler, J.B., 2011, Interim geologic map of the Provo 30′ x 60′ quadrangle, Utah, Wasatch, and Salt Lake Counties, Utah: Utah Geological Survey Open-File Report 586DM, scale 1:100,000.

Duffield, G.M., 2007, AQTESOLV for Windows: HydroSOLVE, Inc., Reston Virginia.

Eckhardt, K., 2005, How to construct recursive digital filters for baseflow separation: Hydrological Processes, v. 19, no. 2, p. 507–515.

ESRI, 2017, ArcMap Geographic Information Systems software, v 10.5: Redlands, California.

Flint, L.E., and Flint, A.L., 2007, Regional analysis of groundwater recharge, *in* Stonestrom, D.A., Constantz, J., Ferre, T.P.A., and Leake, S.A., editors, Ground-water recharge in the arid and semiarid southwestern United States: U.S. Geological Survey Professional Paper 1703, p. 29–59.

Flint, A.L., Flint, L.E., Hevesi, J.A., and Blainey, J.B., 2004, Fundamental concepts of recharge in the desert southwest—a regional modeling perspective, *in* Hogan, J.F., Phillips, F.M., and Scanlon, B.R., editors, Groundwater recharge in a desert environment—the southwestern United States: American Geophysical Union Water Science and Application Series, p. 159–184.

Franciss, F.O., 2010, Fractured Rock Hydraulics: Boca Raton, CRC Press, 188 p.

Gesch, D.B., Oimoen, M.J., and Evans, G.A., 2014, Accuracy assessment of the U.S. Geological Survey National Elevation Dataset, and comparison with other large-area elevation datasets—SRTM and ASTER: U.S. Geological Survey Open-File Report 2014–1008, 18 p.

Hantush, M.S., 1961, Drawdown around a partially penetrating well: Journal of the Hydraulics Division of the American Society of Civil Engineers, v. 87, no. 4, p. 83–98.

Hantush, M.S., and Jacob, C.E., 1955, Non-steady radial flow in an infinite leaky aquifer: Eos, Transactions American Geophysical Union, v. 36, no. 1, p. 95–100.

Heilweil, V.M., and Brooks, L.E., 2011, Conceptual model of the Great Basin carbonate and alluvial aquifer system: U. S. Geological Survey Scientific Investigative Report 2010–5193, 191 p.

Hengl, T., 2007, A practical guide to geostatistical mapping of environmental variables: Luxembourg, Institute for Environment and Sustainability, 291 p.

Hintze, L.F., Willis, G.C., Laes, D.Y.M., Sprinkel, D.A., and Brown, K.D., 2000, Digital geologic map of Utah: Utah Geological Survey Map-179, scale 1:500,000.

Houska, T., Kraft, P., Chamorro-Chavez, A., and Breuer, L., 2015, SPOTting model parameters using a ready-made Python package: PLOS ONE, v. 10, no. 12.

Inkenbrandt, P.C., 2018, Python scripts for Round Valley hydrologic study: Online, https://github.com/inkenbrandt/Round-Valley, accessed February 2018.

Isenmann, G., Bellahcen, S., Vazquez, J., Dufresne, M., Joannis, C., and Mose, R., 2016, Stage–discharge relationship for a pipe overflow structure in both free and submerged flow: Engineering Applications of Computational Fluid Mechanics, v. 10, no. 1, p. 283–295.

Johns, J., Pearce, A.W., Robinson, D., and Hansen, N., 2015, Applying a phosphorus risk index in a mixed-use mountain watershed: Proceedings of the Western Nutrient Management Conference, v. 11, p. 117–122.

Loughlin Water Associates, 2017, Nelson Project Appendix B: Loughlin Water Associates Park City, Utah, 39 p.

Lowe, M., and Wallace, J., 1999, The hydrogeology of Ogden Valley, Weber County, Utah, and recommended wastewater management practices to protect ground-water quality, *in* Spangler, L.E., and Allen, C. J., editors, Geology of northern Utah and vicinity: Utah Geological Association Publication 27, p. 313–336.

Lowe, M.V., Wallace, J., and Bishop, C.E., 2000, Analysis of septic-tank density for three areas in Cedar Valley, Iron County, Utah, - A case study for evalutions of proposed subdivisions in Cedar Valley: Utah Geological Survey Water-Resources Bulletin 27, 73 p.

Lowe, M.V., Wallace, J., Kirby, S.M., and Bishop, C.E., 2007, The hydrogeology of Moab-Spanish Valley, Grand and San Juan Counties, Utah, with emphasis on maps for water-resource management and land-use planning: Utah Geological Survey Special Study 120, 141 p.

Moench, A.F., 1985, Transient flow to a large-diameter well in an aquifer with storative semiconfining layers: Water Resources Research, v. 21, no. 8, p. 1121–1131.

Moench, A.F., 1997, Flow to a well of finite diameter in a homogeneous, anisotropic water table aquifer: Water Resources Research, v. 33, no. 6, p. 1397–1407.

Mu, Q., Zhao, M., Kimball, J.S., McDowell, N.G., and Running, S.W., 2013, A remotely sensed global terrestrial drought severity index: Bulletin of the American Meteorological Society, v. 94, no. 1, p. 83–98.

Mu, Q., Zhao, M., and Running, S.W., 2011, Improvements to a MODIS global terrestrial evapotranspiration algorithm: Remote Sensing of Environment, v. 115, no. 8, p. 1781–1800.

National Water Quality Monitoring Council, 2018, Water quality portal: Online, https://www.waterqualitydata.us/, accessed February 2018.

Natural Resources Conservation Service, 2016, SSURGO/STATSGO2—web soil survey: Online, https://websoilsurvey.sc.egov.usda.gov/App/HomePage.htm, accessed December 2016.

Pearce, A.W., 2017, Assessing phosphorus sources with synoptic sampling in the surface waters of a mixed-use, montane watershed: Provo, Utah, Brigham Young University, M.S. thesis, 67 p.

PRISM Climate Group, 2018, PRISM gridded climate data: Online, http://prism.oregonstate.edu, accessed February 2018.

Provo River Water Users Association, 2016, Deer Creek Dam: Online, https://www.prwua.org/provo-river-project-features/deer-creek-dam-and-reservoir/deer-creek-dam.php, accessed December 2016.

Psomas, 2002, Deer Creek reservoir drainage TMDL study: prepared for the Utah Department of Environmental Quality, 92 p.

Roark, D.M., Holmes, W.F., and Shlosar, H.K., 1991, Hydrology of Heber and Round Valleys, Wasatch County, Utah, with emphasis on simulation of ground-water flow in Heber Valley: Utah Division of Water Rights Technical Publication 101, 101 p.

Ronchetti, E.M., 2009, Robust statistics: Hoboken, New Jersey, Wiley, 380 p.

Sullivan, J.T., Nelson, A.R., LaForge, R.C., Wood, C.K., and Hansen, R.A., 1988, Central Utah regional seismotectonic study for USBR dams in the Wasatch Mountains: U.S. Bureau of Reclamation Seismotectonic Report 88–5, 359 p.

Theis, C.V., Brown, R.H., and Meyer, R.R., 1963, Estimating the transmissivity of aquifers from the specific capacity of wells: U. S. Geological Survey Water-Supply Paper 1536–I, 341 p.

Thorne, J.H., Boynton, R., Flint, L., Flint, A., and N'goc Le, T., 2012, Development and application of downscaled hydroclimatic predictor variables for use in climate vulnerability and assessment studies: California Energy Commission Publication CEC-500-2012-010, 86 p.

U.S. Census Bureau, 2016, Population and housing unit estimates: Online, https://www.census.gov/programs-surveys/popest.html, accessed February 2016.

U.S. Geological Survey, 2015, 3DEP products and services — The National Map: Online, https://www.usgs.gov/core-science-systems/ngp/3dep/about-3dep-products-services, accessed October 2016.

U.S. Geological Survey, 2019, National Water Information System (NWIS)—water data for the nation: Online, https://waterdata.usgs.gov/nwis, accessed May 2019.

Utah Automated Geographic Reference Center (AGRC), 2019, Geographic data for Utah: Online, https://gis.utah.gov/data/, accessed February 2016.

Utah Department of Environmental Quality, 2019, Utah Ambient Water Quality Monitoring System (AWQMS): Online, https://awqms.utah.gov/, accessed May 2019.

Utah Division of Water Rights, 2018, GIS data and related tables — WRPOD: Online, https://www.waterrights.utah.gov/gisinfo/wrcover.asp, accessed February 2018.

Utah Division of Water Rights, 2019, Public water supply water records/use information: Online, https://www.waterrights.utah.gov/cgi-bin/wuseview.exe?Startup, accessed May 2019.

vanRossum, G., 2014, Python: Python Software Foundation.

Wallace, J., and Lowe, M., 1999, A Mass-Balance Approach for Recommending Septic Tank Soil-Absorption System Density/Lot-Size Requirements Based on Potential Water-Quality Degradation Due to Nitrate; Examples from Three Utah Valleys, *in* Spangler, L.E., and Allen, C.J., editors, Geology of Northern Utah and Vicinity: Utah Geological Association Guidebook 27, p. 267–274.

Wasatch Conservation District, 2012, Wallsburg coordinated resource management plan: Wasatch Conservation District, Heber, Utah, 130 p.

Webster, R., and Oliver, M.A., 2001, Geostatistics for environmental scientists: New York, Wiley, 330 p.

UTAH GEOLOGICAL SURVEY
a division of
Utah Department of Natural Resources

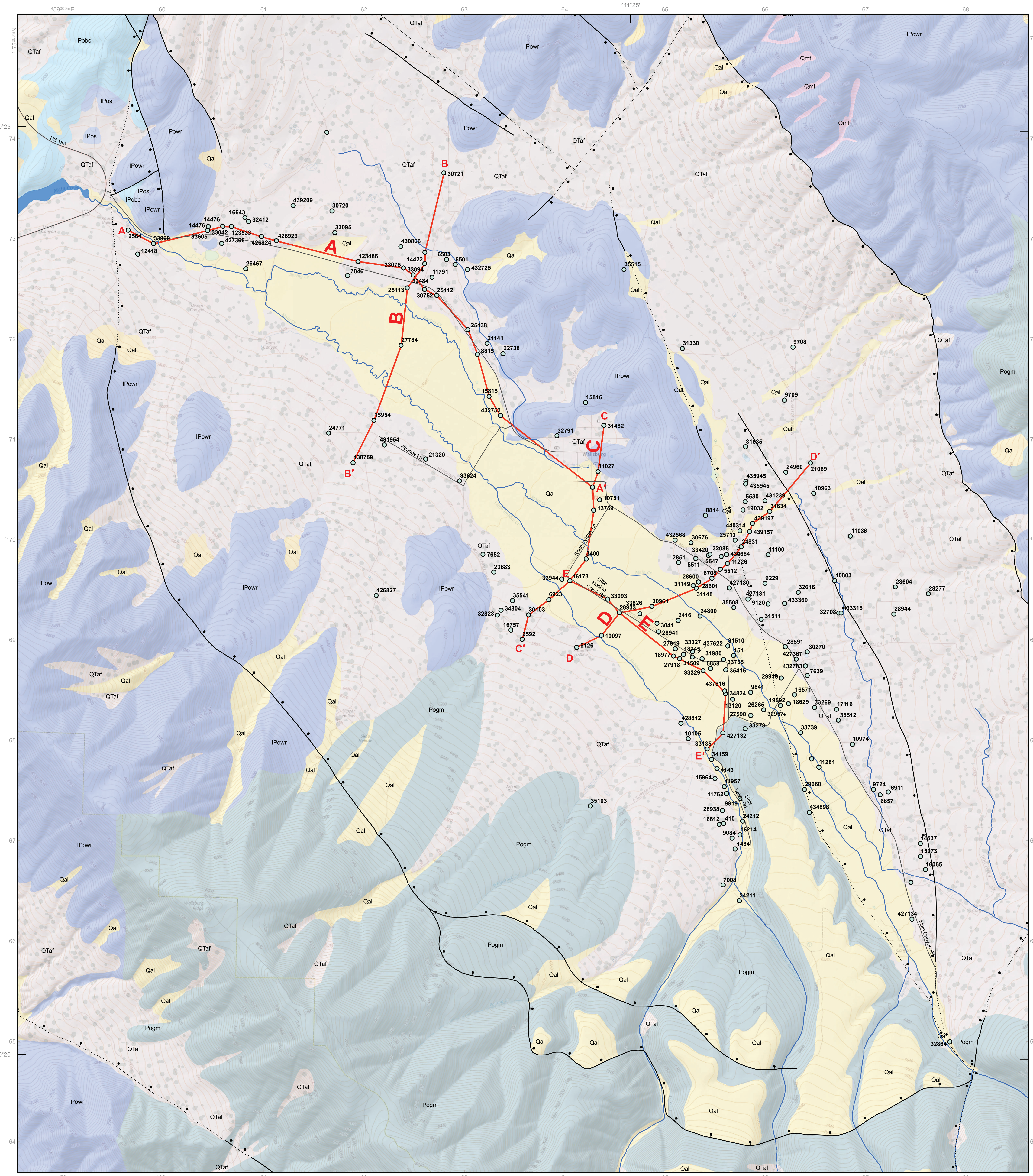

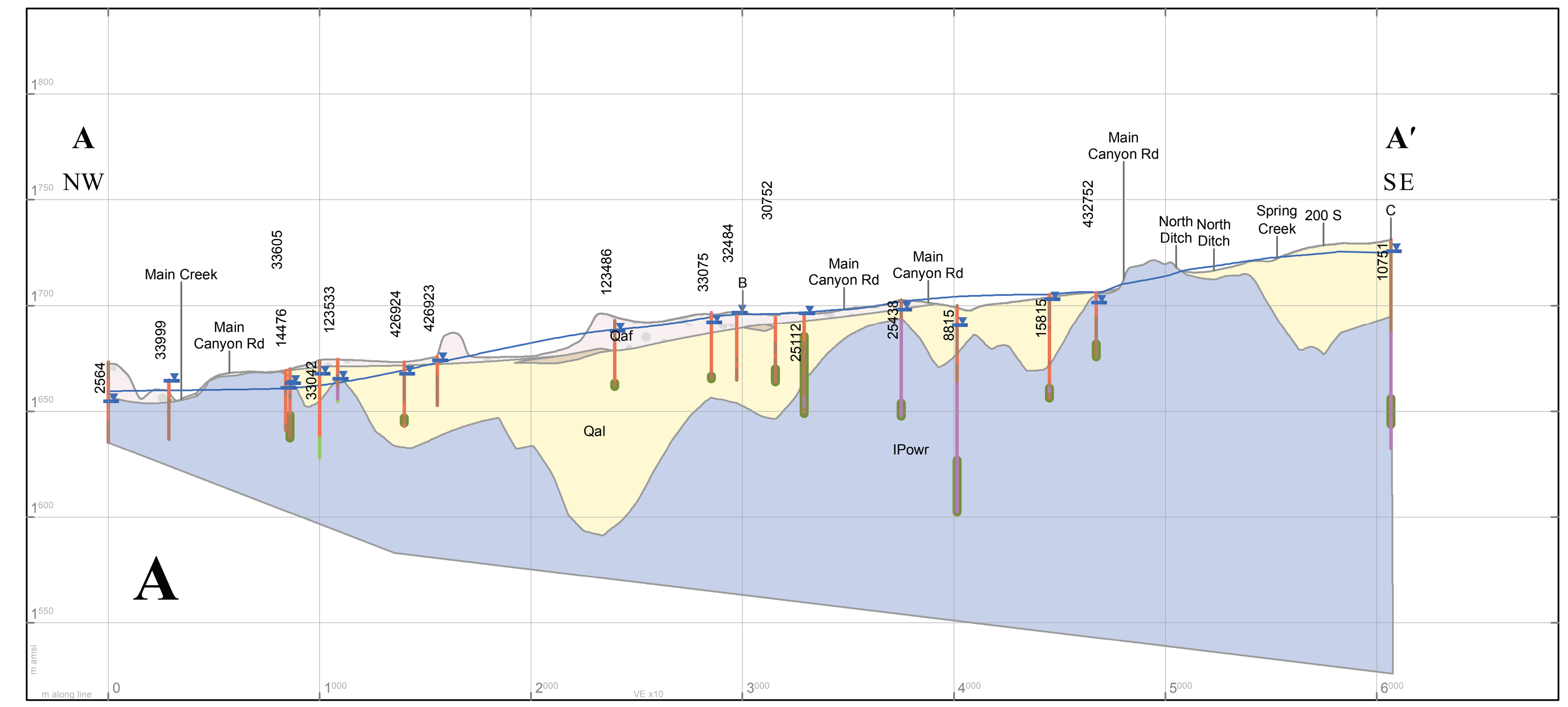

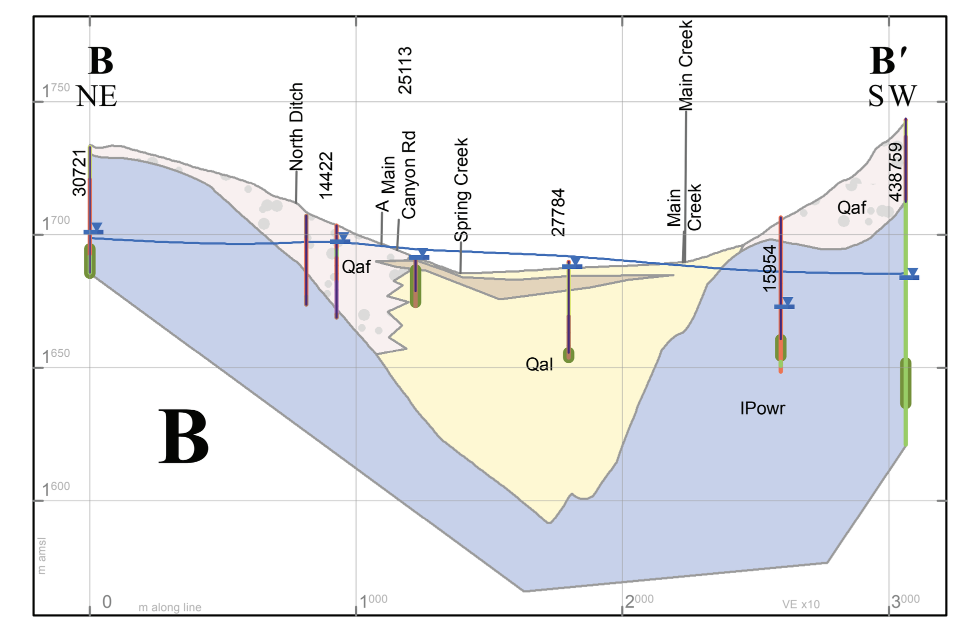

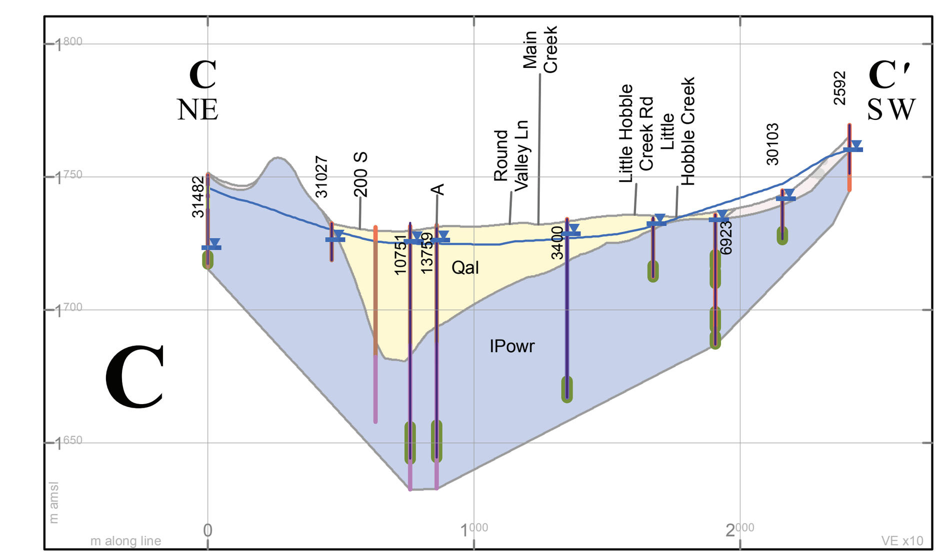

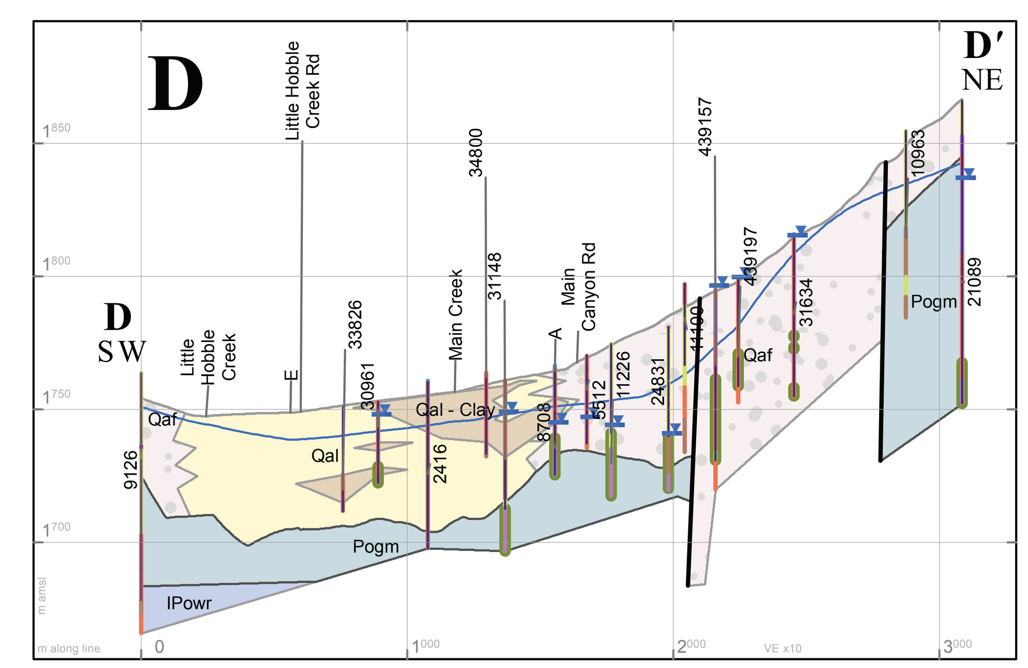

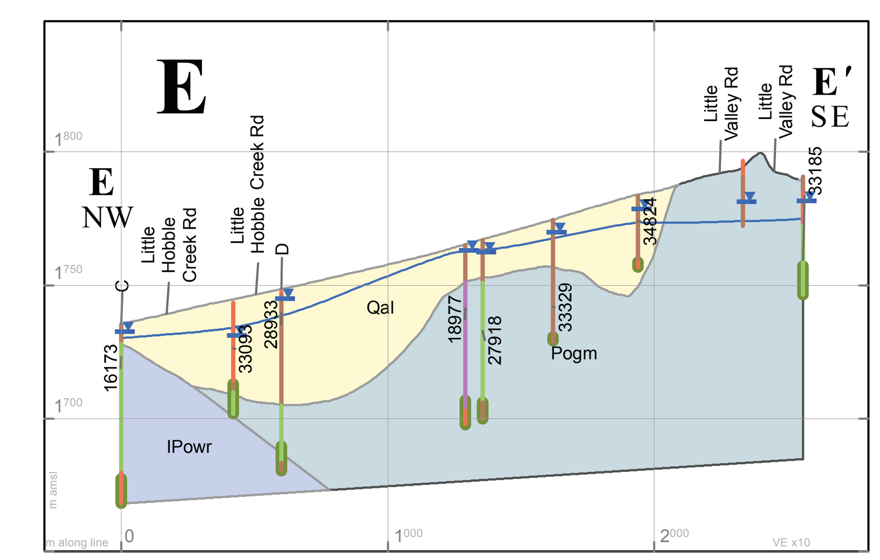

SIMPLIFIED GEOLOGIC MAP, WELL LOCATIONS, AND CROSS SECTIONS OF ROUND VALLEY, UTAH

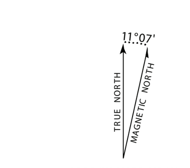

1:24,000

1 0 1 Mile

1 0 1 Kilometer

Base from USGS National Map
Projection and datum for map are UTM NAD83
Cartography and GIS: Paul C. Inkenbrandt
Geology modified from Constenius and others (2011)

Utah Geological Survey
1594 West North Temple, Suite 3110
Salt Lake City, UT 84116
(801) 537-3300
geology.utah.gov

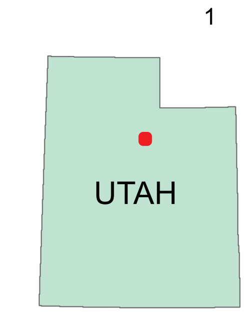

MAP LOCATION

Well location (number represents the WIN*)
Fault, well located
Fault, concealed
Bar and ball on down-thrown side
Stream
Cross section line
Water

*WIN = Utah Division of Water Rights well identification number

Geologic units

- Qal — Alluvium
- Qal - Clay — Clay-rich alluvium
- Qmt — Talus deposits
- QTaf — Alluvial-fan deposits
- Oquirrh Fm
  - Pogm — Granger Mountain Member
  - IPowr — Wallsburg Ridge Member
  - IPos — Shingle Mill Limestone Member
  - IPobc — Bear Canyon Member

Well symbols

Geologic units from well logs

- Sand-cobbles-boulders
- Soil
- Clay
- Clay with boulders
- Gravel and sand
- No information
- Bedrock

Well construction

- Potentiometric Surface
- Reported casing
- Screen intervals